

## *Supplementary Information*

### **Genome mining unveils a class of ribosomal peptides with two amino termini**

Hengqian Ren<sup>1,2,#</sup>, Shravan R. Dommaraju<sup>2,3,#</sup>, Chunshuai Huang<sup>2</sup>, Haiyang Cui<sup>2</sup>, Yuwei Pan<sup>4</sup>, Marko Nestic<sup>2,3</sup>, Lingyang Zhu<sup>5</sup>, David Sarlah<sup>2,3</sup>, Douglas A. Mitchell<sup>2,3,6,\*</sup>, and Huimin Zhao<sup>1,2,3,7,\*</sup>

<sup>1</sup>Department of Chemical and Biomolecular Engineering, University of Illinois at Urbana-Champaign, Urbana, IL, USA.

<sup>2</sup>Carl R. Woese Institute for Genomic Biology, University of Illinois at Urbana-Champaign, Urbana, IL, USA.

<sup>3</sup>Department of Chemistry, University of Illinois at Urbana-Champaign, Urbana, IL, USA.

<sup>4</sup>Department of Molecular and Cellular Biology, University of Illinois at Urbana-Champaign, Urbana, IL, USA.

<sup>5</sup>School of Chemical Sciences, NMR Laboratory, University of Illinois at Urbana-Champaign, Urbana, IL, USA.

<sup>6</sup>Department of Microbiology, University of Illinois at Urbana-Champaign, Urbana, IL, USA.

<sup>7</sup>Department of Bioengineering, University of Illinois at Urbana-Champaign, Urbana, IL, USA.

<sup>#</sup>These authors contributed equally to this work: Hengqian Ren, Shravan R. Dommaraju.

\* To whom correspondence should be addressed: [douglasm@illinois.edu](mailto:douglasm@illinois.edu), [zhao5@illinois.edu](mailto:zhao5@illinois.edu)

## Table of Contents

Supplementary Methods.....	1
Supplementary Table 1: Daptide protein co-occurrence table.....	7
Supplementary Table 2: Comparison of the Dmp chemical shifts observed in 1 (daptide) and hominidin.....	8
Supplementary Table 3: Comparison of the Ala-23 chemical shifts observed in 1 (daptide) and Ala-20 in hominidin .....	9
Supplementary Table 4: Indicator strains and corresponding culturing conditions used in the antimicrobial activity screening .....	10
Supplementary Table 5: Oligonucleotides used for cloning and site-directed mutagenesis.....	11
Supplementary Table 6: DNA sequences of the <i>E. coli</i> codon-optimized <i>mpa</i> genes .....	13
Supplementary Table 7: Naming scheme for daptide biosynthetic genes .....	14
Supplementary Note: Algorithm for pairing of RRE families with precursor peptide families .....	15
Supplementary Figure 1: Generalized workflow for bioinformatic analysis of the RRE-Finder exploratory mode dataset.....	17
Supplementary Figure 2: Daptide precursor peptide sequence logo .....	18
Supplementary Figure 3: HHpred results for MpaB .....	19
Supplementary Figure 4: Alternative identified daptide BGCs .....	20
Supplementary Figure 5: Daptide precursor peptide frequency within a BGC .....	21
Supplementary Figure 6: Taxonomic comparison of daptide protease lengths .....	22
Supplementary Figure 7: Phylogenetic tree of aminotransferases.....	23
Supplementary Figure 8: Annotation of the cloned region from <i>M. paraoxydans</i> DSM 15019.....	24
Supplementary Figure 9: Media and host screen for <i>mpa</i> BGC expression .....	25
Supplementary Figure 10: Purification of daptides 1-3.....	26
Supplementary Figure 11: HR-MS/MS analysis of 1.....	27
Supplementary Figure 12: HR-MS/MS analysis of 2.....	28
Supplementary Figure 13: HR-MS/MS analysis of 3.....	29
Supplementary Figure 14: NMR spectra of compound 1 in 1,1,3,3,3-hexafluoroisopropanol- <i>d</i> <sub>2</sub> (HFIP- <i>d</i> <sub>2</sub> )..	47
Supplementary Figure 15: NMR spectra of authentic ( <i>R</i> )-Dmp and ( <i>S</i> )-Dmp standards .....	53
Supplementary Figure 16: Determination of MpaA1 amino acid stereochemistry using LC-MS .....	54
Supplementary Figure 17: Determination of MpaA1 Dmp stereochemistry.....	55
Supplementary Figure 18: The <i>sca</i> BGC identified from <i>Streptomyces capuensis</i> NRRL B-3501.....	56
Supplementary Figure 19: Heterologous expression and product characterization of <i>sca</i> .....	57
Supplementary Figure 20: Determination of ScaA1/A2 residue stereochemistry .....	58
Supplementary Figure 21: Secondary structure of daptides 1-3.....	60
Supplementary Figure 22: Comparison of melittin to daptide 1 .....	61
Supplementary Figure 23: Hemolytic activity of daptides 1-3.....	62
Supplementary Figure 24: Heterologous expression and <i>mpa</i> gene omissions in <i>S. albus</i> J1074.....	63
Supplementary Figure 25: Expression of the refactored <i>mpaABCDE</i> under various cultivation conditions ...	64
Supplementary Figure 26: Expression of the refactored <i>mpaABCDE</i> with chaperone plasmids .....	65
Supplementary Figure 27: Expression of the refactored <i>mpaABCDE</i> with pGro7 chaperone plasmid under various arabinose concentrations.....	66

Supplementary Figure 28: Expression of the refactored <i>mpaABCDE</i> with pGro7 chaperone plasmid with extended expression time .....	67
Supplementary Figure 29: MALDI-TOF-MS analysis of MpaA1 leader region variants co-expressed with MpaB and MpaC .....	68
Supplementary Figure 30: MALDI-TOF-MS analysis of MpaA1 C-terminal Thr variants that were co-expressed with MpaB and MpaC .....	69
Supplementary Figure 31: MALDI-TOF-MS analysis of MpaA1 insertion and deletion variants at the C-terminus that were co-expressed with MpaB and MpaC.....	70
Supplementary Figure 32: MALDI-TOF-MS analysis of MpaA1 variants in the core peptide region that were co-expressed with MpaB and MpaC .....	71
Supplementary Figure 33: Assessment of the AlphaFold-Multimer prediction for the MpaB-MpaC-MpaA1 complex.....	72
Supplementary Figure 34: Electrostatic surface potential of MpaB and MpaC. ....	73
Supplementary Figure 35: Identification of a hominycin-like BGC from <i>Staphylococcus pseudintermedius</i> ..	74
Supplementary Figure 36: The plasmid map of directly cloned <i>mpa</i> for heterologous expression in <i>S. albus</i> J1074 .....	75
Supplementary Figure 37: Plasmid maps of gene omission for heterologous expression in <i>S. albus</i> J1074: pSET-mpaABCDMPT.....	76
Supplementary Figure 38: Plasmid maps of gene omission for heterologous expression in <i>S. albus</i> J1074: pSET-mpaABCDMP .....	77
Supplementary Figure 39: Plasmid maps of gene omission for heterologous expression in <i>S. albus</i> J1074: pSET-mpaABCDM .....	78
Supplementary Figure 40: Plasmid maps of gene omission for heterologous expression in <i>S. albus</i> J1074: pSET-mpaA1BCD.....	79
Supplementary Figure 41: Plasmid maps of codon-optimized and refactored genes for heterologous expression in <i>E. coli</i> : MpaA1A2A3BCDM.....	80
Supplementary Figure 42: Plasmid maps of codon-optimized and refactored genes for heterologous expression in <i>E. coli</i> : MpaABCDM .....	81
Supplementary Figure 43: Plasmid maps of codon-optimized and refactored genes for heterologous expression in <i>E. coli</i> : MpaABCD.....	82
Supplementary Figure 44: Plasmid maps of codon-optimized and refactored genes for heterologous expression in <i>E. coli</i> : MpaABCM .....	83
Supplementary Figure 45: Plasmid maps of codon-optimized and refactored genes for heterologous expression in <i>E. coli</i> : MpaABDM.....	84
Supplementary Figure 46: Plasmid maps of codon-optimized and refactored genes for heterologous expression in <i>E. coli</i> : MpaABC.....	85
Supplementary Figure 47: Plasmid maps of codon-optimized and refactored genes for heterologous expression in <i>E. coli</i> : MpaAB .....	86
Supplementary Figure 48: Plasmid maps of codon-optimized and refactored genes for heterologous expression in <i>E. coli</i> : MpaAC .....	87

## Supplementary Methods

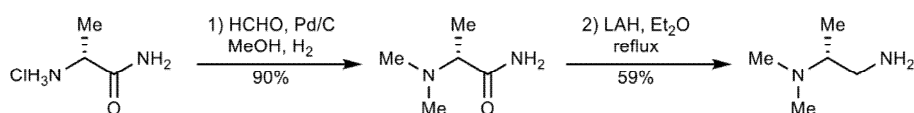
**Bacterial strains and reagents.** *E. coli* strain NEB10 $\beta$  was used for all cloning experiments. *E. coli* strain WM6026 which was a gift from William Metcalf (University of Illinois at Urbana-Champaign) was used as a conjugation donor for *Streptomyces* heterologous hosts<sup>1</sup>. *S. albus* J1074 and *S. lividans* TK24 were used for heterologous expression of the cloned *mpa* BGC. *E. coli* BL21(DE3) was used for the expression of refactored *mpa* pathway. *M. paraoxydans* DSM 15019 was obtained from the German Collection of Microorganisms and Cell Cultures GmbH (Braunschweig, Germany). *S. albus* J1074 and *S. lividans* TK24 were obtained from the Agricultural Research Service Culture Collection (Peoria, IL). *E. coli* strain NEB10 $\beta$  and BL21(DE3) were purchased from New England Biolabs (Ipswich, MA). Components of cell culture media were purchased from ThermoFisher Scientific (Waltham, MA). Antibiotics were purchased from GoldBio (St. Louis, MO). The hexafluoroisopropanol-*d*<sub>2</sub> (HFIP; (CF<sub>3</sub>)<sub>2</sub>CDOD;  $\geq 99$  atom % D) was purchased from Sigma-Aldrich (St. Louis, MO). The (*R*)-2-(dimethylamino)propionamide and (*S*)-2-(dimethylamino)propionamide were purchased from Alfa Chemistry (Ronkonkoma, NY). All other chemicals were purchased from ThermoFisher Scientific (Waltham, MA). No further purification was performed for any purchased chemicals before use. Restriction enzymes, NEBuffers, T4 DNA polymerase, *E. coli* DNA ligase, dNTPs, NAD<sup>+</sup>, NEBuilder HiFi DNA assembly mastermix, and Q5 DNA polymerase were purchased from New England Biolabs (Ipswich, MA). All DNA oligonucleotides were ordered from Integrated DNA Technologies (Coralville, IA). Codon optimized genes were synthesized by Twist Bioscience (South San Francisco, CA).

**High-resolution mass spectrometry.** Lyophilized, HPLC-purified daptides **1-3** were resuspended in aq. 60% acetonitrile/0.1% acetic acid. Samples were directly infused onto a ThermoFisher Scientific Orbitrap Fusion ESI-MS using an Advion TriVersa Nanomate 100. Calibration was performed with Pierce LTQ Velos ESI Positive Ion Calibration Solution (ThermoFisher). The MS was operated with the following parameters: 100,000 resolution, 2 *m/z* isolation width (MS/MS), 0.4 activation *q* value (MS/MS), and 30 ms activation time (MS/MS). Fragmentation was performed using collision-induced dissociation (CID) at normalized collision energy. Each peptide was subjected to 30, 70, and 100

normalized collision energy (MS/MS). Data analysis was conducted using the Qualbrowser application of Xcalibur software (version 4.1.31.9, ThermoFisher Scientific).

**NMR spectroscopy.** The sample was prepared by dissolving ~5 mg of **1** (HPLC-purified and lyophilized) in 500  $\mu$ L of hexafluoroisopropanol-d2 (HFIP; (CF<sub>3</sub>)<sub>2</sub>CDOD;  $\geq$ 99 atom % D, Sigma-Aldrich). NMR spectra were recorded on an Agilent VNMRS 750 MHz narrow bore magnet spectrometer equipped with a 5 mm triple resonance (<sup>1</sup>H-<sup>13</sup>C-<sup>15</sup>N) triaxial gradient probe and pulse-shaping capabilities. Samples were held at 25 °C during acquisition. Standard Varian pulse sequences were used for the following experiments: <sup>1</sup>H, <sup>13</sup>C, <sup>1</sup>H-<sup>1</sup>H COSY, <sup>1</sup>H-<sup>13</sup>C HSQC, and <sup>1</sup>H-<sup>13</sup>C HMBC. Spectra were recorded with VNMRJ 3.2A software. All NMR data were processed using MestReNova 11.0.3. Chemical shifts were referenced internally to the solvent peak ( $\delta_{\text{H}} = 4.4$  ppm,  $\delta_{\text{C}} = 68.1$ , HFIP).

#### Synthetic procedure for the (*R*)-/(*S*)-Dmp standards



1) (*R*)-2-(dimethylamino)propionamide was prepared according to a known procedure<sup>2</sup>: A mixture of (*R*)-alaninamide hydrochloride (500 mg, 4.01 mmol, 1 equiv.), HCHO (37% aqueous, 0.97 mL) and Pd/C (10% wt, 50 mg) in MeOH (15 mL) was stirred in a flask equipped with a H<sub>2</sub> balloon for 16 h. Upon completion, the mixture was filtered through celite. The filtrate was evaporated, diluted with a mixture of MeOH/DCM (10 mL/10 mL), basified with NH<sub>4</sub>OH (28% aqueous, 1 mL), and concentrated. Flash column chromatography (SiO<sub>2</sub>) of the residue with DCM/MeOH/28% aqueous NH<sub>4</sub>OH (60:10:1) afforded (*R*)-2-(dimethylamino)propionamide (420 mg, 3.62 mmol, 90%).

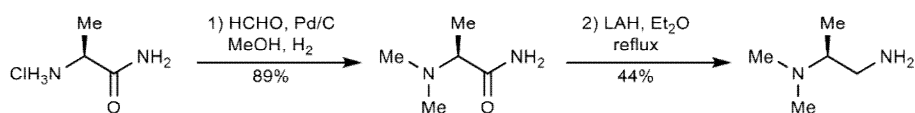
2) Conditions for amide reduction were reported previously<sup>3</sup>. To a solution of (*R*)-2-(dimethylamino)propionamide (420 mg, 3.62 mmol) in dry ether (18 mL) was added LAH (412 mg, 10.8 mmol, 3 equiv) at 0 °C portionwise. Upon completed addition, the mixture was heated to reflux and left to stir overnight. The mixture was cooled down to 0 °C, followed by sequential addition of water (0.5 mL), 15% aqueous NaOH (0.5 mL) and water (1.5 mL). After 15 min of stirring, the obtained precipitate was removed by filtration, and the filtrate was dried with MgSO<sub>4</sub>. Careful evaporation of ether in vacuo (the product is

highly volatile) afforded (*R*)-*N*<sub>2</sub>,*N*<sub>2</sub>-dimethyl-1,2-propanediamine [(*R*)-Dmp] as a colorless oil (218 mg, 2.13 mmol, 59%). Since this compound co-evaporated with diethyl ether, a small amount of ether was always present in the final sample.

$$[\alpha]_{\text{D}}^{22} = -13.1^{\circ} \text{ (c = 0.35 mg/mL, Et}_2\text{O)}$$

<sup>1</sup>H NMR (500 MHz, DMSO-*d*<sub>6</sub>) δ 3.32 (br, 2H), 2.50 (m, 1H), 2.40 – 2.32 (m, 2H), 2.16 (d, *J* = 2.0 Hz, 1H), 2.12 (s, 6H), 0.82 (d, *J* = 6.3 Hz, 3H).

<sup>13</sup>C NMR (126 MHz, DMSO-*d*<sub>6</sub>) δ 64.9, 44.9, 40.3, 10.4.



1) (*S*)-2-(dimethylamino)propionamide was prepared according to a known procedure<sup>2</sup>. A mixture of (*S*)-alaninamide hydrochloride (500 mg, 4.01 mmol, 1 equiv), HCHO (37% aqueous, 0.97 mL) and Pd/C (10% wt, 50 mg) in MeOH (15 mL) was stirred in a flask equipped with a H<sub>2</sub> balloon for 16 h. Upon completion, the mixture was filtered through celite. The filtrate was evaporated, diluted with a mixture of MeOH/DCM (10 mL/10 mL), basified with NH<sub>4</sub>OH (28% aqueous, 1 mL), and concentrated. Flash column chromatography (SiO<sub>2</sub>) of the residue with DCM/MeOH/28% aqueous NH<sub>4</sub>OH (60:10:1) afforded (*S*)-2-(dimethylamino)propionamide (416 mg, 3.58 mmol, 89%).

2) Reduction conditions were reported previously<sup>3</sup>. To a solution of (*S*)-2-(dimethylamino)propionamide (416 mg, 3.62 mmol) in dry ether (18 mL) was added LAH (408 mg, 10.7 mmol, 3 equiv) at 0 °C portionwise. Upon completed addition, the mixture was heated to reflux and left to stir overnight. The mixture was cooled down to 0 °C, followed by sequential addition of water (0.5 mL), 15% aqueous NaOH (0.5 mL) and water (1.5 mL). After 15 min of stirring, the obtained precipitate was removed by filtration, and the filtrate was dried with MgSO<sub>4</sub>. Careful evaporation of ether in vacuo (the product is highly volatile) afforded (*S*)-*N*<sub>2</sub>,*N*<sub>2</sub>-dimethyl-1,2-propanediamine [(*S*)-Dmp] as a colorless oil (160 mg, 1.57 mmol, 44%). Since this compound co-evaporated with diethyl ether, a small amount of ether was always present in the final sample.

$$[\alpha]_D^{22} = 16.4^\circ \text{ (c = 0.40 mg/mL, Et}_2\text{O)}$$

<sup>1</sup>H NMR (500 MHz, DMSO-*d*<sub>6</sub>) δ 3.32 (br, 2H), 2.50 (m, 1H), 2.40 – 2.32 (m, 2H), 2.16 (d, *J* = 2.0 Hz, 1H), 2.12 (s, 6H), 0.82 (d, *J* = 6.3 Hz, 3H).

<sup>13</sup>C NMR (126 MHz, DMSO-*d*<sub>6</sub>) δ 64.9, 44.9, 40.3, 10.4.

**Characterization of stereochemistry by Marfey's assays.** Purified **1** (400 μg) was dried in vacuo in a Schlenk flask. To the dried peptide, 300 μL of a 1:1 mixture 12 M DCl (35% *w/v*, Aldrich) and D<sub>2</sub>O (Cambridge Isotope Laboratory) containing 3% phenol (*w/v*) was added. The solution was equilibrated under nitrogen gas and subjected to one freeze-pump-thaw cycle. The sample was then frozen, subjected to vacuum, and sealed. Once equilibrated back to room temperature, the sample was heated to 95 °C for 2 h under reduced pressure. For the ScaA1/A2 peptide mixture, the same hydrolysis procedure was conducted in 1.6 mL of the 1:1 mixture 12 M DCl and D<sub>2</sub>O and heated at 95 °C for 16 hr. After cooling back to room temperature, insoluble debris was removed by centrifugation for 5 min, and supernatant was dried using a Speedvac concentrator (Savant ISS110).

The hydrolysate of **1** was dissolved in 150 μL 1M aq. NaHCO<sub>3</sub> and 150 μL acetone containing 4 mg/mL 1-fluoro-2-4-dinitrophenyl-5-L-alanine amide (L-FDAA, Thermo Scientific) was added. For the ScaA1/A2 sample, the hydrolysate was dissolved in 150 μL 1M aq. NaHCO<sub>3</sub> and 150 μL acetone containing 12 mg/mL L-FDAA. Contents were mixed, and the reaction vessel was heated to 60 °C for 2 h without shaking using an Eppendorf ThermoMixer C. The reaction mixture was then quenched using 40 μL 6 M HCl dropwise. Sample was dried using a Speedvac concentrator (Savant ISS110). Amino acid standards were prepared by drying down 150 μL L-amino acid solution (0.5 μmol/mL), followed by dissolution in 1 M aq. NaHCO<sub>3</sub> and mixing with acetone containing 4 mg/mL L-FDAA as above. D-amino standards were generated by reacting the L-amino acid solution with 1-fluoro-2-4-dinitrophenyl-5-D-alanine amide (D-FDAA, Toronto Research Chemicals). These reaction products are enantiomers to the hypothetical D-amino acid and L-FDAA coupled products, where both are chromatographically identical using an achiral stationary phase. Standards for (*R*)-*N*<sub>2</sub>,*N*<sub>2</sub>-dimethyl-1,2-propanediamine and (*S*)-*N*<sub>2</sub>,*N*<sub>2</sub>-dimethyl-1,2-propanediamine were prepared by adding 1 μL of

synthesized standard to 149  $\mu\text{L}$  1M aq.  $\text{NaHCO}_3$  and mixed with acetone containing 4 mg/mL L-FDAA as above.

Derivatized amino acid standards, Dmp standards, and MpaA1 hydrolysate were reconstituted in 300  $\mu\text{L}$  15% aq. MeCN + 0.1% formic acid (LC-MS grade). Samples were sonicated for 5 minutes in a sonication bath and insoluble material was removed by filtration with a 0.2  $\mu\text{m}$  centrifugal filter (Pall Corporation) or by centrifugation for 5 min. Amino acid stereochemistry was determined using a Shimadzu LC-MS 2020 with a quadrupole detector and a Macherey-Nagel Nucleodur C18 column (250 $\times$ 4.6 mm, 5  $\mu\text{m}$  particle size, 100  $\text{\AA}$  pore size). Samples were analyzed in batch using the following conditions: solvent A 0.1% aq. formic acid, solvent B MeCN + 0.1% formic acid, 1 mL/min flow rate, and the following method: 15% B for 7 min, 15-50% B over 45 min, hold at 50% B for 5 min followed by wash and re-equilibration in starting conditions. Analyte (20  $\mu\text{L}$ ) was injected and the  $[\text{M}+\text{H}]^+$  ions of the amino acid-Marfey's reagent adducts were selective monitored as follows ( $m/z$ ): Ser, 358; Trp, 457; Asp, 386; Phe, 418; Tyr, 434; Glu (amide of Gln hydrolyzed), 400; Val, 370; Ile/Leu, 384; Ala, 342; FDAA(bis)-Tyr, 686. For the ScaA1/A2 sample, the following ions were selectively monitored ( $m/z$ ): Ala, 342; Phe, 418; Ile/Leu, 384; Thr, 372; Val, 370; FDAA(bis)-Tyr, 686. To clarify Asp and Ser stereochemistry for **1**, amino acid-Marfey's reagent adduct standards were mixed 3:1 with MpaA1 hydrolysate, and 20  $\mu\text{L}$  of the resulting mixtures were injected on the LC-MS as above. Dmp stereochemistry was determined by co-injection of derivatized MpaA1 hydrolysate with derivatized Dmp standards on a Thermo Vanquish Duo binary pump UHPLC system and a Thermo Scientific Accucore C18 column (150 $\times$ 4.6 mm, 2.6  $\mu\text{m}$  particle size, 80  $\text{\AA}$  pore size). Samples were analyzed using the following conditions: solvent A 0.1% aq. formic acid, solvent B MeCN + 0.1% formic acid, 2 mL/min flow rate and the following method: 15% B for 0.5 min and 15-22% B over 7 min, followed by wash and re-equilibration in starting conditions. To obtain optimal peak resolution, derivatized Dmp standards and MpaA1 hydrolysate were diluted >100 fold before injection of 20  $\mu\text{L}$  of sample in each run.

**Circular dichroism spectrometry.** CD spectra were acquired using a JASCO spectropolarimeter J-715 with Peltier temperature control. Stock solutions of **1**, **2**, and **3** (10 mM in HFIP) were diluted by



water to 50  $\mu\text{M}$  [final concentration of HFIP at 0.5% (v/v)] immediately prior to data acquisition. Spectra were recorded from 260 to 200 nm at a scan rate of 200 nm/min at 0.1 nm resolution at 10 °C. The data shown are the average of three acquisitions.

**Supplementary Table 1: Daptide protein co-occurrence table.** RODEO<sup>4</sup> annotation used the Pfam<sup>5</sup>, TIGRFAM<sup>6</sup>, and custom RiPP recognition element (RRE) profile hidden Markov models (pHMMs)<sup>7</sup>. The top three hits for each annotated CDS were compiled and counted for frequency. The top 32 highest occurring pHMM hits in daptide BGCs are listed with custom pHMM models for daptide detection shown in red.

Count	% Co-occurrence	pHMM ID	pHMM description
486	101%	PF00202	Aminotransferase class-III
486	101%	TIGR00707	argD: transaminase, acetylmornithine/succinylornithine family
484	100%	TIGR00508	bioA: adenosylmethionine-8-amino-7-oxononanoate transaminase
456	94%	PF13649	Methyltransferase domain
452	94%	TIGR01188	drxA: daunorubicin resistance ABC transporter, ATP-binding protein
381	79%	PF08241	Methyltransferase domain
377	78%	TIGR03740	galliderm_ABC: lantibiotic protection ABC transporter, ATP-binding subunit
375	78%	TIGR03522	GldA_ABC_ATP: gliding motility-associated ABC transporter ATP-binding subunit GldA
319	66%	<b>Actino_DapB_RRE</b>	C-terminal RRE domain from Actinomycetota DapB proteins
307	64%	PF00465	Iron-containing alcohol dehydrogenase
302	63%	TIGR03405	Phn_Fe-ADH: phosphonate metabolism-associated iron-containing alcohol dehydrogenase
289	60%	<b>Actino_DapP_RRE</b>	N-terminal RRE domain from Actinomycetota DapP proteins
192	40%	PF13561	Enoyl-(Acyl carrier protein) reductase
185	38%	TIGR02638	lactal_redase: lactaldehyde reductase
183	38%	PF12698	ABC-2 family transporter protein
178	37%	PF13489	Methyltransferase domain
176	36%	<b>Bacill_DapB_RRE</b>	C-terminal RRE domain from Bacillota DapB proteins
163	34%	TIGR01830	3oxo_ACP_reduc: 3-oxoacyl-[acyl-carrier-protein] reductase
154	32%	PF00528	Binding-protein-dependent transport system inner membrane component
145	30%	PF02163	Peptidase family M50
142	29%	PF00583	Acetyltransferase (GNAT) family
142	29%	<b>Bacill_DapP_RRE</b>	N-terminal RRE domain from Bacillota DapP proteins
139	29%	PF02624	YcaO cyclodehydratase, ATP-ad Mg <sup>2+</sup> -binding
134	28%	TIGR03604	TOMM_cyclo_SagD: thiazole/oxazole-forming peptide maturase, SagD family component
124	26%	PF00069	Protein kinase domain
123	26%	PF00296	Luciferase-like monooxygenase
120	25%	TIGR03564	F420_MSMEG_4879: F420-dependent oxidoreductase, MSMEG_4879 family
120	25%	TIGR03841	F420_Rv3093c: probable F420-dependent oxidoreductase, Rv3093c family
120	25%	PF08242	Methyltransferase domain
105	22%	TIGR01575	rimI: ribosomal-protein-alanine acetyltransferase
104	22%	PF12730	ABC-2 family transporter protein
96	20%	PF05147	Lanthionine synthetase C-like protein

**Supplementary Table 2: Comparison of the Dmp chemical shifts observed in 1 (daptide) and hominidin<sup>8</sup>.** Data was obtained in 1,1,1,3,3,3-hexafluoroisopropanol-*d*<sub>2</sub> (HFIP-*d*<sub>2</sub>) for 1 and H<sub>2</sub>O + D<sub>2</sub>O for hominidin, respectively. <sup>§</sup>Data not available. \*Signals assigned to *N*-methyl groups are not distinguished in the original paper. Dmp: (*S*)-*N*<sub>2</sub>,*N*<sub>2</sub>-dimethyl-1,2-propanediamine.

No.	1 (daptide)		Hominidin	
	$\delta_C$ type	$\delta_H$ multi	$\delta_C$ type	$\delta_H$ multi
1	39.1 CH <sub>2</sub>	3.91 overlapped 3.38 d (15.2)	39.9 CH <sub>2</sub>	3.46 d (6.3) 3.41 m
2	61.7 CH	3.75 m	60.9 CH	3.48 m
3	6.9 CH <sub>3</sub>	1.34 brs	10.9 CH <sub>3</sub>	1.23 d (6.7)
4	34.1 CH <sub>3</sub>	2.80 s	38.2 CH <sub>3</sub>	2.75* s
5	41.6 CH <sub>3</sub>	2.97 s	41.0 CH <sub>3</sub>	2.80* s
NH		N/A <sup>§</sup>		8.24 t (5.9)

**Supplementary Table 3: Comparison of the Ala-23 chemical shifts observed in 1 (daptide) and Ala-20 in homininin<sup>8</sup>.** Data was obtained in 1,1,1,3,3,3-hexafluoroisopropanol-*d*<sub>2</sub> (HFIP-*d*<sub>2</sub>) for 1 and H<sub>2</sub>O + D<sub>2</sub>O for homininin, respectively. <sup>§</sup>Data not available. \*Carbonyl carbon of Ala-22 in 1 and Ile-19 in homininin.

No.	1 (daptide)		Hominicin	
	$\delta_C$ type	$\delta_H$ multi	$\delta_C$ type	$\delta_H$ multi
1'	51.0 CH	4.22 overlapped	50.0 CH	4.18 m
2'	13.7 CH <sub>3</sub>	1.57 d (6.9)	16.4 CH <sub>3</sub>	1.29 d (7.4)
NH		N/A <sup>§</sup>		8.32 d (5.8)
CO	175.8 C		175.5 C	
CO*	176.4 C		173.3 C	

**Supplementary Table 4: Indicator strains and corresponding culturing conditions used in the antimicrobial activity screening.** Recipes for mediums used in the bioassay are as the following: lysogeny broth (LB): 10 g/L tryptone, 10 g/L NaCl, and 5 g/L yeast extract; brain heart infusion broth (BHI): 5 g/L beef heart (infusion from 250 g), 12.5 g/L calf brains (infusion from 200 g), 2.5 g/L Na<sub>2</sub>HPO<sub>4</sub>, 2 g/L glucose, 10 g/L peptone, and 5 g/L NaCl; international Streptomyces project-2 medium (ISP2): 10 g/L malt extract, 4 g/L yeast extract, and 4 g/L glucose; ATCC medium 172 (ATCC 172): 10 g/L glucose, 20 g/L soluble starch, 5 g/L yeast extract, 5 g/L N-Z Amine Type A (Sigma C0626), and 1 g/L CaCO<sub>3</sub>; yeast extract–peptone–dextrose medium (YPD): 10 g/L yeast extract, 20 g/L peptone, and 20 g/L glucose.

Phylum	Strain	Medium	Temperature (°C)
Bacillota	<i>Bacillus cereus</i> TZ417	LB	30
	<i>Bacillus subtilis</i> ATCC 6633	LB	30
	<i>Lactococcus lactis</i> CNRZ 481	LB	30
	<i>Staphylococcus epidermidis</i> 15X154	LB	37
	<i>Staphylococcus aureus</i> USA300	BHI	37
	<i>Streptococcus mutans</i> ATCC 25175	BHI	37
Actinomycetota	<i>Micrococcus luteus</i> ATCC 4698	LB	30
	<i>Streptomyces albus</i> J1074	ISP2	30
	<i>Streptomyces lividans</i> TK24	ISP2	30
	<i>Streptomyces coelicolor</i> M145	ISP2	30
	<i>Microbacterium aurum</i> B-24210	ATCC 172	30
	<i>Microbacterium esteraromaticum</i> B-24213	ATCC 172	30
	<i>Microbacterium hominis</i> B-24220	ATCC 172	30
	<i>Microbacterium ketosireducens</i> B-24221	ATCC 172	30
<i>Microbacterium kitamiense</i> B-24226	ATCC 172	30	
Pseudomonadota	<i>Escherichia coli</i> DH5a	LB	37
	<i>Enterobacter cloacae</i>	LB	30
	<i>Pseudomonas fluorescens</i> Pf-5	LB	30
	<i>Pseudomonas putida</i> mt-2	LB	30
Ascomycota	<i>Saccharomyces cerevisiae</i> YSG50	YPD	30
	<i>Aspergillus terreus</i>	YPD	30

**Supplementary Table 5: Oligonucleotides used for cloning and site-directed mutagenesis.** The primers are named for the annealing region and whether the primer was for the forward (F) or reverse (R) direction.

Name	Nucleotide Sequence (5' to 3' direction)
pBE44 F	ttaccaatgcttaatcagtgaggcacc
pBE45 R	atctttatagtcctgtcgggtttcg
pBE44-DSM15019-ami R	accgtgttcgtcttcccggatctcaacaccggcaacaacaacttatatcgtatggggctg
pBE45-DSM15019-ami F	cactccccgccttcccaccgttctccacacccttctctgacgctcagtggaacgaaaac
DSM15019-g1 F	aattaatacgaactcactataggaatttctactggtgtagatccggatctcaacaccggc
DSM15019-g1 R	gccggtggtgagatccggatctacaacagtagaaattccctatagtgagtcgtattaatt
DSM15019-g2 F	aattaatacgaactcactataggaatttctactggtgtagatccaccgttctccacacc
DSM15019-g2 R	gggtgtggagaacggtggatctacaacagtagaaattccctatagtgagtcgtattaatt
pBE44-B3501-ami R	ggtcacctgcgcttcttccaacatgtccgagccgtacaacaacttatatcgtatggggctgacttc
pBE45-B3501-ami F	cgcacagaagctttgaaggcgaagggataggatcgcgctcagtggaacgaaaac
B3501-g1 F	aattaatacgaactcactataggaatttctactggtgtagatctccaacatgtccgagcc
B3501-g1 R	ggctcggacatggttcaaatctacaacagtagaaattccctatagtgagtcgtattaatt
B3501-g2 F	aattaatacgaactcactataggaatttctactggtgtagataaggcgaagggatagg
B3501-g2 R	cctatccctttcgaccttactacaacagtagaaattccctatagtgagtcgtattaatt
pSET (XbaI)-mpaB F	gacggccagtgccaagcttgggctgcaggtcgactctagacgccgcccgaacgagagaa
mpaP R	gcgacgccgatcgggtcgag
mpaM F	tcctcagcactcccgcgcc
Yeast-mpaT3 R	ttatagcacgtgatgaaaaggaccagggtggcacttttcgccaggaatcctacgtcgctt
mpaT3-Yeast F	acgtgtcgtagcgtctcaggaggcgcgtaggattcctggcgaaaagtgccacctgggtc
pSET (EcoRI)-Yeast R	cacacaggaacagctatgacatgattacgaattcgcacatcacagtatcgtgatgacagtg
Yeast-mpaP R	tagcacgtgatgaaaaggaccagggtggcacttttcgctcatcctctctcctcctcgtcgtc
mpaP-Yeast F	cccgtggcagctctcagcagcggaggagagaggatgacgaaaagtgccacctgggtc
Yeast-mpaM R	ttatagcacgtgatgaaaaggaccagggtggcacttttcgctcatcggcggcccttccat
mpaM-Yeast F	cacgacctcccgcgcccgggatggaaggggcccgggatgacgaaaagtgccacctgggtc
Yeast-mpaA1 R	tatagcacgtgatgaaaaggaccagggtggcacttttcggcgtccctccttctctcc
mpaA1-Yeast F	cgtccggcagcaccgatcggagaaaggaaggaggacgccgaaaagtgccacctgggtc
BbsI-mpaA1 F	acgtgaagacaaaatgatgaatccacagaaatgtcgatccg
BbsI-mpaA1 R	acgtgaagacaaaaccgtcaggctcgtcggcgtgc
mpaA1 E13A R	ttccatcgggtccagcgttgaaagcggatcga
mpaA1 E13A F	tcgatccgctttcaagcgtggaccgatggaa
mpaA1 L14A R	ggcttccatcgggtccgcctcttgaaagcggat
mpaA1 L14A F	atccgctttcaagagcggaccgatggaagcc
mpaA1 D15A R	gggggcttccatcggcggcagctcttgaaagcg
mpaA1 D15A F	cgctttcaagagctggcggcggatggaagcccc
mpaA1 P16A R	actgggggcttccatcgcgtccagctcttgaaa
mpaA1 P16A F	tttcaagagctggacgcgatggaagccccagt
mpaA1 M17A R	ccaactggggcttccgcgggtccagctcttg
mpaA1 M17A F	caagagctggacccggcggaaagccccagttgg
mpaA1 E18A R	atcccaactggggcggccatcgggtccagctc
mpaA1 E18A F	gagctggaccgatggcggccccagttgggat

mpaA1 P20A R	aaaggaatcccaactcgcggttccatcgggtc
mpaA1 P20A F	gaccgatggaagccgaggtggattccttt
Bbsl-mpaA1 Ser R	acgtgaagacaaaccgtcagctcgctgccgctgccaatac
Bbsl-mpaA1 Cys R	acgtgaagacaaaccgtcagcacgctgccgctgccaatac
Bbsl-mpaA1 Asp R	acgtgaagacaaaccgtcaatccgctgccgctgccaatac
Bbsl-mpaA1 Asn R	acgtgaagacaaaccgtcagttcgctgccgctgccaatac
Bbsl-mpaA1 Glu R	acgtgaagacaaaccgtcattccgctgccgctgccaatac
Bbsl-mpaA1 Gln R	acgtgaagacaaaccgtcactgctgccgctgccaatac
Bbsl-mpaA1 Gly R	acgtgaagacaaaccgtcagcccgtgccgctgccaatac
Bbsl-mpaA1 Ala R	acgtgaagacaaaccgtcacgccgctgccgctgccaatac
Bbsl-mpaA1 Phe R	acgtgaagacaaaccgtcaaacgctgccgctgccaatac
Bbsl-mpaA1 Lys R	acgtgaagacaaaccgtcatttcgctgccgctgccaatac
Bbsl-mpaA1 Arg R	acgtgaagacaaaccgtcaacgctgccgctgccaatac
Bbsl-mpaA1 Val R	acgtgaagacaaaccgtcacaccgctgccgctgccaatac
Bbsl-mpaA1 +44A R	acgtgaagacaaaccgtcaggtcgccgctgccgctgccaatac
Bbsl-mpaA1 -43A R	acgtgaagacaaaccgtcaggttgccgctgccaataaccga
Bbsl-mpaA1 +45A R	acgtgaagacaaaccgtcacggtcgctgccgctgccaatac
Bbsl-mpaA1 G39P R	acgtgaagacaaaccgtcaggtcgctgccgctgccgaataccgatc
Bbsl-mpaA1 G37P R	acgtgaagacaaaccgtcaggtcgctgccgctgccaatacgggatcaggaca
Bbsl-mpaA1 V34P R	acgtgaagacaaaccgtcaggtcgctgccgctgccaataccgatcagcggaagcgtc
Bbsl-mpaA1 G31P R	acgtgaagacaaaccgtcaggtcgctgccgctgccaataccgatcaggacaagcgggatgac acct
Bbsl-mpaA1 G28P R	acgtgaagacaaaccgtcaggtcgctgccgctgccaataccgatcaggacaagcgtccgatgac cggttgataaaag

**Supplementary Table 6: DNA sequences of the *E. coli* codon-optimized *mpa* genes.**

Gene	Nucleotide Sequence (5' to 3' direction)
<i>mpaA1</i>	atgaatgaatccacagaaatgtcgatccgctttcaagagctggaccgatggaagccccagttgggattccttttatc aagggtgcatcggagcgcttgctcctgatcggatttggcgcagcggcagcgacctga
<i>mpaA2</i>	atgatgaaatgcccgcgtgctccttagagtttacggagctggaagctatggatgcgcccggcgatgcagatgattata tccgtgcttctcgtggtggcggttatcatcgggatttctcgcctgacctaa
<i>mpaA3</i>	atgcaatcaacatcccttgaatttctggaattagaacagatcgacactccattggaatggtgggaacatgcgagttaca ttattgcaattattggtggtgcagctgccattgocagctga
<i>mpaB</i>	atgggaacctcagctacgaccgcacgccaagacgacggctcaaccggcgaagatccgttatttaggcctcatgtccttc gcgatgggtaaccggcgccacgcccggctgctcgttttctcgtgagggcagaacgggtgcggaagcgttagc tgcagcggctgatccggaagatgtcattctcggagccagcgggttctcgcctcgtccaggagcagccggtgctggtggg tatggcggacgcctggcggatattgggtgatgaactcttctcggcgaacgaggatggagctgcaagactatcgcgcg ccagttcgttcagatcgttgggtcccacggccatgcttcttcttgatgaggtctcctggcgtgccttctcgcgatgatgc cgatctcgcacgtggcaccggcgtggttgcgcggcaatgctggaccacgctgcttattggccgaccgctcagcactg gcgcccgcaggaagtggagacgcccacgctgacgcatcgacgggacgggtggtgctgacttaggcctgacggcggc aggcaattggctcatgttgacgatcttccagacgcctgggttggcgcttaacctcgtgcttcaatgcttgggtggttcc tggctcggccgatctcgttgcgaacttgatacgcgctccatggttacgcgcctacctcgaatgctgaggaccttcgtaaa atggtacgcctgcccgaatggcaccgacgctattgcaggctacgggttggcattactggatgacgatctggcggaaagcgg aagccttgccgatgaccttttctttagataccgcccgaaggttttctggtggcggatgctgctacacctcgcgcgtca cttactttcgcctttaaaccgcccgggtgggtggatgcccacagactagtagcacgcgctggctcgtgctgcccacgctg gctcgcctctggtgctgcccggatgcccacgcccaccatttgggttggaaagcgttagcagctctggcgcttccacttag gggcacgcaccgaggacgcatctgggtgatggggcagcttga
<i>mpaC</i>	atgactgtacccttcacagcccgcgttccgaccttatggcaccggcagtcgcgacgcgagcgcgatggtaggctcactg cgggctgataccctgggtgctggctgacgcggcggtagcgcaccccttgccactcctcaatcgggcccgcactatgac cgtcgacgcccgcggctcgacgagttgggaattctctgatcgcggaagaactggctcgcctcgcctgaagtgatc gtggcggctcgttggcggctcagttctggatgcctctaagattgcgcgcctggctctctcctcggcgcttgccttgatt tcgcacttcgtcagcagccacgtctgctcttaccatcttaccggacgctccccgcagtggaacatttggcggatgcc aacgaccttggaaacctctcggaaaccaacagcgtggccatccttcgtaaatcgttggcgctcgtctgcttggggga cgtcccttacgtccgcgccaacgcagctctggaccggaccagctggccactttgaccctgcagcgggtcgtgaggggc ctcttgaggcgtttctccgctcgcggagcagtagctaccacgctacagcccgcgcagcggatgacgctgactctt aggcgcgcttggcggagcggctgacgctgataatgtctacgacggctcgtctcctcgttgccttagccttagcgcg gccactcagcgcactgcccgtctcctggtggcctgaccgctattctgacgcccactggtaacttggccaatgaggttagcct tccacctgggagtgccgcaaaatgacggcaactgcccagctgattgacgcccgatggcaacgcacatcggctcggggcagccc gcgctggggtgacgctgcccagcttggacgcattttgggctggagttgacgaggaacggcgttacctcgtgatcctgca gctggaatcgcgctagtggttagatcaggcggggttaccagcccaccagcccagcgcgctgagattgatcgtattg cggacgcagtcgaacgctgcccggagatcatcgcctatgttgcgcggcattcgcgcgctgatgacgctgacgttctt gcacgactcccgtggagcccttccccggtaggcgatcgtcgtcctcgttggcagagcgtcgttga
<i>mpaD</i>	atgagcgttccgcatgcccttggacctctatgcttccagcagacaccgcatttccgcccagcgcgctcgcctcgggg ccgagccaccgttggctcagcagacgggtcgtatcgtttagcctacaagtggttgggaacgtaccgttggg atttgggaatccagcgggtcaccgaggtgctctcagcgcgactcgtgacgctcctacctgagcttattcctgctccc caccgttacgcagaggtatgcccggatgcttgaatttgcgctcgcaggaagcagcgttaccgcccgcctcatttagca ctagtgccggcgcgcaaatgatgcccctatgaaactcgcctgcaataattgggcaacaaggctgctggttagcgttcc tttagtagttggttacgcggttagctatcatggtacgatgatggctcccacgttcttccggcgacgatctgctgacg tcggtgataggctcgcaccgtcgtacggtacgccagtaagtcacacggatgaaagggctgagctggaagcgttgcctgg agcgcgaaggttcccgtgctgcccagctgcttgcgagccggtaactgggttccagtgcccacgcttctcgtgctcatt cgtgctcgttgcctcagcttgcgcgaacgccatgggttctgcttagttgcccagaggttagccaccgggttgcctcgt acgggcccagctgcttgcaccatgaaggttgggcagcccgtccagatgctccttctgtatcaaaaggcgtcaccgaatggag ctatggcgcagcagcgtccttgggtgggtgatcgattgcaaccgccttggcgcgtggcggctggacatttggttcacgg tgagacacaagccgggacgcctgcctgtgacgcccgtgctcctgcccgttatcgaagcagctcgtcgtattgacgtcgag ggcaccactcaagcgtggttagcagcttacatcgttggcccgcacgtggcaagaggacggcatcgtgaccgatgta gcggaagtgggttctcgtgggtgtaggattacgcccgtcctgacggttccagctcgtgagcggaaaccgacgtgctggaag gggttagtgccattgcccgatccggcgttgggtgacatcctggcccgtcattcattcaggttaacccctggctacggtttt acacctgcagaggtagcggaaactgaccgcccgggtgctggtggcggcttggcacgtgcccgtgagggcgggtggcatga
<i>mpaM</i>	atgacctcgttggattaccgagactgtcgcgcccgtctggaccttgggtggtaccgcccgtgcgcaagacttgtatg caggcgcgggtacagactttaaagatgcctcgttaggtcccgatcgtgcccgaattcgtgaggtactgggttagccca caccgaccccgtccggtaactggacctcgcagcgggttctggccggttgaacaattcctcctgcccgttagtggccaccgc gtgacagcgtggaccttagtgccgataatggttagccggttgcggtggcgcagctcccgcagtgccacccttagaatgcg ttgtggctgatagcgtgacttagcacttggcggacacttccgctggtagttctcggagcaacgctcgatcaccctgct cgaccgcgaagatcgcgcacgcctctacgcccgtgctgctcgtcattctgcatcagcaggtgctcttgcattgaccatt gcccagcgtgctcagtcagacacgcttgcgatcccacggcaccgcaaatcaggttctcgttccgcaggtgtagtagc cttacttattcgcacaacaatcgaggtatgaggtgctgcccgtcttggtaaaactgggtccgctggctgacatcgcgcc acgtgcagaagttccgggtgtaacatcacgcttgcacgctttaaaccacagaggtcctggctggcggagttagtagcagcc gggtttacagcaccgagcgtcgcgggttgcactccggcaggtggtgagatttgggtgtaaacgacctcgcgcgccc gggacggacgcggtcgtcgttaa



**Supplementary Table 7: Naming scheme for daptide biosynthetic genes.** Custom pHMM models for daptide detection are shown in red.

Gene Name	Function	pHMM annotations for identification
<b>DapA</b>	Precursor peptide	N/A
<b>DapB</b>	DUF-RRE fusion protein	<i>Actino_DapB_RRE, Bacill_DapB_RRE</i>
<b>DapC</b>	Oxidative decarboxylase (alcohol dehydrogenase)	PF00465, PF13561
<b>DapD</b>	Aminotransferase	PF00202
<b>DapM</b>	Methyltransferase	PF13649, PF08241, PF13489, PF08242, <i>etc.</i>
<b>DapP</b>	Intramembrane protease	PF02163, <i>Actino_DapP_RRE, Bacill_DapP_RRE</i>
<b>DapT</b>	ABC transporter	TIGR01188, TIGR03740, PF00528, <i>etc.</i>

## Supplementary Note: Algorithm for pairing of RRE families with precursor peptide families.

```
import argparse
import sys
import os
import re

def __main__():

    input_file = open(RRE_ALL_BY_ALL_BLAST_FILE, 'r')
    input_precursor_file = open(PRECURSOR_ALL_BY_ALL_BLAST_FILE, 'r')
    enzyme_edge_data = input_file.read().split("\n")
    precursor_edge_data = input_precursor_file.read().split("\n")
    input_file.close()
    input_precursor_file.close()
    cutoff = 50
    print("Starting enzyme edge filtering...")

    enzyme_edges_withAS = []
    for line in enzyme_edge_data:
        values = line.split()
        try:
            enzyme_edges_withAS.append([values[0], values[1], float(values[11])])
        except:
            pass

    print("Starting ID mapping...")

    precursor_edges_withids = []
    for line in precursor_edge_data:
        try:
            node1, node2, BS = re.split("\t", line)
            if float(BS) > 10:
                precursor_edges_withids.append([node1, node2])
        except:
            pass

    open("temp.tsv", 'w').close()

    enzyme_cluster_generate(output_file_name="temp.tsv", enzyme_edges_withAS=enzyme_edges_withAS,
cutoff=cutoff, precursor_edges_withids=precursor_edges_withids)

def enzyme_cluster_generate(output_file_name, enzyme_edges_withAS=[], cutoff=1000,
precursor_edges_withids=[]):

    print("Starting enzyme graph generation... cutoff = ", cutoff)

    enzyme_edges = []
    for edge in enzyme_edges_withAS:
        if edge[2] > cutoff and edge[0] < edge[1]:
            enzyme_edges.append([edge[0], edge[1]])
    enzyme_clusters = sorted(connected_components(enzyme_edges), key=len, reverse=True)

    print("Starting precursor graph generation...")

    for se in enzyme_clusters:
        print("Cutoff: ", cutoff, "Enzyme cluster size: ", len(se))
        if len(se) < 30:
            print("Too small:", len(se))
            break
        precursor_edges = []
        new_precursor_edges_withids = []
        for edge in precursor_edges_withids:
            if edge[0].split("_")[0] in se and edge[1].split("_")[0] in se:
                precursor_edges.append([edge[0], edge[1]])
                new_precursor_edges_withids.append(edge)
        edge_count = 0
        for enzyme_edge in enzyme_edges:
            if enzyme_edge[0] in se and enzyme_edge[1] in se:
                edge_count += 1
        enzyme_connectivity = ((2 * edge_count) / float(len(se))) / float((len(se)-1))
        print("Enzyme connectivity: " + str(enzyme_connectivity))

        precursor_clusters = sorted(connected_components(precursor_edges), key=len, reverse=True)
        try:
            x = precursor_clusters[0]
        except:
            return
        if len(x) < 5:
            return
        print("Precursor cluster size: ", len(x))
        cluster_found=False

        if len(x) > 0.1 * len(se) and enzyme_connectivity>0.2:
```

```

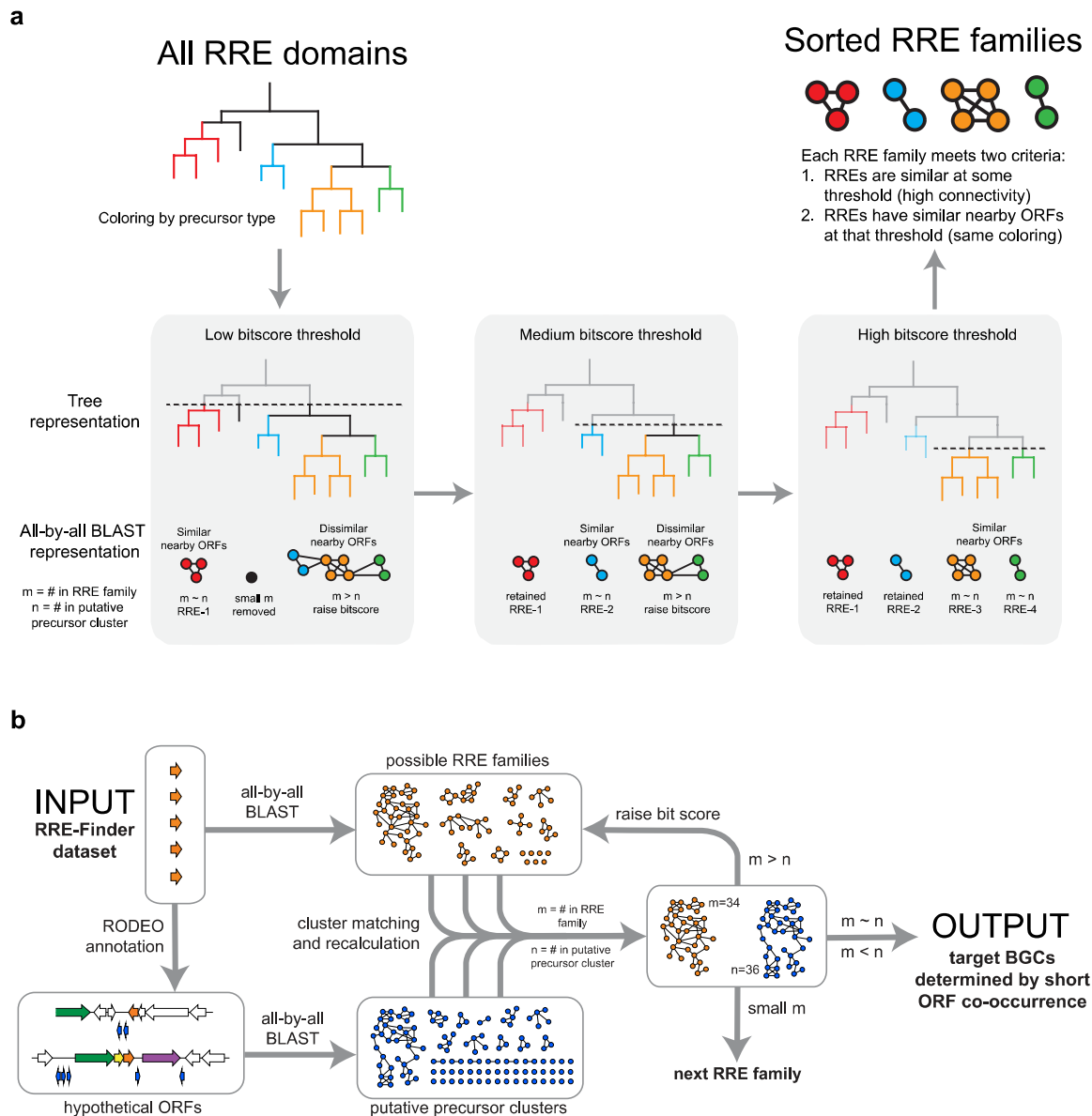
        print("Precursor cluster size: " + str(len(x)) + " Enzyme cluster size: " + str(len(se)) + "
BS cutoff: " + str(cutoff))
        cluster_found=True
        precursor_edge_count = 0
        for z in precursor_edges:
            if z[0] in x and z[1] in x and z[0] != z[1]:
                precursor_edge_count+=1
        precursor_connectivity = precursor_edge_count / len(x) / (len(x)-1)
        print("Precursor connectivity: " + str(precursor_connectivity))

    new_enzyme_edges=[]
    real_node_list = []
    for edge in enzyme_edges_withAS:
        if edge[0] in se and edge[1] in se:
            new_enzyme_edges.append(edge)
            if edge[0] not in real_node_list:
                real_node_list.append(edge[0])
            if edge[1] not in real_node_list:
                real_node_list.append(edge[1])
    if cluster_found==False:
        enzyme_cluster_generate(output_file_name=output_file_name,
enzyme_edges_withAS=new_enzyme_edges, cutoff=cutoff+10,
precursor_edges_withids=new_precursor_edges_withids)
    else:
        precursor_sequences = open(PRECURSOR_FASTA_FILE, 'r').read().split(">")
        output_file = open(output_file_name, 'a')
        output_file.write(str(cutoff) + "\t" + ",".join(se) + "\t" + str(len(se)) + "\t" +
str(enzyme_connectivity)+"\t")
        for precursor in precursor_sequences:
            header = precursor.split("\n")[0]
            if header in x:
                output_file.write(">" + header + " " + ",".join(precursor.split("\n")[1:]) + ",")
            continue
        output_file.write("\t" + str(len(x)) + "\t"+str(precursor_connectivity) + "\t" +
",".join(real_node_list) + "\t" + str(len(real_node_list)) + "\n")
        output_file.close()

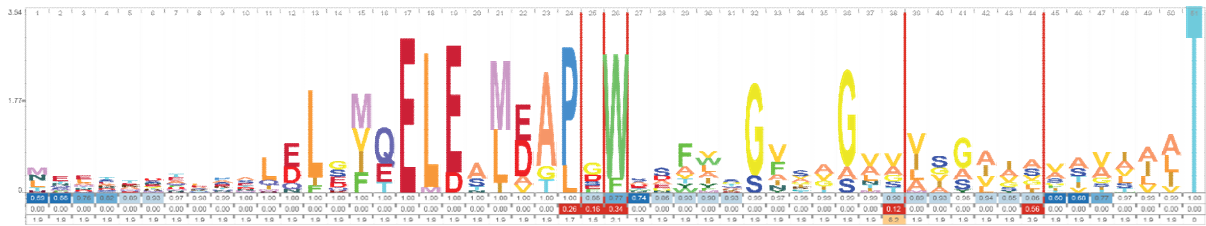
def connected_components(pairs):
    components = []
    for a, b in pairs:
        a_num = -1
        b_num = -2
        for i, component in enumerate(components):
            if a in component:
                a_num = i
            if b in component:
                b_num = i
            if a_num != -1 and b_num != -2:
                break
        if a_num == -1:
            if b_num == -2:
                components.append([a,b])
                #print(a,b)
            else:
                components[b_num].append(a)
                #print(a,b,components[b_num])
        elif b_num == -2:
            components[a_num].append(b)
            #print(a,b,components[a_num])
        elif a_num != b_num:
            components[a_num].extend(components[b_num])
            components[b_num] = []
    return components

if __name__=="__main__":
    __main__()

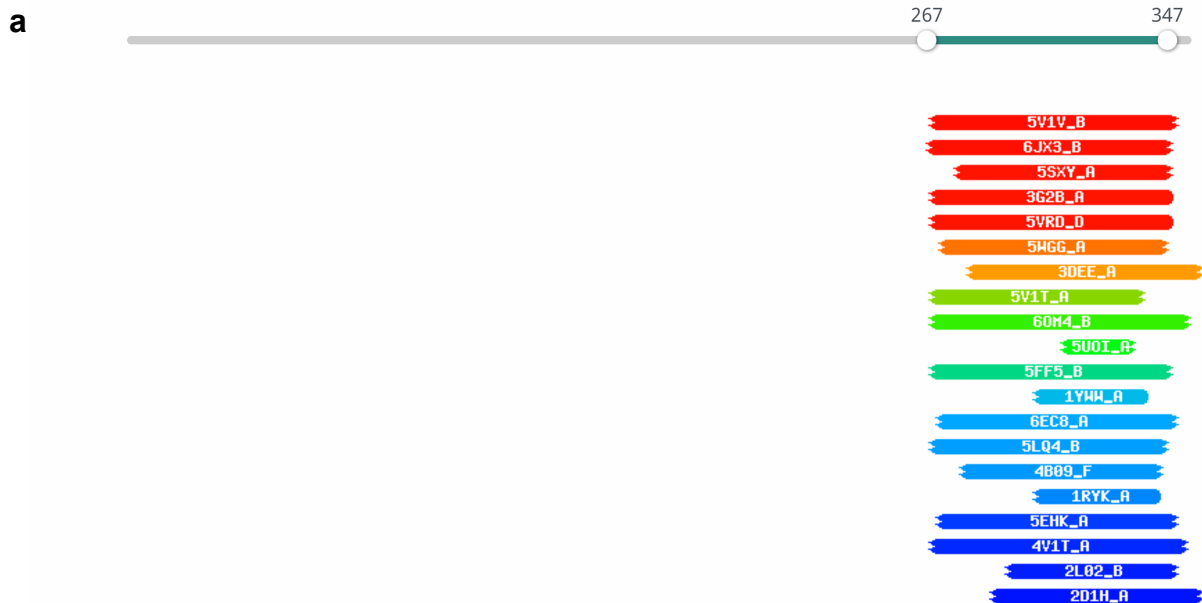
```



**Supplementary Figure 1: Generalized workflow for bioinformatic analysis of the RRE-Finder exploratory mode dataset.** The comprehensive description for this workflow is in the Methods section, and code used for implementation is on Github (<https://github.com/the-mitchell-lab/rodeo2>) and in the **Supplementary Note**. Phylogenetic trees, sequence similarity networks, and biosynthetic gene clusters depicted in this figure are stylized. **(a)** Logical basis for finding new RRE-dependent RiPP pathways. Analysis of RRE domain clusters is performed iteratively with increasing bitscore thresholds. Examination of each cluster for high similarity nearby open-reading frames (ORFs) allows categorization of RRE families based on sequence similarity of the RRE domains and co-occurrence with high-likelihood precursor peptides. **(b)** Workflow of bioinformatics and algorithmic logic. RRE domains predicted by RRE-Finder were annotated by RODEO to identify hypothetical precursors in intergenic ORFs. The RRE domains were sorted into families using an all-by-all BLAST search and the predicted ORFs were also sorted into clusters. For each RRE family, putative precursor peptide clusters were filtered for ORFs in the same genomic neighborhood, and the sizes of the families were compared. Small RRE families were discarded from the algorithm. Cases where the size of the largest precursor peptide cluster matched the RRE family were output from the algorithm for further analysis. All other cases were re-entered into the algorithm with a higher bitscore threshold for RRE family generation.



**Supplementary Figure 2: Daptide precursor peptide sequence logo.** The daptide precursor peptide pHMM ( $n = 184$ ) was generated from precursor peptides identified by the workflow in **Supplementary Figure 1**. The pHMM was converted to a sequence logo using Skylign<sup>9</sup> with the information content above background setting, and the direct output is provided. The invariant Thr residue at the C-terminus is evident (cyan color), along with highly conserved features in the N-terminal leader region.



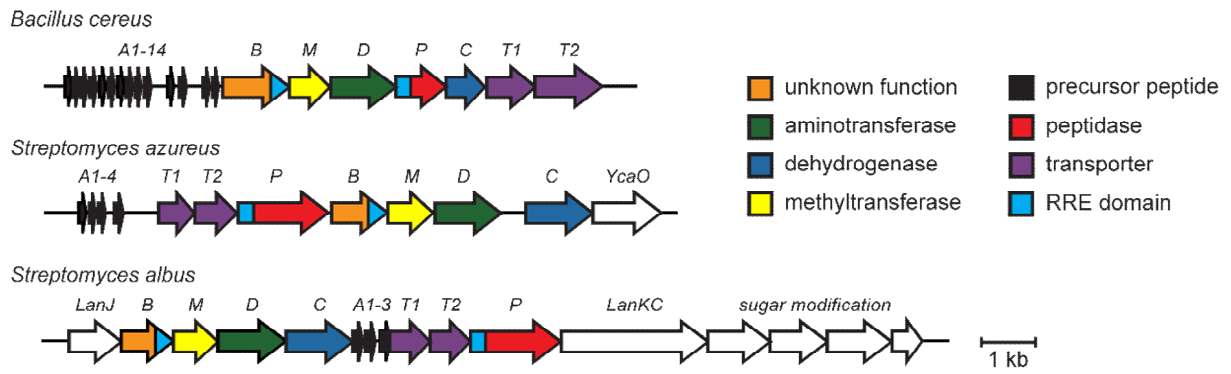
**b**

### Hitlist

Show  Entries Search:

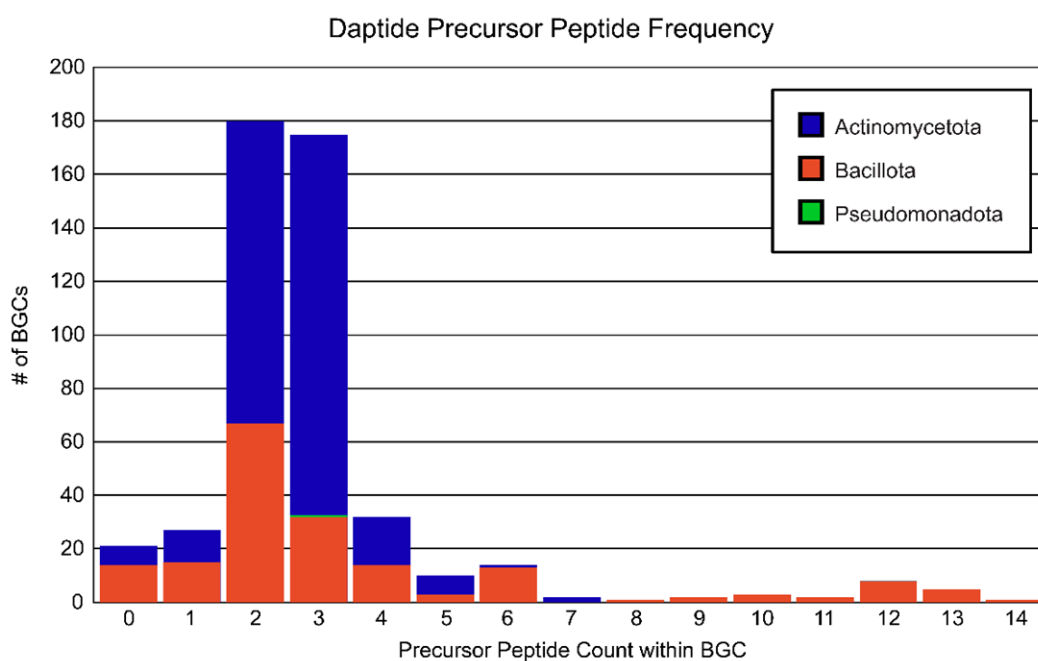
Nr	Hit	Name	Probability	E-value	Score	SS	Aligned cols	Target Length
<input type="checkbox"/>	5V1V_B	TbiB1; Lasso Peptide, RiPP, Peptide Binding, PROTEIN BINDING; 1.35A {Thermobaculum terrenum (strain ATCC BAA-798 / YNP1)}	98.85	1e-7	72.32	12.4	81	91
<input type="checkbox"/>	6JX3_B	TfuB1; lasso peptide, RRE, PEPTIDE BINDING PROTEIN; 1.7A {Thermobifida fusca}	98.64	8e-7	67.55	11.7	80	99
<input type="checkbox"/>	5SXY_A	Bifunctional coenzyme PQQ synthesis protein C/D; RiPP RRE peptide scaffolding, CHAPERONE; NMR {Methylobacterium extorquere}	98.35	0.0000077	61.76	10.3	69	94
<input type="checkbox"/>	3G2B_A	Coenzyme PQQ synthesis protein D; helix-turn-helix, PQQ biosynthesis, BIOSYNTHETIC PROTEIN; 1.66A {Xanthomonas campestris}	98.34	0.0000082	62.04	10.3	78	95
<input type="checkbox"/>	5VRD_D	Bifunctional coenzyme PQQ synthesis protein C/D; PQQ, oxidase, alpha-helical bundle, OXIDOREDUCTASE; 2.85A {Methylobacte}	98.33	0.0000043	82.98	11.1	78	392

**Supplementary Figure 3: HHpred results for MpaB.** (a) Depicted annotation of MpaB (RefSeq ID: WP\_060922562.1) analyzed using HHpred<sup>10</sup> with the PDB\_mmCIF70\_12\_Oct database. The N-terminal domain of the protein is not annotated by HHpred, while the C-terminal domain is annotated with RREs. (b) Hitlist table of HHpred analysis.



**Supplementary Figure 4: Alternative identified daptide BGCs.** Depicted BGCs are from two bacterial phyla (Bacillota and Actinomycetota) with differing genomic architectures, tailoring genes, and precursor peptide count.

**a**



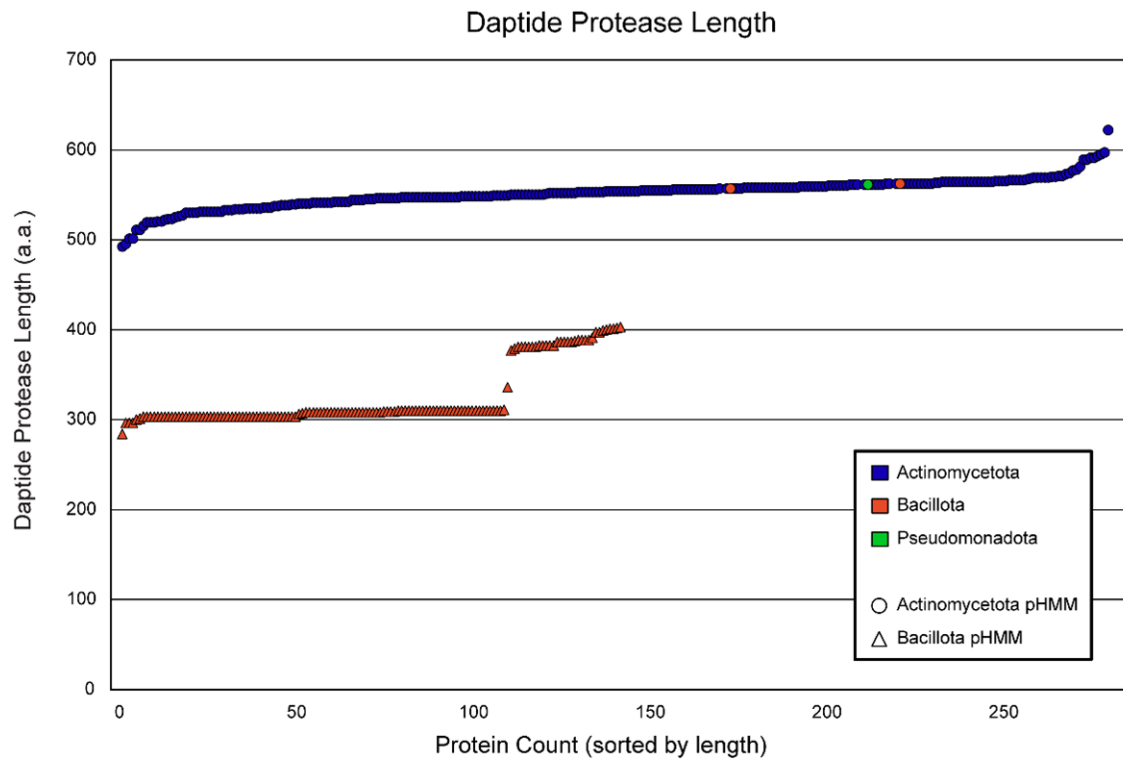
**b**

Precursor Peptide Count within BGC

	0	1	2	3	4	5	6	7	8	9	10	11	12	13	14	Total
<b>Actinomycetota</b>	7	12	113	142	18	7	1	2								302
<b>Bacillota</b>	14	15	67	32	14	3	13		1	2	3	2	8	5	1	180
<b>Pseudomonadota</b>				1												1
<b>Total</b>	21	27	180	175	32	10	14	2	1	2	3	2	8	5	1	483

**Supplementary Figure 5: Daptide precursor peptide frequency within a BGC.** (a) Histogram of daptide precursor peptides per BGC. (b) Numerical values used to generate the histogram are given in table format. Each BGC that lacked an identified precursor peptide originated from a short contig, and the BGC was presumed to be incomplete.

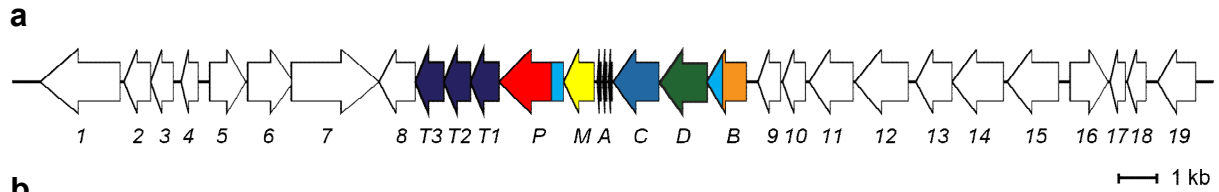




**Supplementary Figure 6: Taxonomic comparison of daptide protease lengths.** All full-length hits for the Actino\_DapP\_RRE and Bacill\_DapP\_RRE found using RODEO and within daptide BGCs were compiled. Protein lengths in amino acids (a.a.) were sorted into two series based on which pHMM best retrieved each protein (circle and triangle) prior to sorting by length. The color coding is based on GenBank taxonomic classification.



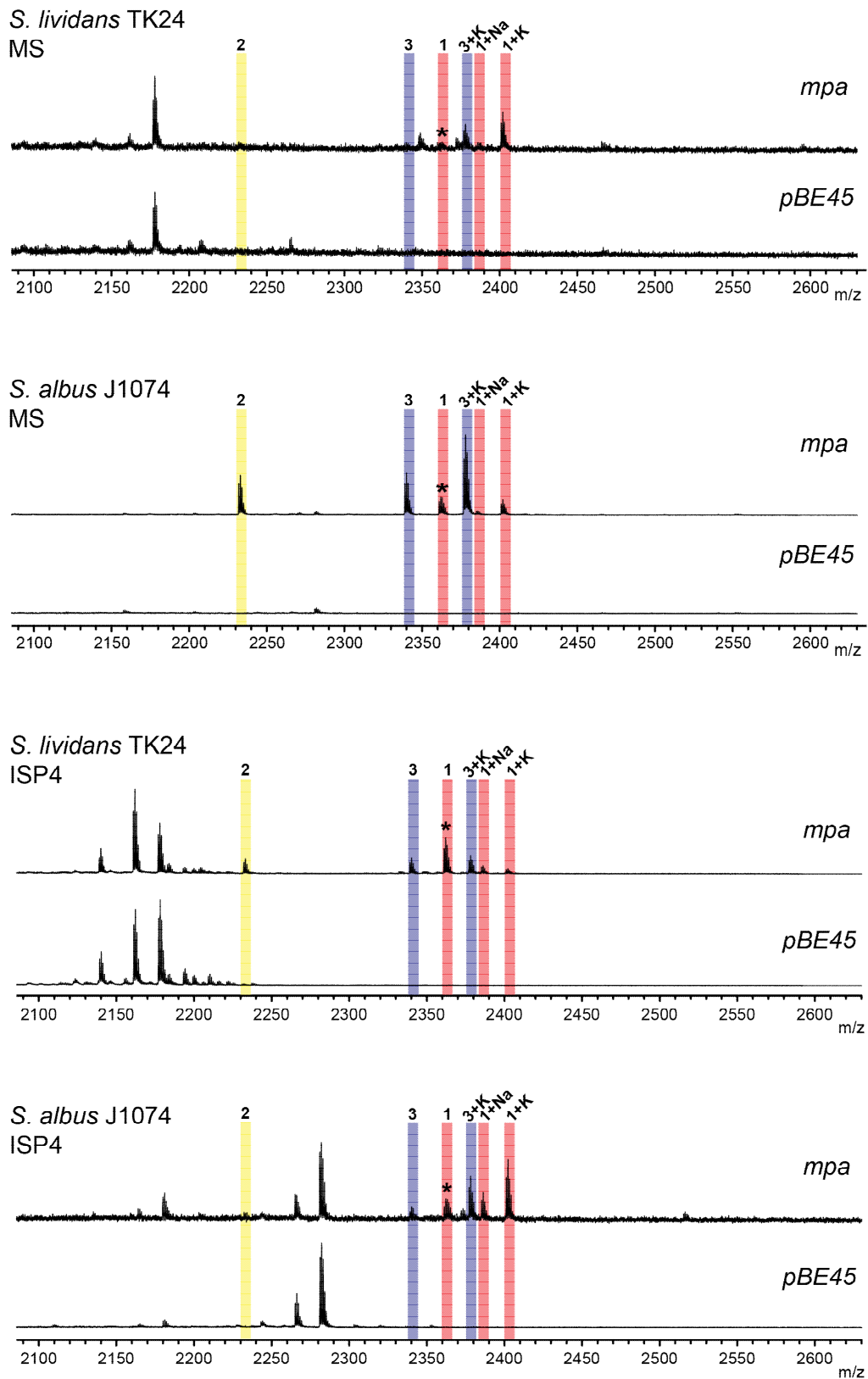
**Supplementary Figure 7: Phylogenetic tree of aminotransferases.** Maximum-likelihood phylogenetic tree of all 483 identified daptide aminotransferases and three outgroup aminotransferases (from aminotransferase class-III<sup>11</sup>). The tree is rooted using gamma-aminobutyrate transaminase 3 (UniProt/GenBank CDS identifiers: Q84P52/BAG16484.1 - Streptophyta). Two additional outgroups are included (P9WQ81/CCP44332.1 - Actinomycetota and P53555/AAB17458.1 - Bacillota) that perform related reactions in biotin biosynthesis.



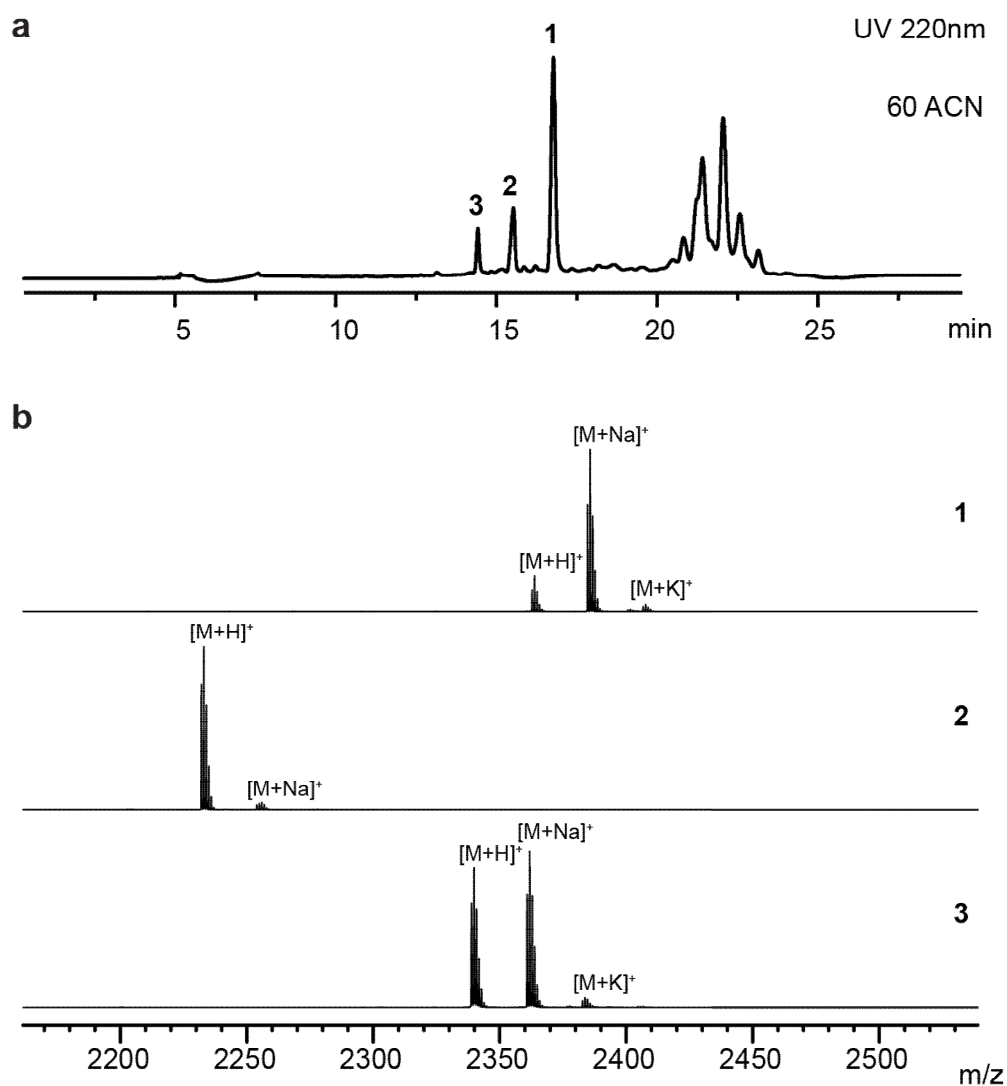
**b**

Gene	NCBI Accession	Description (per NCBI listing)
<i>orf1</i>	WP_060923289.1	Phosphate acetyltransferase
<i>orf2</i>	WP_157547021.1	Hypothetical protein
<i>orf3</i>	WP_060922551.1	Rhomboid family intramembrane serine protease
<i>orf4</i>	WP_157547022.1	Hypothetical protein
<i>orf5</i>	WP_060922553.1	MoxR family ATPase
<i>orf6</i>	WP_060922554.1	DUF58 domain-containing protein
<i>orf7</i>	WP_060922555.1	DUF3488 and transglutaminase-like domain-containing protein
<i>orf8</i>	WP_060922556.1	Rhodanese-related sulfurtransferase
<i>mpaT3</i>	WP_083370907.1	Hypothetical protein
<i>mpaT2</i>	WP_060922557.1	Hypothetical protein
<i>mpaT1</i>	WP_157547023.1	ATP-binding cassette domain-containing protein
<i>mpaP</i>	WP_060922558.1	Hypothetical protein
<i>mpaM</i>	WP_060922559.1	Class I SAM-dependent methyltransferase
<i>mpaA3</i>	N/A <sup>a</sup>	Precursor peptide
<i>mpaA2</i>	N/A <sup>a</sup>	Precursor peptide
<i>mpaA1</i>	N/A <sup>a</sup>	Precursor peptide
<i>mpaC</i>	WP_060922560.1	Iron-containing alcohol dehydrogenase
<i>mpaD</i>	WP_060922561.1	Aminotransferase class III-fold pyridoxal phosphate-dependent enzyme
<i>mpaB</i>	WP_060922562.1	Hypothetical protein
<i>orf9</i>	WP_174521438.1	GNAT family N-acetyltransferase
<i>orf10</i>	WP_060922563.1	Phosphatase PAP2 family protein
<i>orf11</i>	WP_060922564.1	Cystathionine gamma-synthase
<i>orf12</i>	WP_025104232.1	Cystathionine beta-synthase
<i>orf13</i>	WP_025104231.1	Carbohydrate ABC transporter permease
<i>orf14</i>	WP_025104230.1	Sugar ABC transporter permease
<i>orf15</i>	WP_060923551.1	Bacterial extracellular solute-binding protein
<i>orf16</i>	WP_083371072.1	LacI family transcriptional regulator
<i>orf17</i>	WP_025104227.1	Ribosomal protein
<i>orf18</i>	WP_025104226.1	Ribosomal protein
<i>orf19</i>	WP_157547024.1	Hypothetical protein

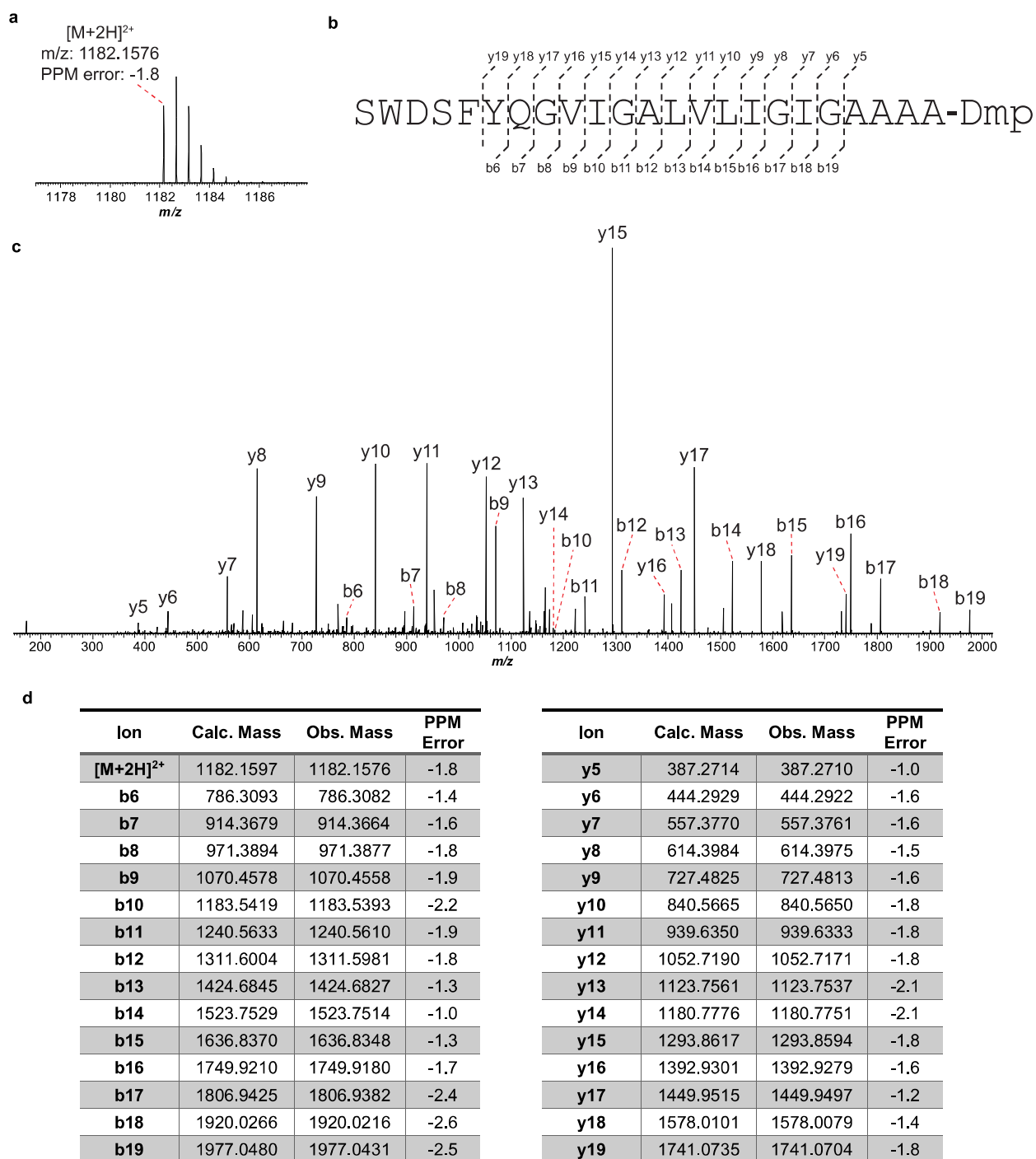
**Supplementary Figure 8: Annotation of the cloned region from *M. paraoxydans* DSM 15019. (a)** Gene arrangement of the cloned region. **(b)** Accession numbers and annotation of corresponding genes in NCBI. <sup>a</sup>Not annotated as gene.



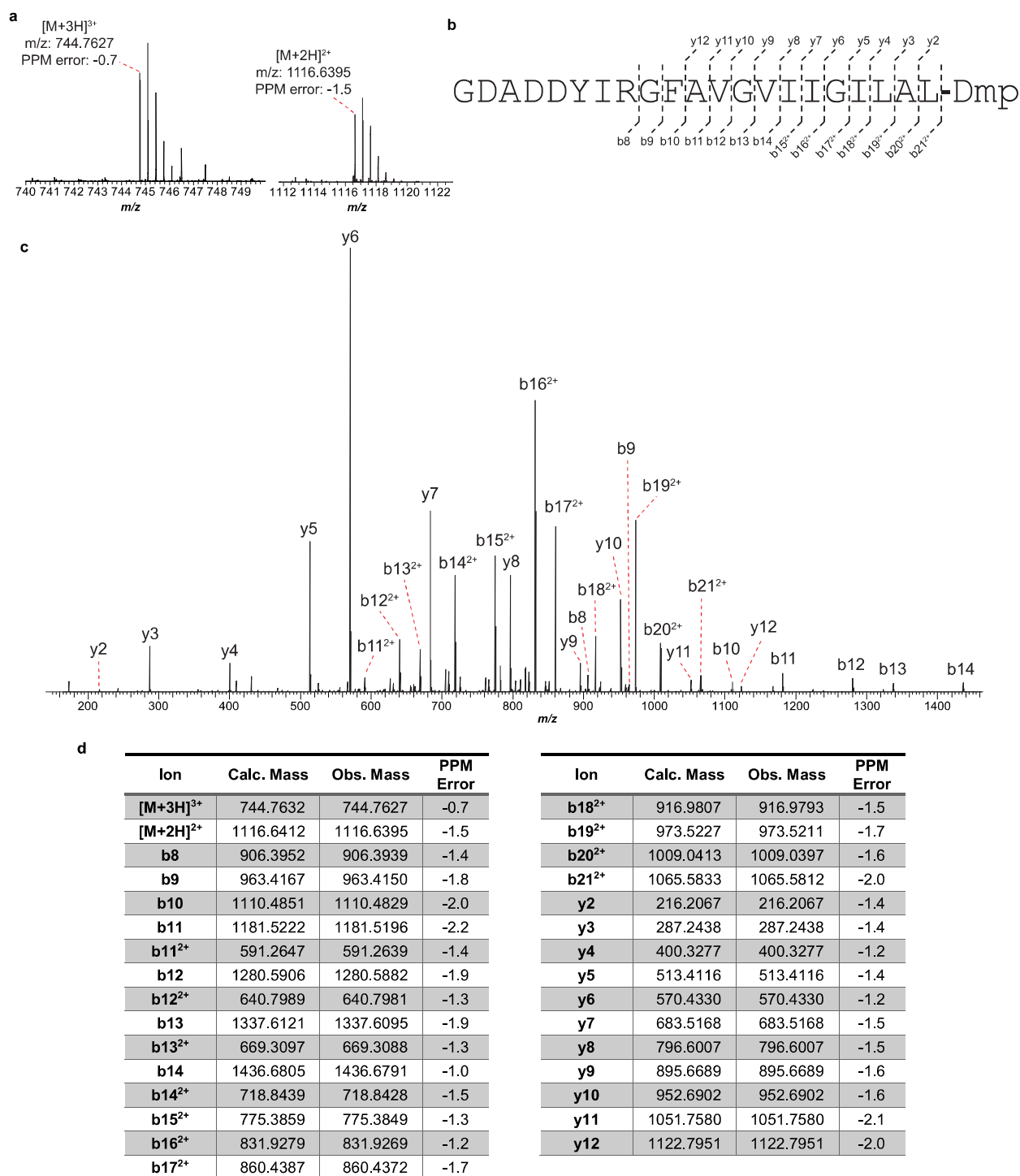
**Supplementary Figure 9: Media and host screen for *mpa* BGC expression.** MALDI-TOF mass spectra of methanolic extracts of *S. lividans* TK24 and *S. albus* J1074 colonies that were transformed with *mpa* or the pBE45 empty vector and cultivated on MS and ISP4 agar media. Possible overlapped peaks of  $[1+H]^+$  and  $[3+Na]^+$  are indicated with an asterisk.



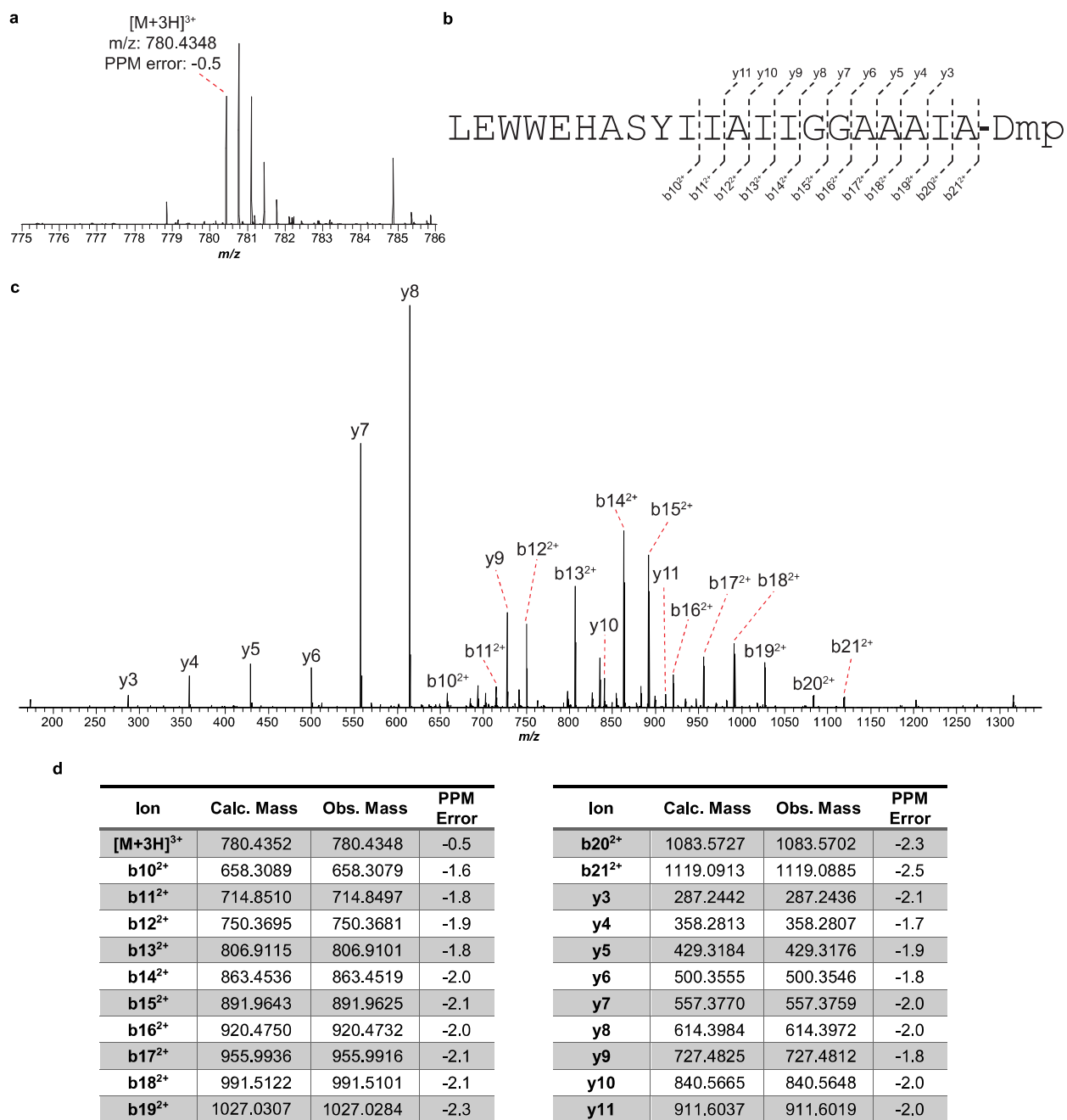
**Supplementary Figure 10: Purification of daptides 1-3.** (a) Reverse phase (C18) HPLC chromatograms with UV absorbance (220 nm) monitoring of solid phase extraction eluents using 60% acetonitrile. (b) MALDI-TOF-MS analysis of the collected fractions.



**Supplementary Figure 11: HR-MS/MS analysis of 1.** (a) Broad band high-resolution mass spectrum of compound 1. (b) Summary of collision-induced dissociation (CID) daughter ions for 1. Observed b- and y-ions are annotated. Ions are in the +1 charge state except where indicated. Dmp:  $N_2,N_2$ -dimethyl-1,2-propanediamine. (c) CID spectrum of 1. (d) Table of daughter ion assignments for 1.



**Supplementary Figure 12: HR-MS/MS analysis of 2.** (a) Broad band high-resolution mass spectrum of compound 2. The  $[M+3H]^{3+}$  ion was selected for fragmentation. (b) Summary of collision-induced dissociation (CID) daughter ions for 2. Observed b- and y-ions are annotated. Ions are in the +1 charge state except where indicated. Dmp: *N*<sub>2</sub>,*N*<sub>2</sub>-dimethyl-1,2-propanediamine. (c) CID spectrum of 2. (d) Table of daughter ion assignments for 2.

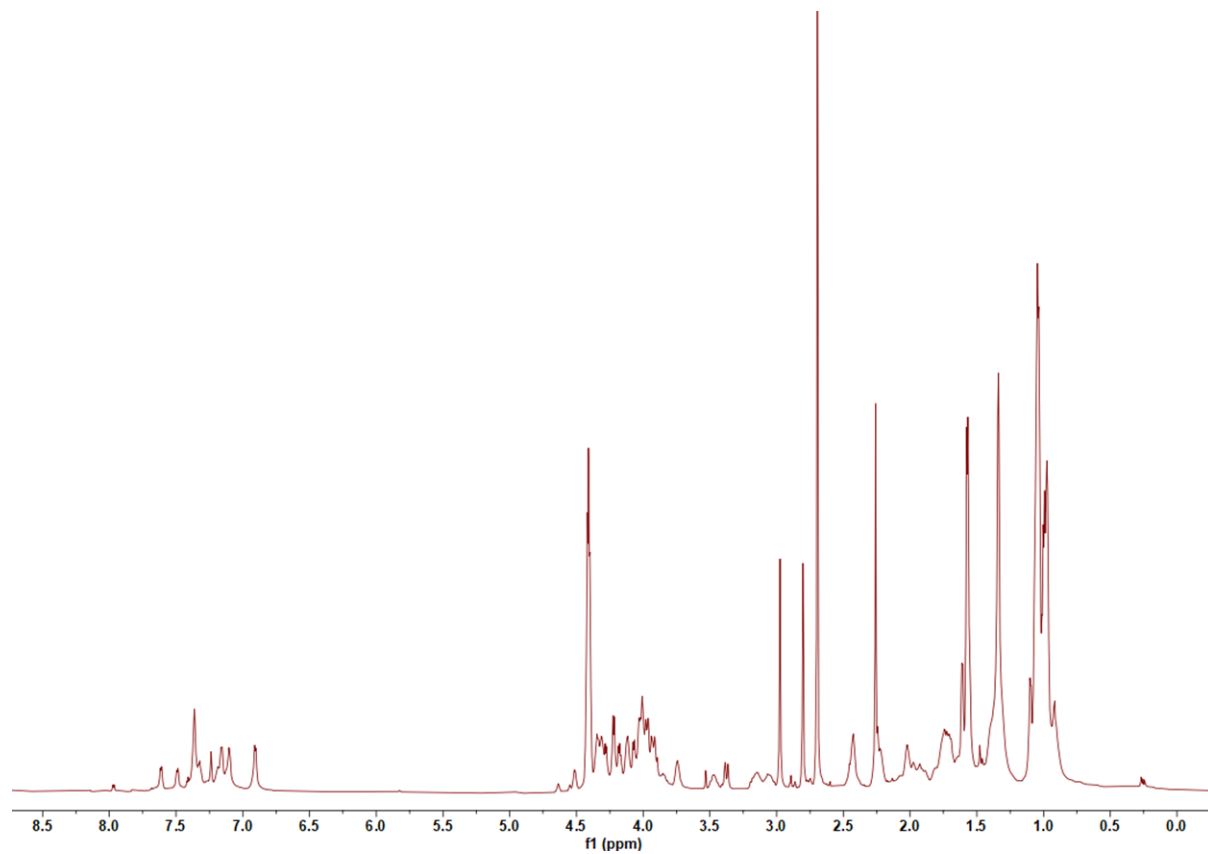


**Supplementary Figure 13: HR-MS/MS analysis of 3.** (a) Broad band high-resolution mass spectrum of compound 3. (b) Summary of collision-induced dissociation (CID) daughter ions for 3. Observed b- and y-ions are annotated. Ions are in the +1 charge state except where indicated. Dmp:  $N_2,N_2$ -dimethyl-1,2-propanediamine. (c) CID spectrum of 3. (d) Table of daughter ion assignments for 3.



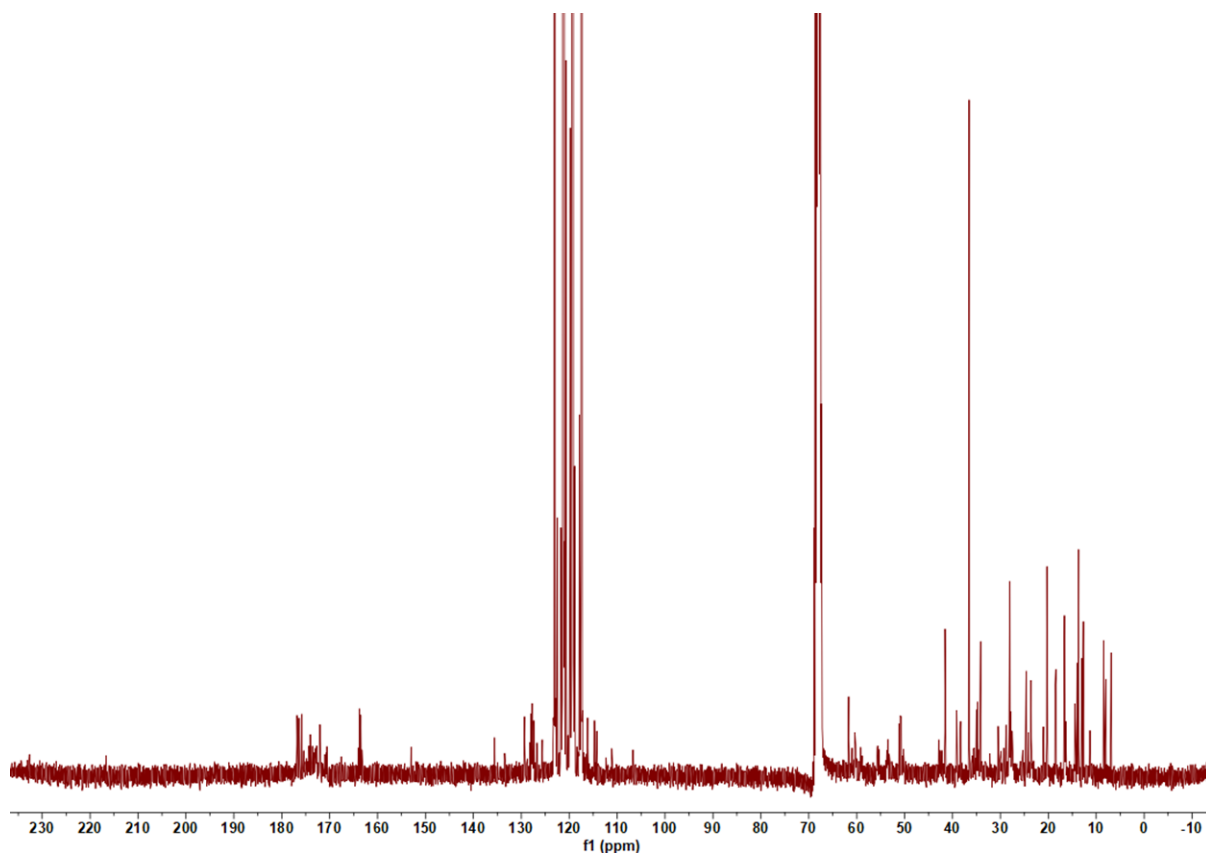
**a**

$^1\text{H}$  NMR, 1,1,1,3,3,3-Hexafluoroisopropanol- $d_2$  (HFIP- $d_2$ ), 750 MHz. The solvent peak appears at 4.41 ppm.



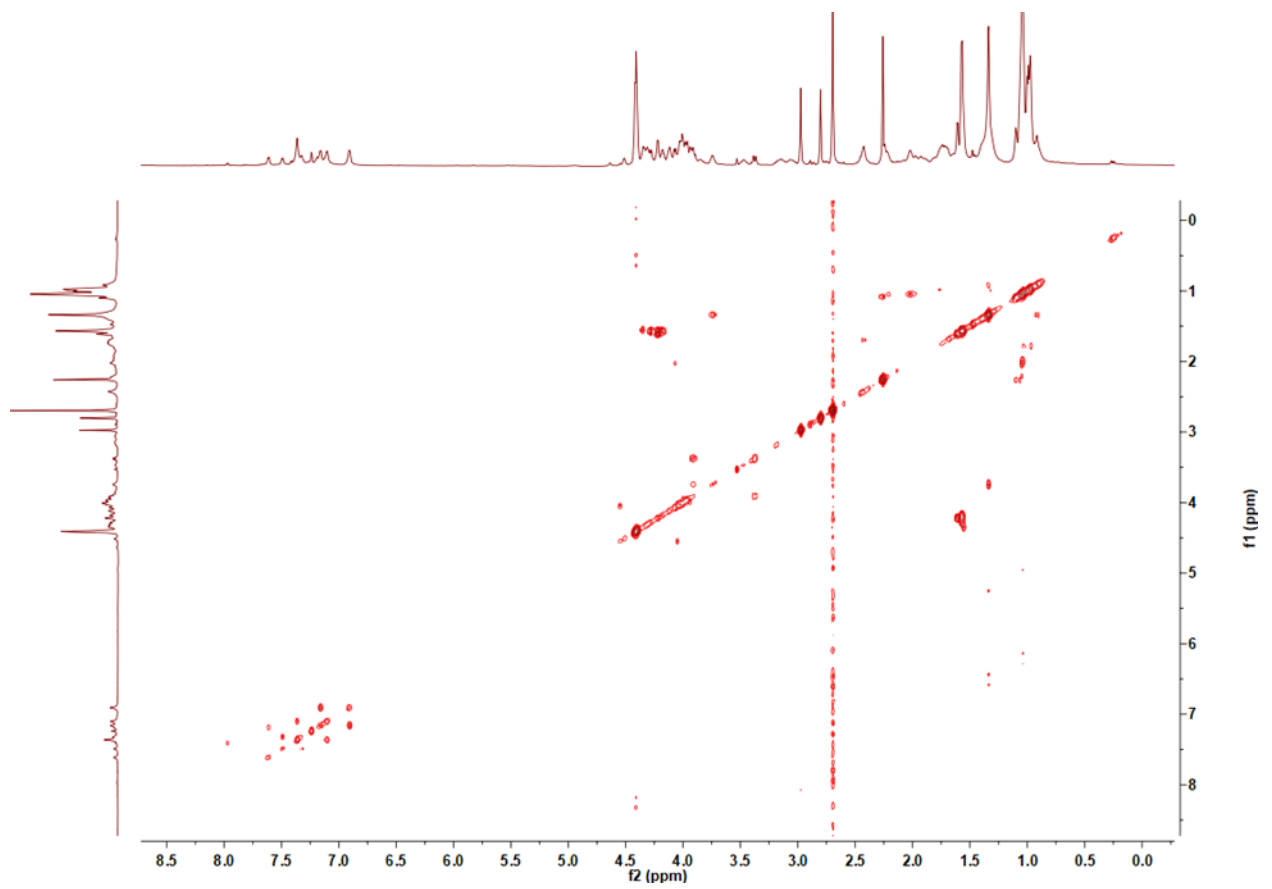
**b**

$^{13}\text{C}$  NMR, 1,1,1,3,3,3-Hexafluoroisopropanol- $d_2$  (HFIP- $d_2$ ), 750 MHz. The solvent peaks appear at 68.1 and 120.7 ppm.



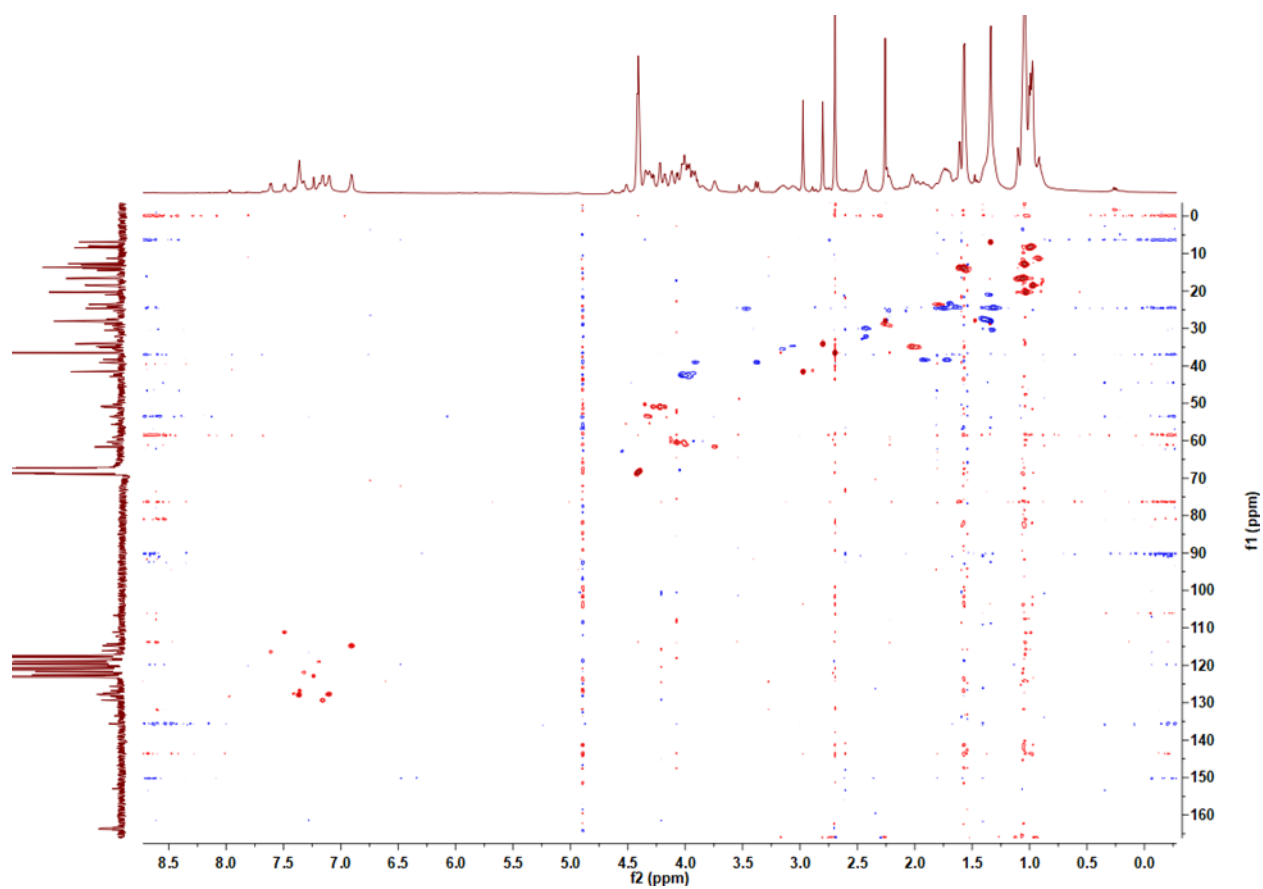
**c**

$^1\text{H}$ - $^1\text{H}$  COSY NMR, 1,1,1,3,3,3-Hexafluoroisopropanol- $d_2$  (HFIP- $d_2$ ), 750 MHz.



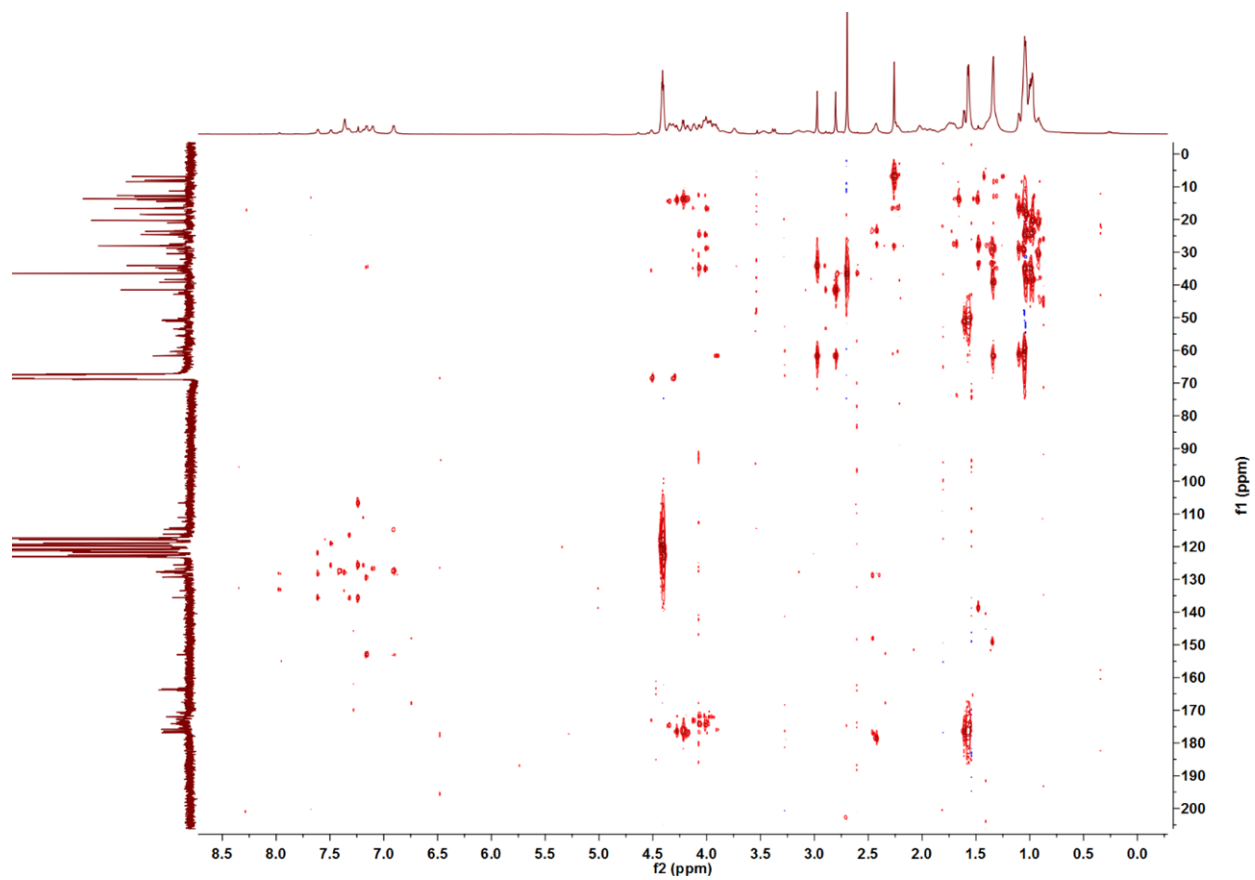
**d**

$^1\text{H}$ - $^{13}\text{C}$  HSQC NMR, 1,1,1,3,3,3-Hexafluoroisopropanol- $d_2$  (HFIP- $d_2$ ), 750 MHz. Multiplicity-edited HSQC was performed. Signals of  $\text{CH}_2$  and  $\text{CH}/\text{CH}_3$  are shown in blue and red, respectively.



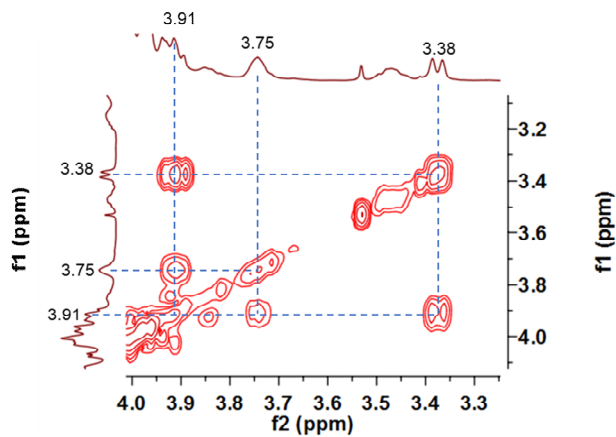
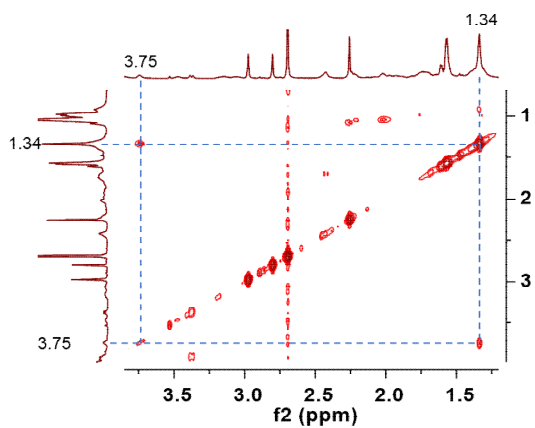
e

$^1\text{H}$ - $^{13}\text{C}$  HMBC NMR, 1,1,1,3,3,3-Hexafluoroisopropanol- $d_2$  (HFIP- $d_2$ ), 750 MHz.



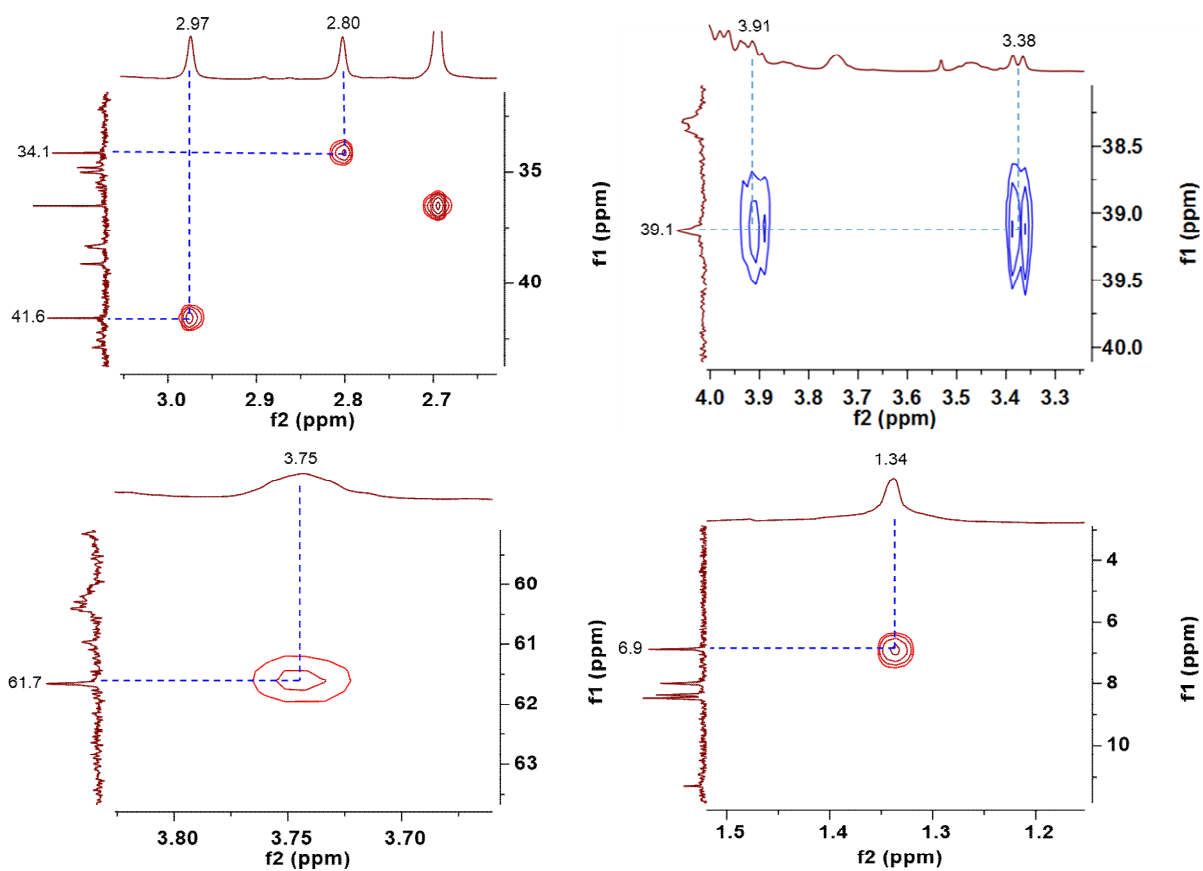
**f**

COSY focusing on the Dmp region. Dmp: *N,N*-dimethyl-1,2-propanediamine.



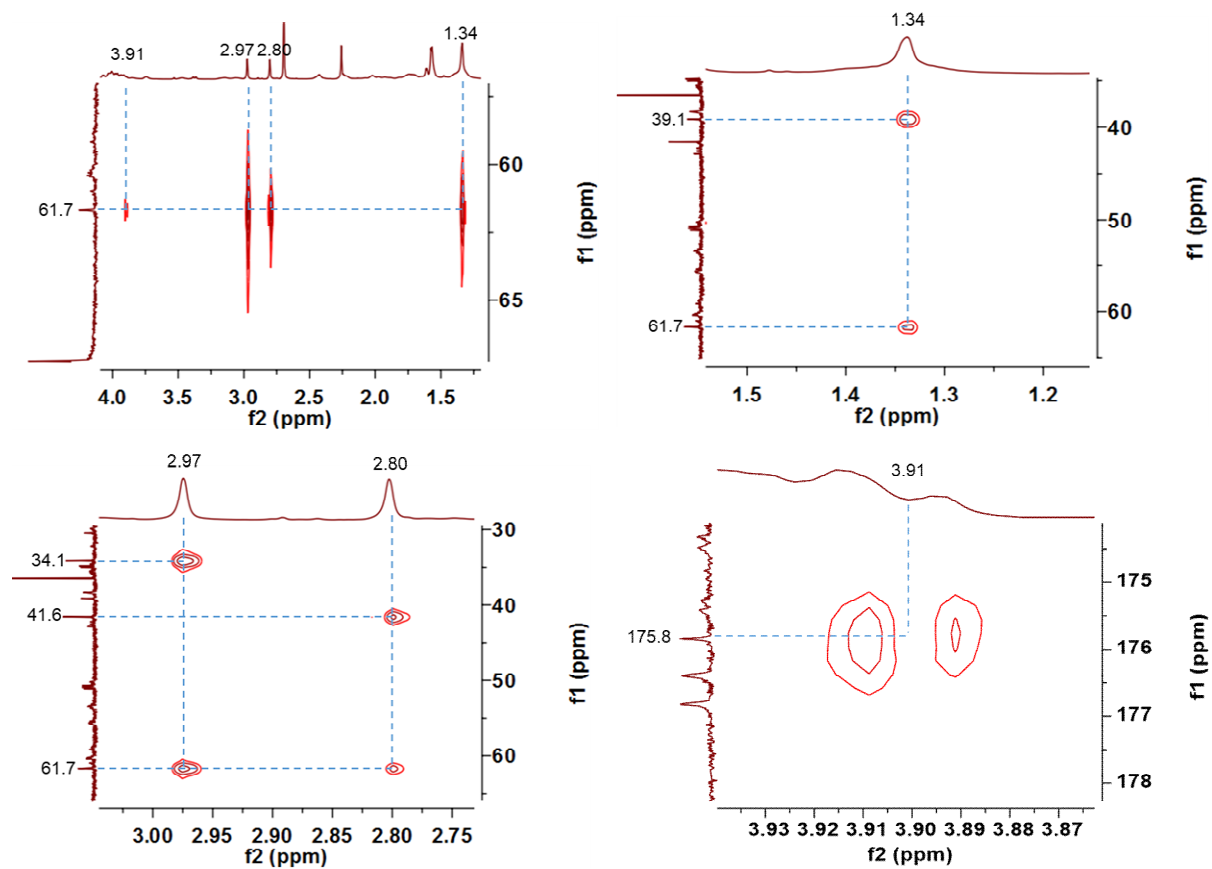
**g**

HSQC focusing on the Dmp region. Multiplicity-edited HSQC was performed. Signals of CH<sub>2</sub> and CH/CH<sub>3</sub> are shown in blue and red, respectively. Dmp: *N*<sub>2</sub>,*N*<sub>2</sub>-dimethyl-1,2-propanediamine.



**h**

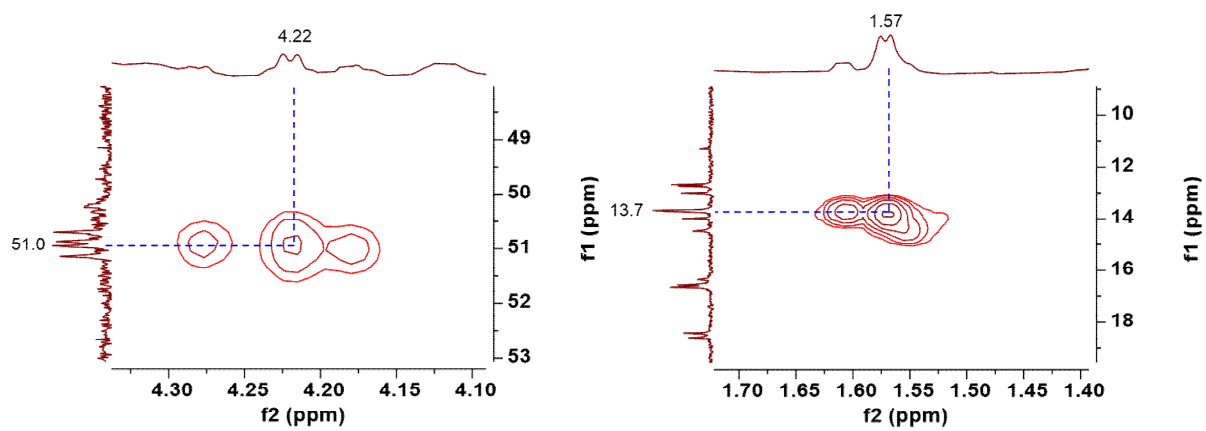
HMBC focusing on the Dmp region. Dmp:  $N_2,N_2$ -dimethyl-1,2-propanediamine.





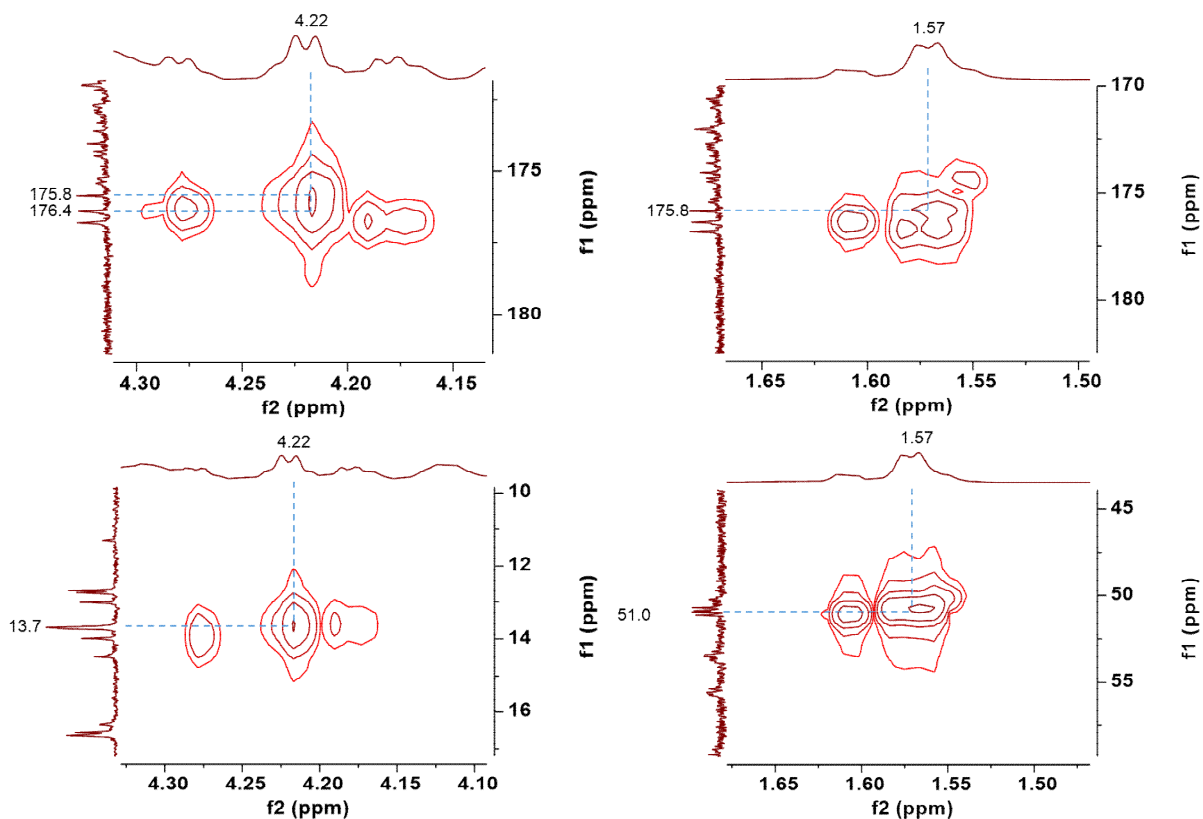
**i**

HSQC focusing on the Ala-23 region. Multiplicity-edited HSQC was performed. Signals of CH<sub>2</sub> and CH/CH<sub>3</sub> are shown in blue and red, respectively.



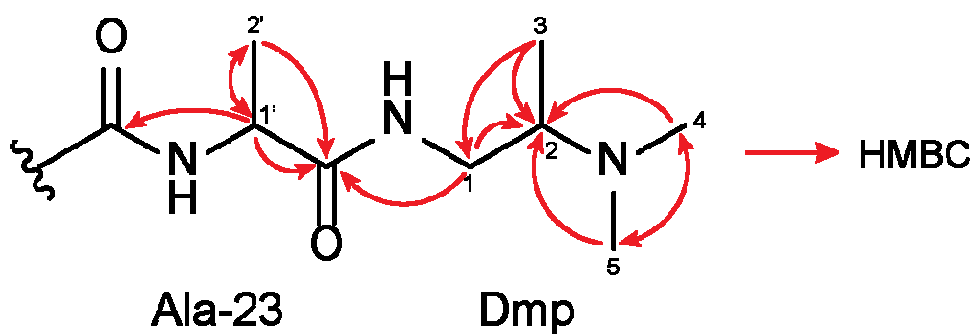
**j**

HMBC focusing on the Ala-23 region.



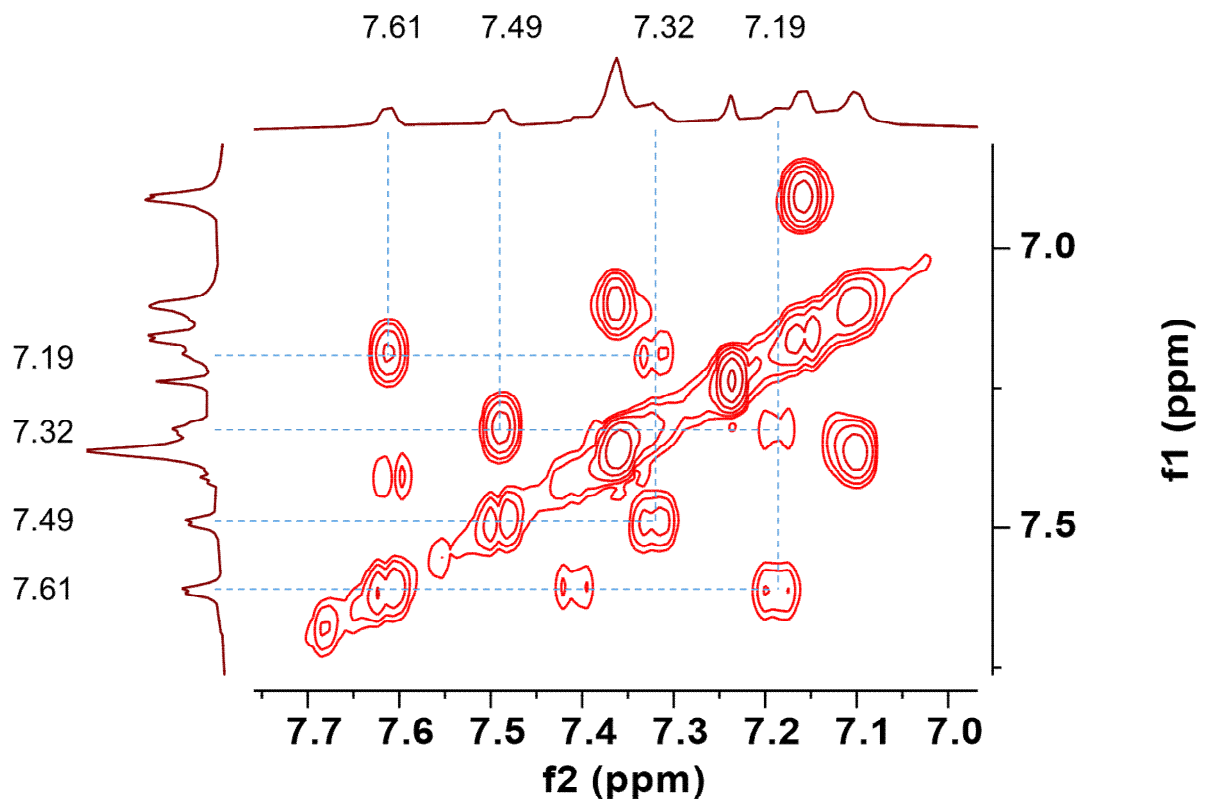
**k**

Summary of HMBC correlations in the Dmp and Ala-23 region. Dmp: *N,N*-dimethyl-1,2-propanediamine.



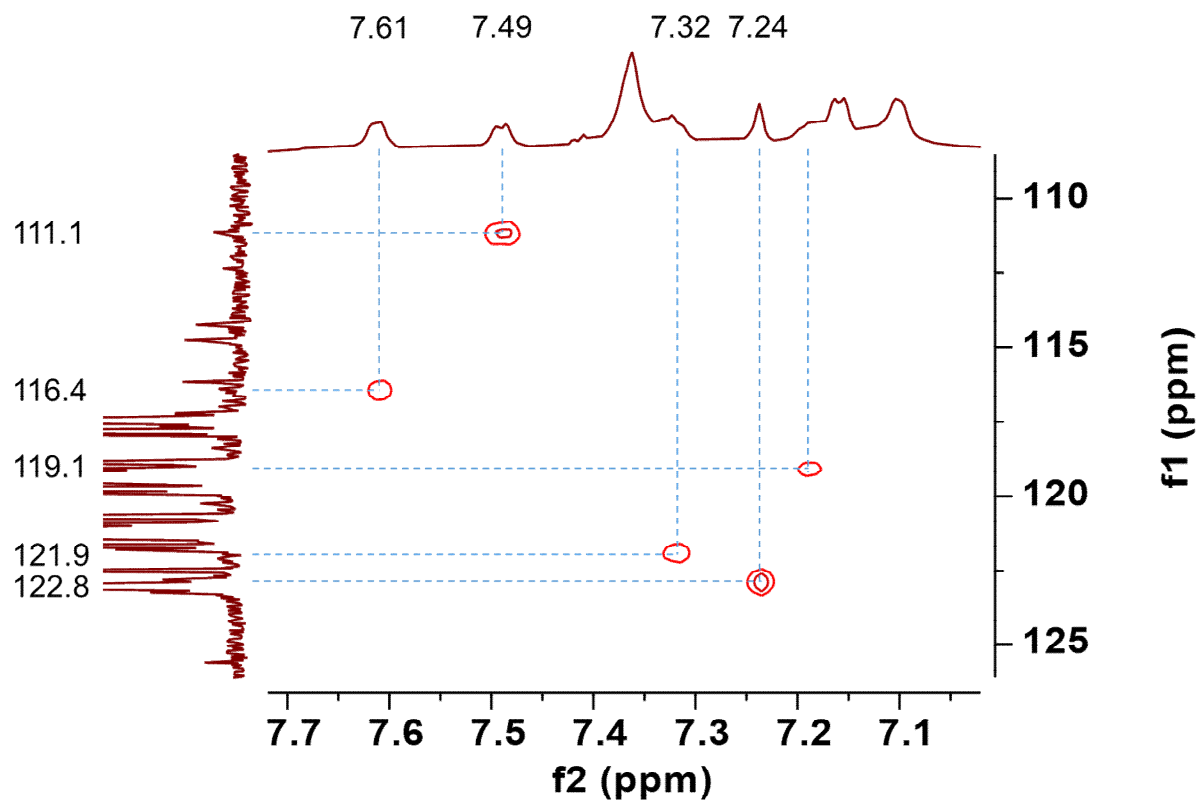
I

COSY focusing on the Trp-2 region



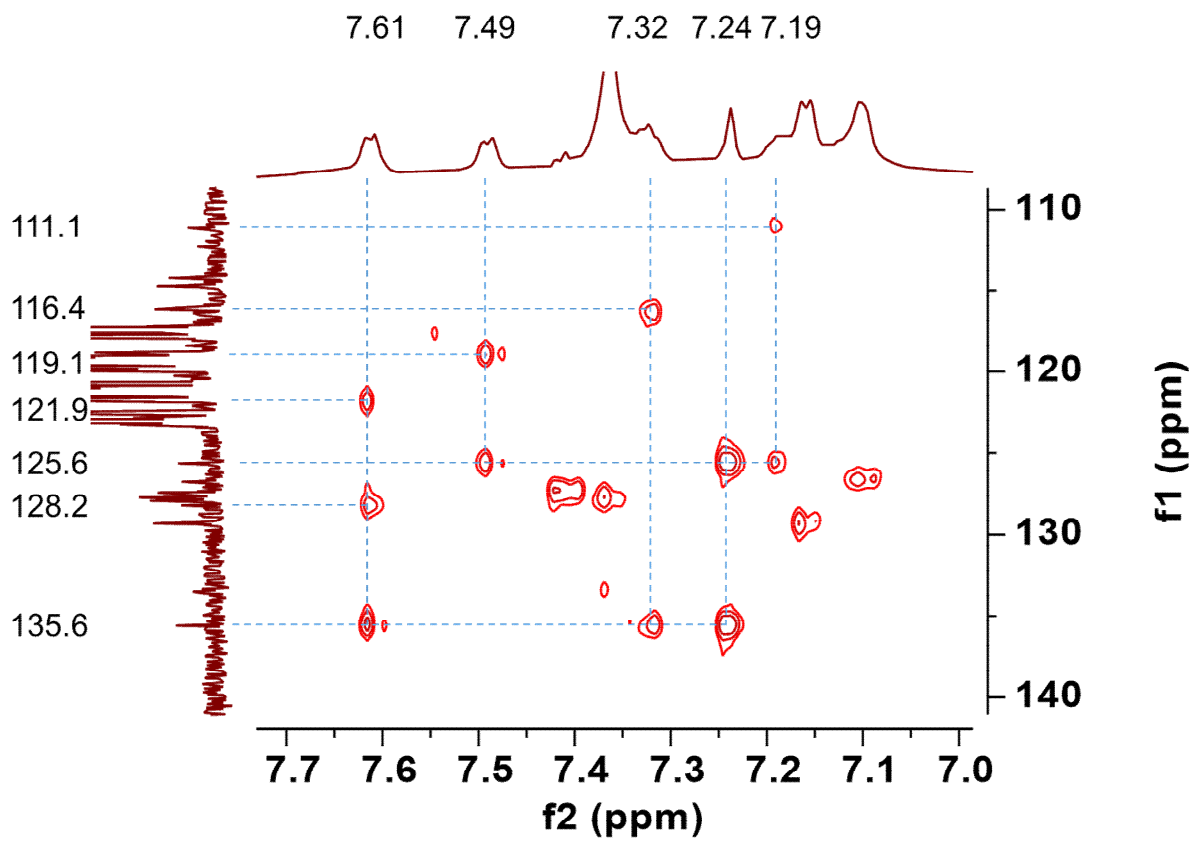
**m**

HSQC focusing on the Trp-2 region. Multiplicity-edited HSQC was performed. Signals of CH<sub>2</sub> and CH/CH<sub>3</sub> are shown in blue and red, respectively.



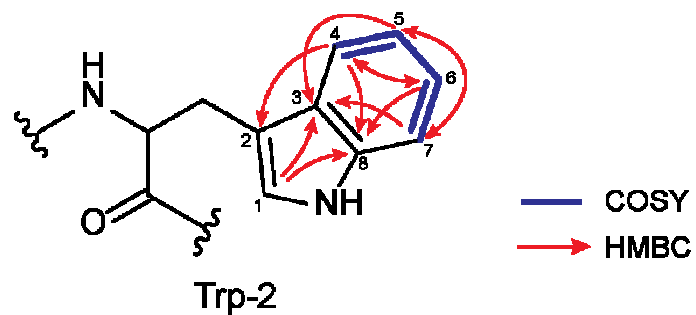
**n**

HMBC focusing on the Trp-2 region.



o

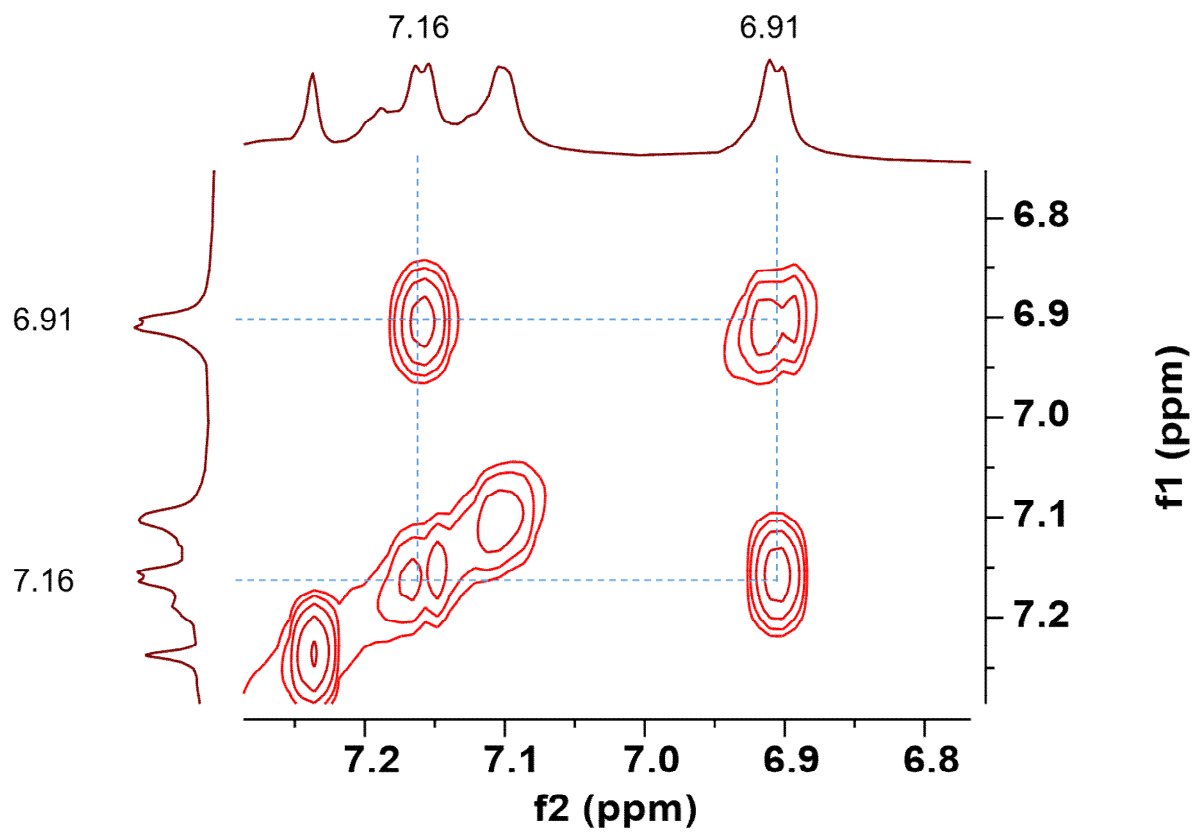
Summary of COSY and HMBC correlations in the Trp-2 region.



No.	1 (daptide)	
	$\delta_C$ type	$\delta_H$ multi
1	122.8 CH	7.24 s
2	128.2 C	
3	125.6 C	
4	116.4 CH	7.61 d (7.1)
5	119.1 CH	7.19 overlapped
6	121.9 CH	7.32 overlapped
7	111.1 CH	7.49 d (7.9)
8	135.6 C	

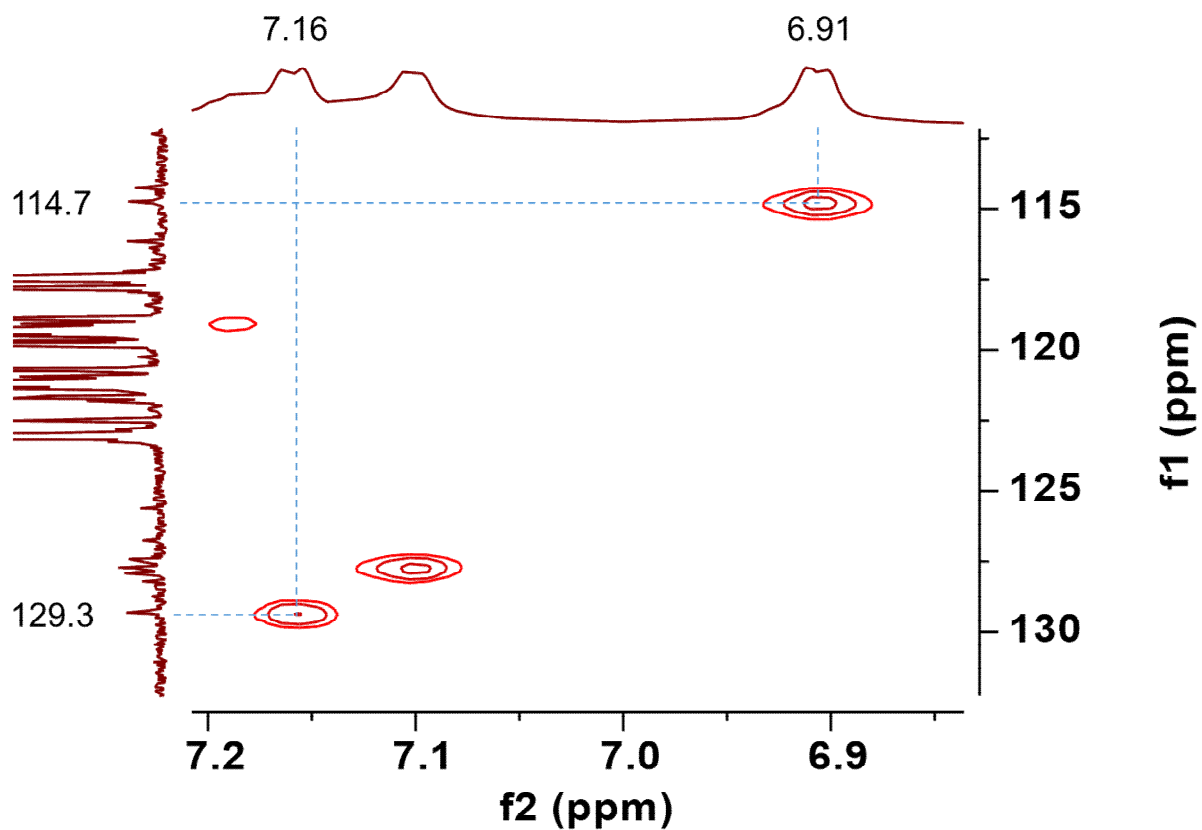
**p**

COSY focusing on the Tyr-6 region



q

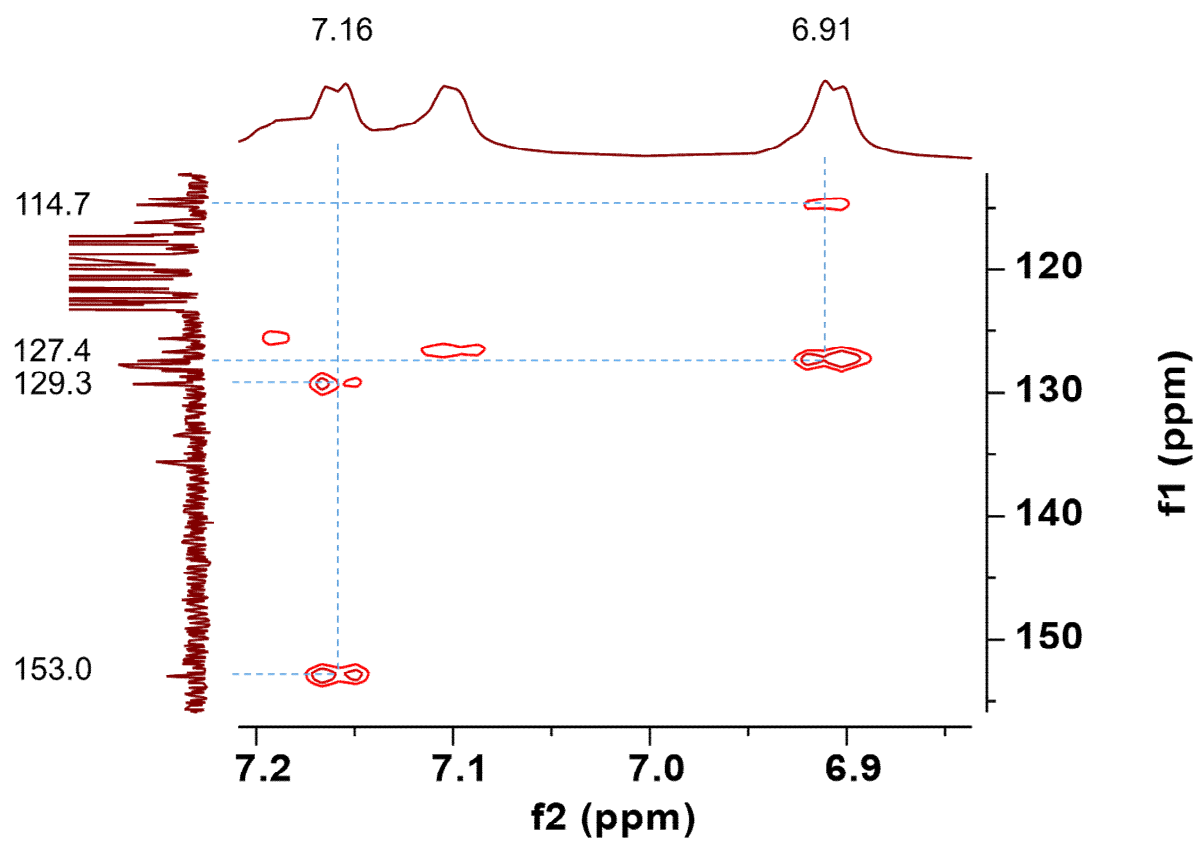
HSQC focusing on the Tyr-6 region. Multiplicity-edited HSQC was performed. Signals of CH<sub>2</sub> and CH/CH<sub>3</sub> are shown in blue and red, respectively.





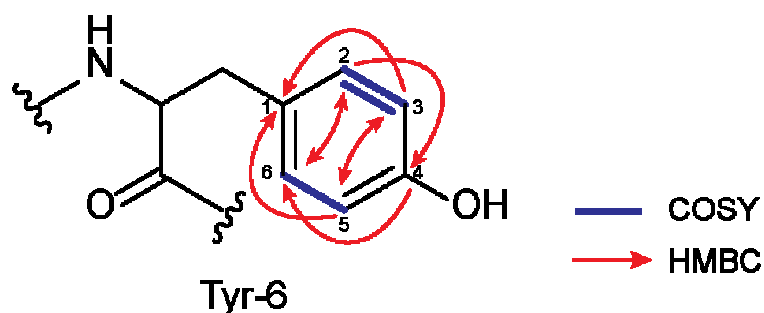
**r**

HMBC focusing on the Tyr-6 region.



**S**

Summary of COSY and HMBC correlations in the Tyr-6 region.

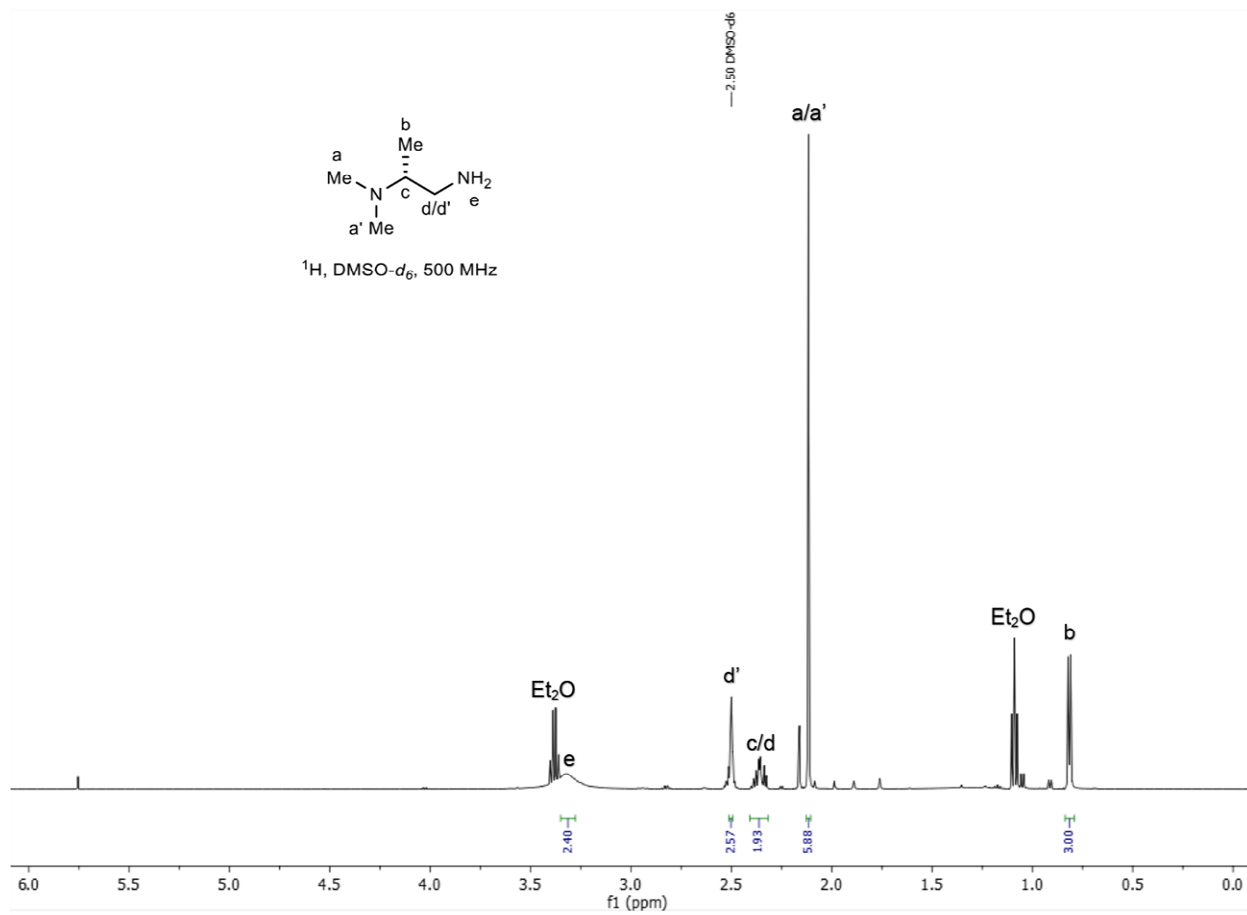


No.	1 (daptide)	
	$\delta$ C type	$\delta$ H multi
1	127.4 C	
2	129.3 CH	7.16 overlapped
3	114.7 CH	6.91 d (7.1)
4	153.0 C	
5	114.7 CH	6.91 d (7.1)
6	129.3 CH	7.16 overlapped

**Supplementary Figure 14: NMR spectra of compound 1 in 1,1,3,3,3-hexafluoroisopropanol-d2 (HFIP-*d*2).** (a)  $^1\text{H}$  NMR. The solvent peak appears at 4.41 ppm. (b)  $^{13}\text{C}$  NMR. The solvent peaks appear at 68.1 and 120.7 ppm. (c)  $^1\text{H}$ - $^1\text{H}$  COSY NMR. (d)  $^1\text{H}$ - $^{13}\text{C}$  HSQC NMR. Multiplicity-edited HSQC was performed. Signals of  $\text{CH}_2$  and  $\text{CH}/\text{CH}_3$  are shown in blue and red, respectively. (e)  $^1\text{H}$ - $^{13}\text{C}$  HMBC NMR. (f) COSY focusing on the Dmp region. Dmp: *N*<sub>2</sub>,*N*<sub>2</sub>-dimethyl-1,2-propanediamine. (g) HSQC focusing on the Dmp region. Multiplicity-edited HSQC was performed. Signals of  $\text{CH}_2$  and  $\text{CH}/\text{CH}_3$  are shown in blue and red, respectively. (h) HMBC focusing on the Dmp region. (i) HSQC focusing on the Ala-20 region. Multiplicity-edited HSQC was performed. Signals of  $\text{CH}_2$  and  $\text{CH}/\text{CH}_3$  are shown in blue and red, respectively. (j) HMBC focusing on the Ala-20 region. (k) Summary of HMBC correlations in the Dmp and Ala-20 region. Dmp: *N*<sub>2</sub>,*N*<sub>2</sub>-dimethyl-1,2-propanediamine. (l) COSY focusing on the Trp-2 region. (m) HSQC focusing on the Trp-2 region. Multiplicity-edited HSQC was performed. Signals of  $\text{CH}_2$  and  $\text{CH}/\text{CH}_3$  are shown in blue and red, respectively. (n) HMBC focusing on the Trp-2 region. (o) Summary of COSY and HMBC correlations in the Trp-2 region. (p) COSY focusing on the Tyr-6 region (q) HSQC focusing on the Tyr-6 region. Multiplicity-edited HSQC was performed. Signals of  $\text{CH}_2$  and  $\text{CH}/\text{CH}_3$  are shown in blue and red, respectively. (r) HMBC focusing on the Tyr-6 region. (s) Summary of COSY and HMBC correlations in the Tyr-6 region.

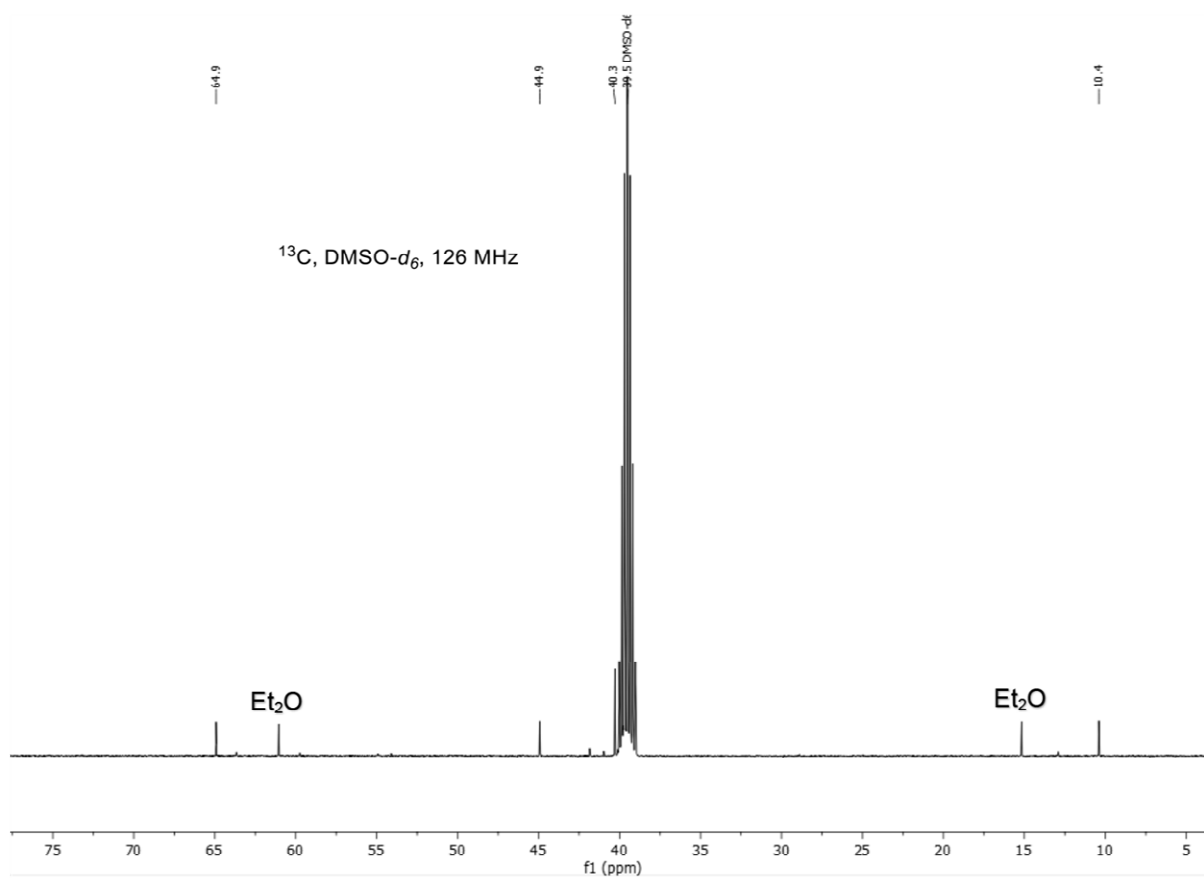
**a**

(*R*)-Dmp  $^1\text{H}$  NMR,  $\text{DMSO-}d_6$ , 500 MHz.



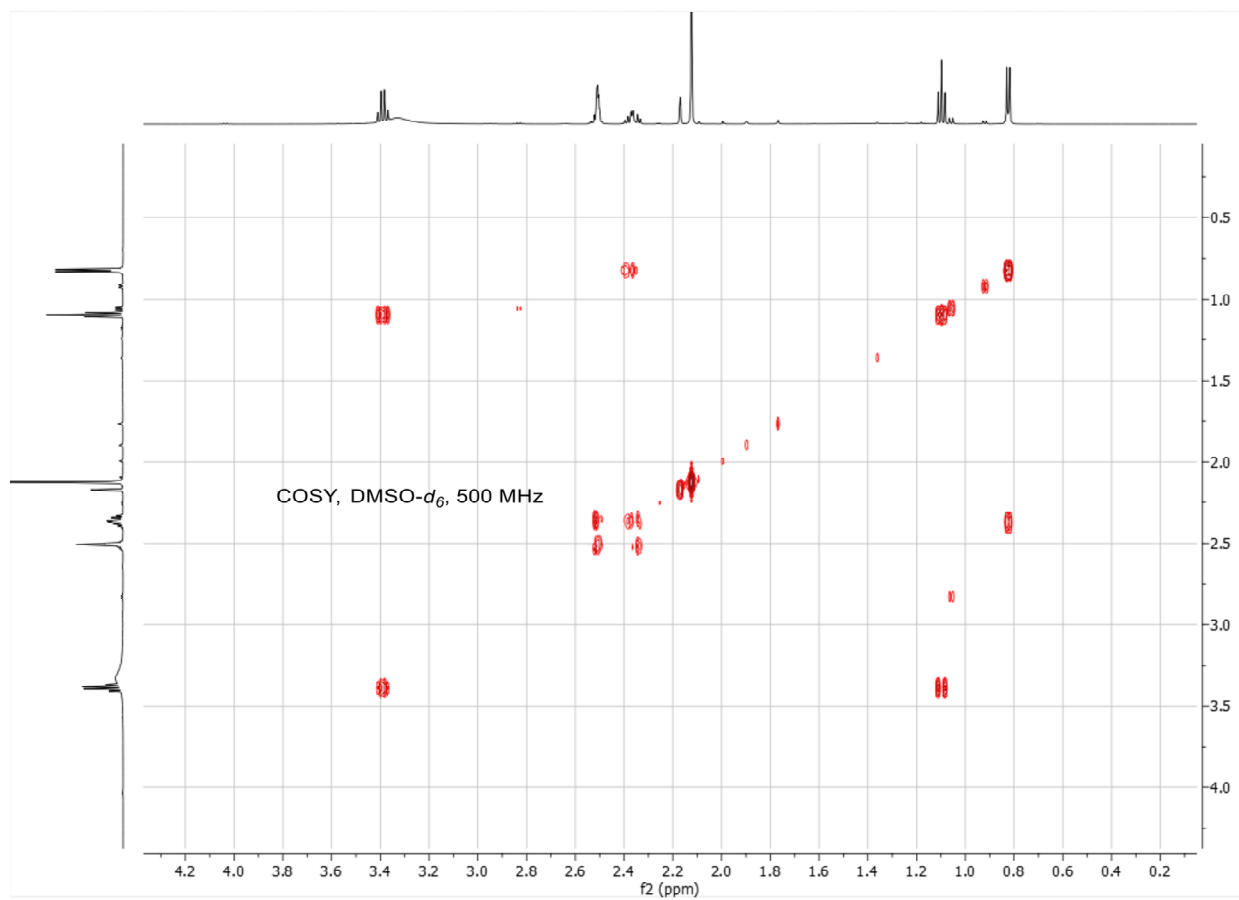
**b**

(*R*)-Dmp  $^{13}\text{C}$  NMR,  $\text{DMSO-}d_6$ , 126 MHz.



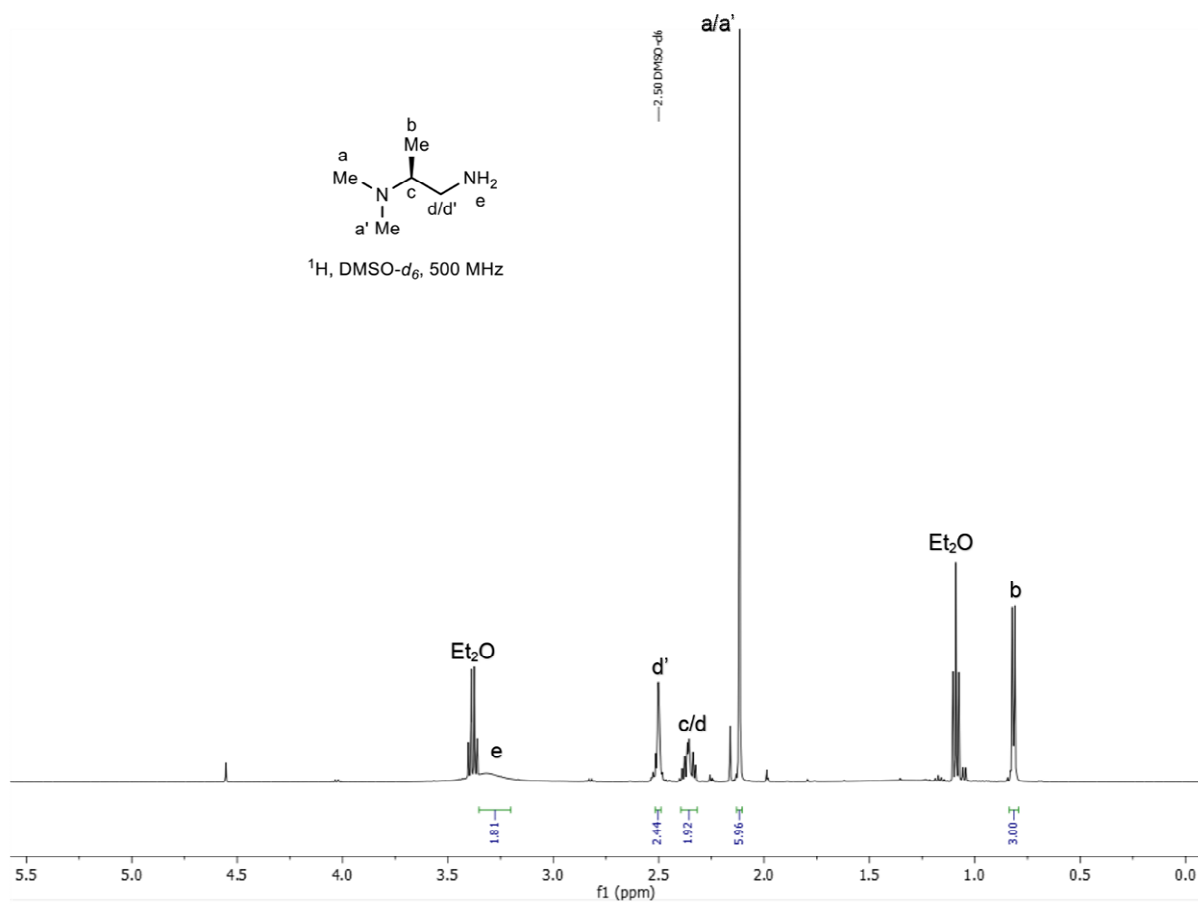
**c**

(*R*)-Dmp  $^1\text{H}$ - $^1\text{H}$  COSY NMR, DMSO- $d_6$ , 500 MHz.



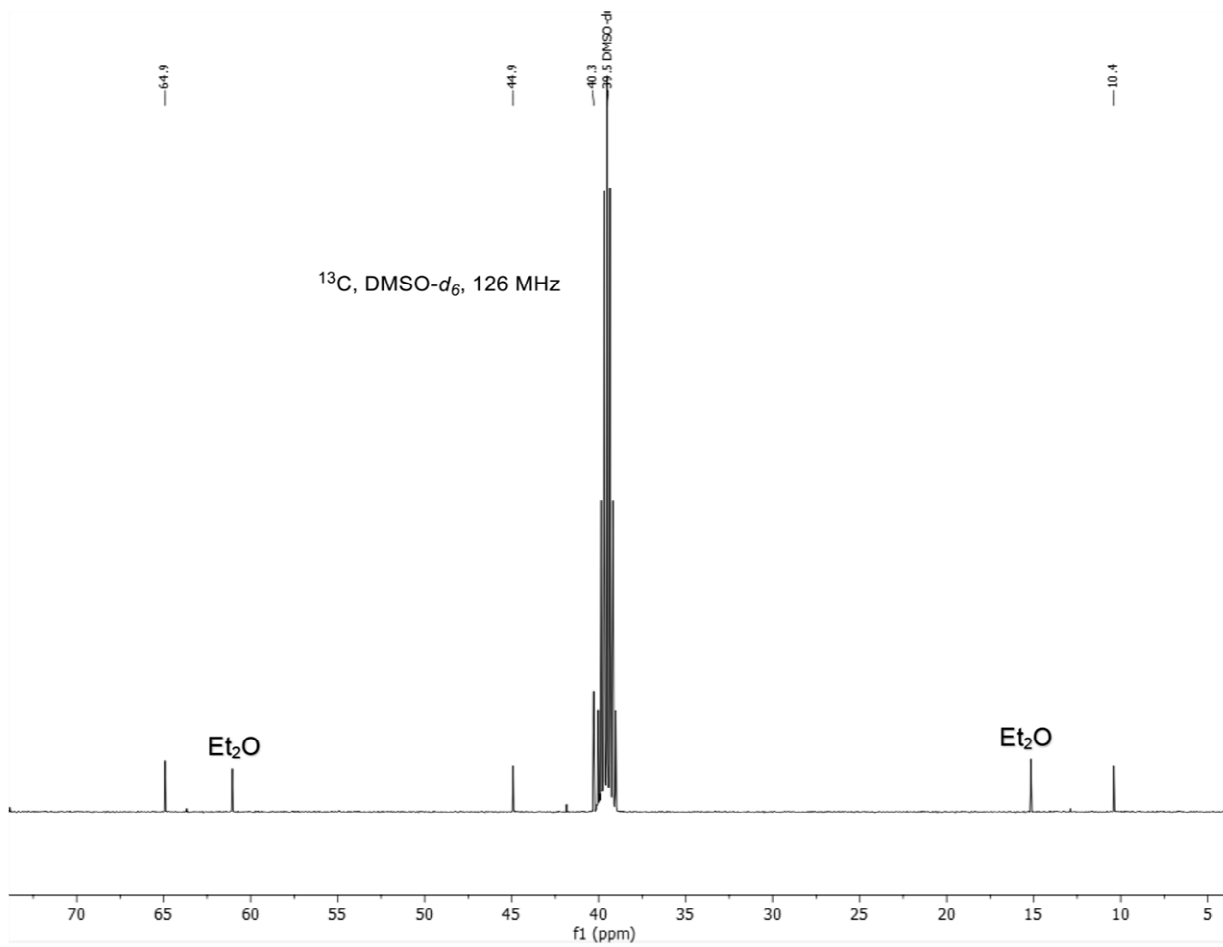
**d**

(*S*)-Dmp  $^1\text{H}$  NMR,  $\text{DMSO-}d_6$ , 500 MHz.



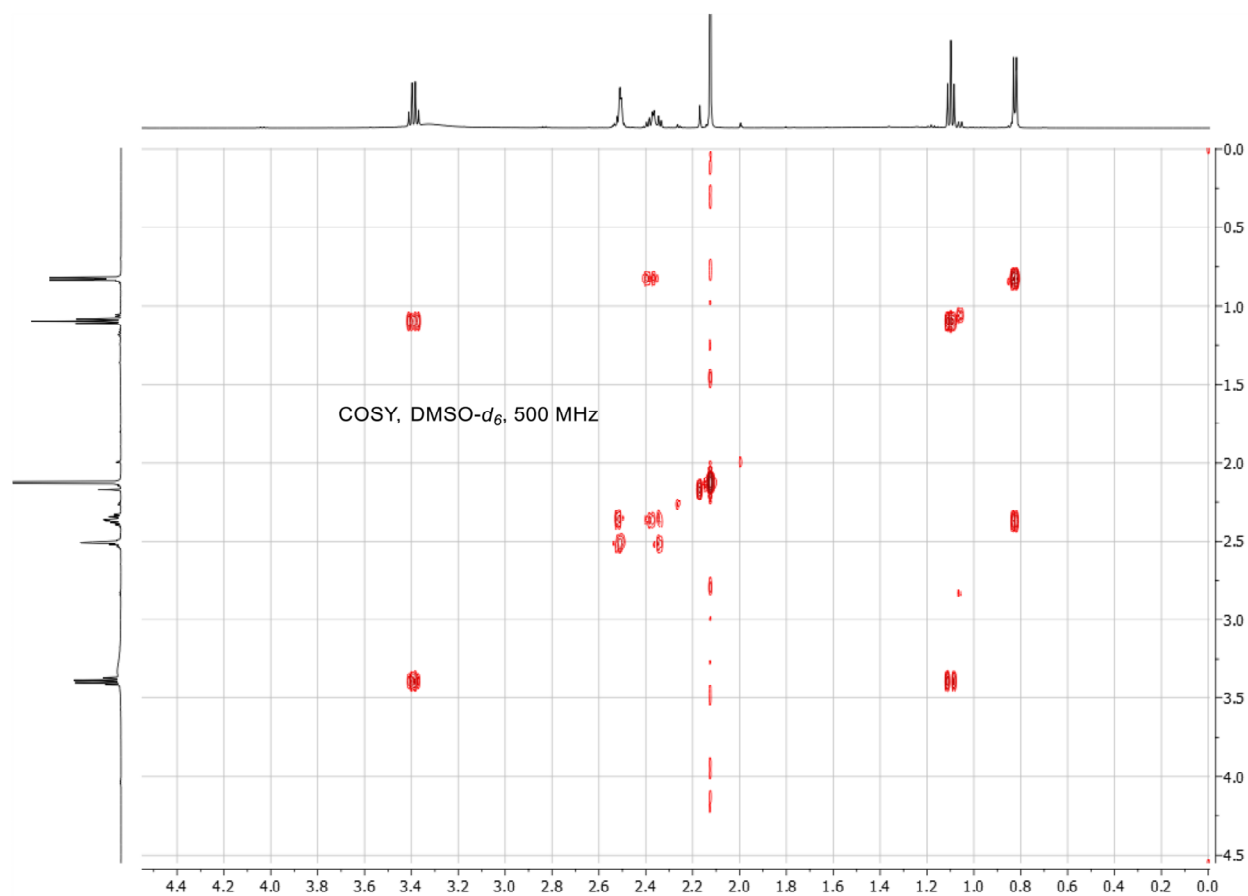
**e**

(*S*)-Dmp  $^{13}\text{C}$  NMR, DMSO- $d_6$ , 126 MHz.



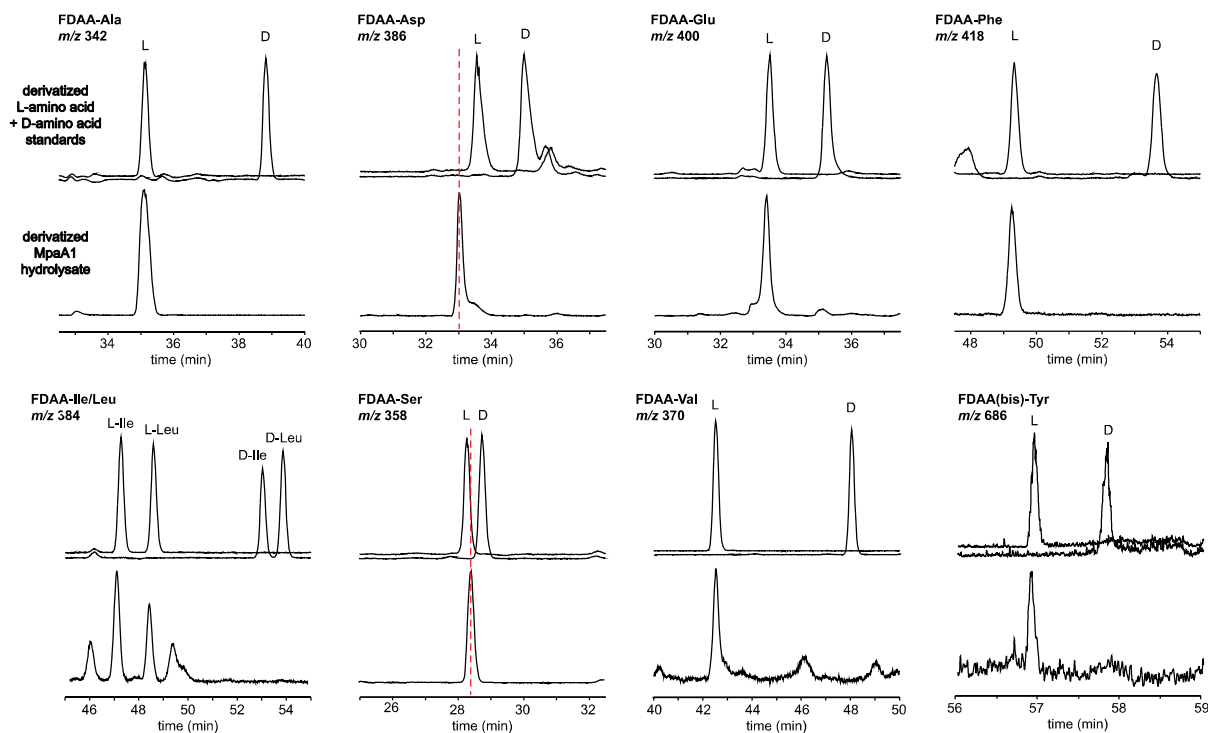
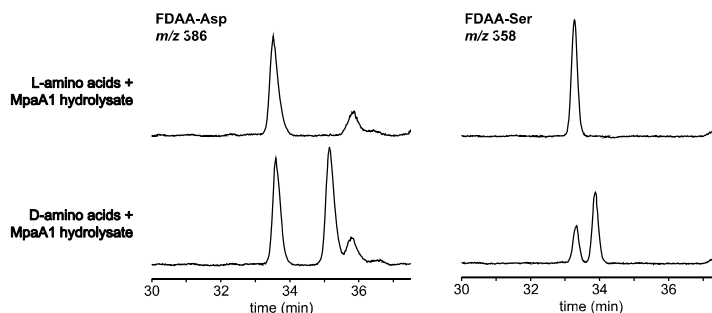
**f**

(*S*)-Dmp  $^1\text{H}$ - $^1\text{H}$  COSY NMR, DMSO- $d_6$ , 500 MHz.

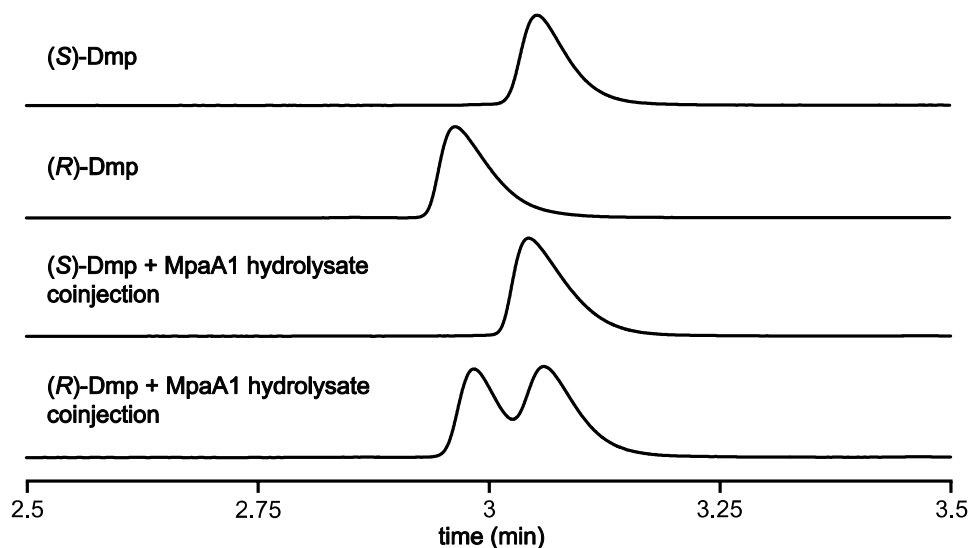


**Supplementary Figure 15: NMR spectra of authentic (*R*)-Dmp and (*S*)-Dmp standards.** Dmp:  $N_2,N_2$ -dimethyl-1,2-propanediamine. (a) (*R*)-Dmp  $^1\text{H}$  NMR, DMSO- $d_6$ , 500 MHz. (b) (*R*)-Dmp  $^{13}\text{C}$  NMR, DMSO- $d_6$ , 126 MHz. (c) (*R*)-Dmp  $^1\text{H}$ - $^1\text{H}$  COSY NMR, DMSO- $d_6$ , 500 MHz. (d) (*S*)-Dmp  $^1\text{H}$  NMR, DMSO- $d_6$ , 500 MHz. (e) (*S*)-Dmp  $^{13}\text{C}$  NMR, DMSO- $d_6$ , 126 MHz. (f) (*S*)-Dmp  $^1\text{H}$ - $^1\text{H}$  COSY NMR, DMSO- $d_6$ , 500 MHz.

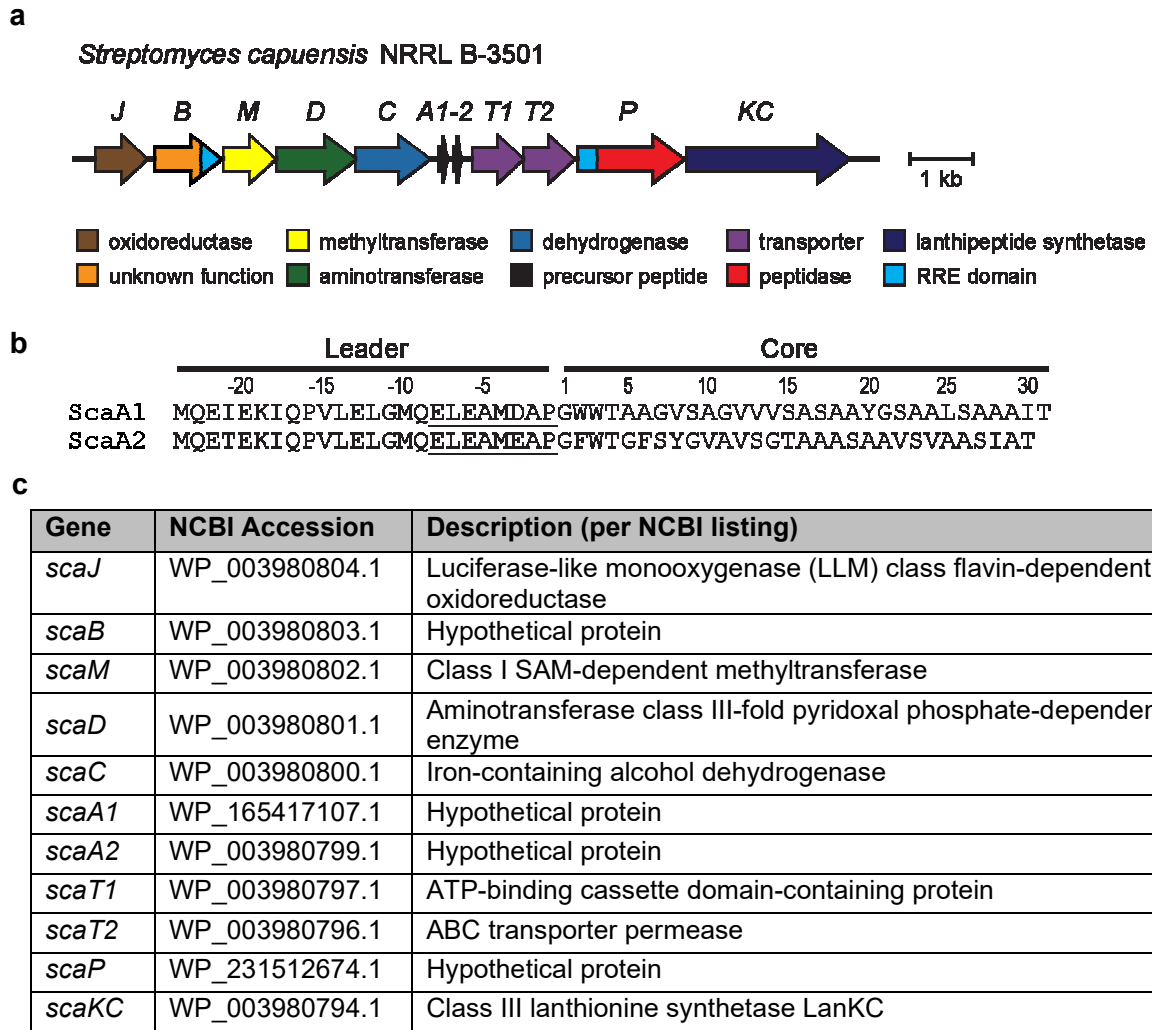


**a****b****Supplementary Figure 16: Determination of MpaA1 amino acid stereochemistry using LC-MS.**

(a) Ion count-normalized LC-MS chromatograms are shown for derivatized amino acid standards and for 1-fluoro-2-4-dinitrophenyl-5-alanine amide (FDAA)-derivatized hydrolysate of **1**. L- and D-amino acid standards were run individually. FDAA-Trp adducts were not observed<sup>12</sup>. FDAA-Glu was monitored instead of FDAA-Gln due to the hydrolysis of MpaA1. Assignment of Asp and Ser was initially ambiguous owing to retention time drift. (b) LC-MS chromatograms for co-injections of derivatized amino acid standards with derivatized MpaA1 hydrolysate.

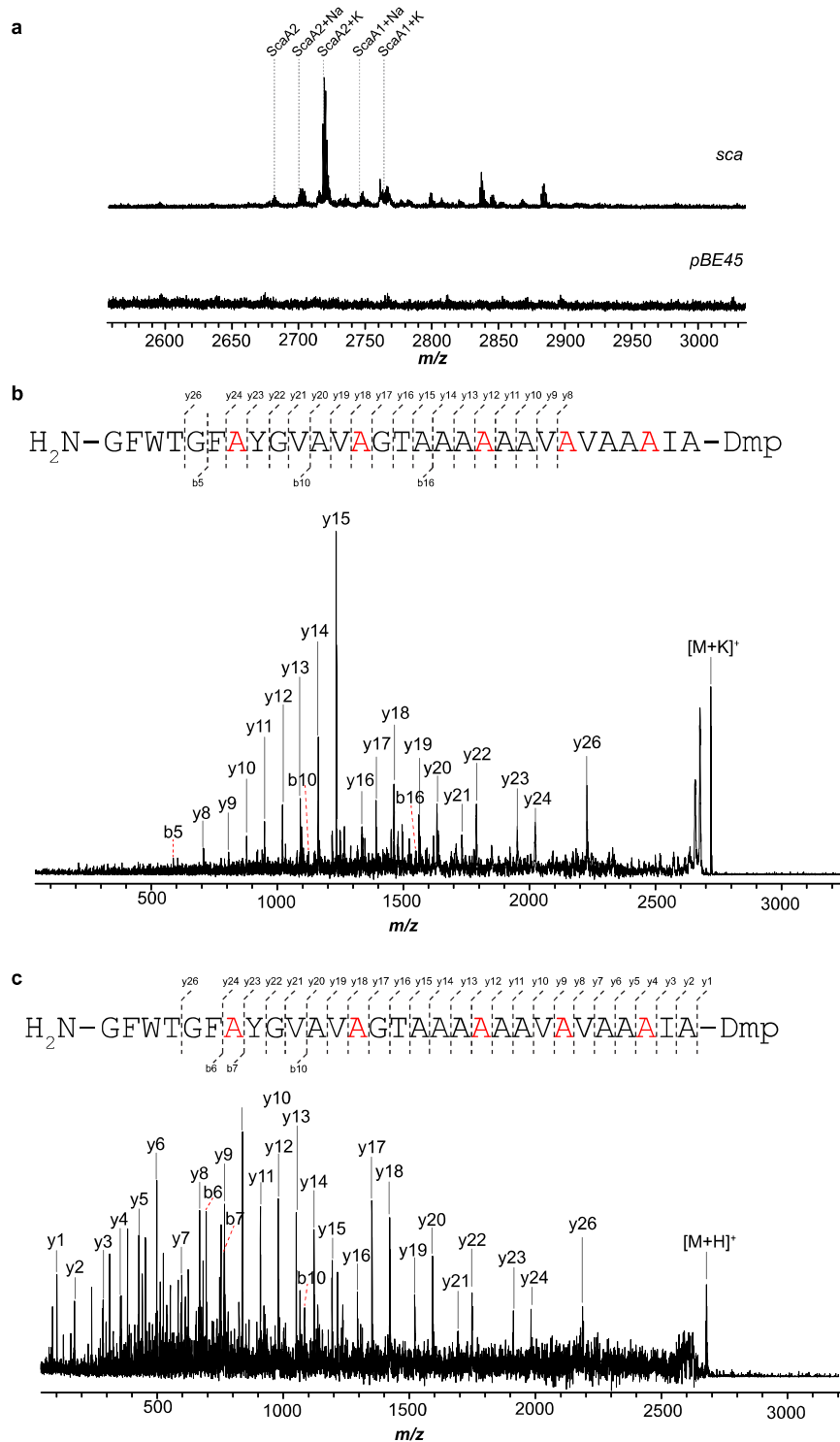


**Supplementary Figure 17: Determination of MpaA1 Dmp stereochemistry.** Absorbance-normalized chromatograms are shown for single injections of FDAA-derivatized (*R*)-Dmp and (*S*)-Dmp, along with co-injections of derivatized hydrolysate of **1**. Absorbance was monitored at 340 nm. Dmp: *N*<sub>2</sub>,*N*<sub>2</sub>-dimethyl-1,2-propanediamine.

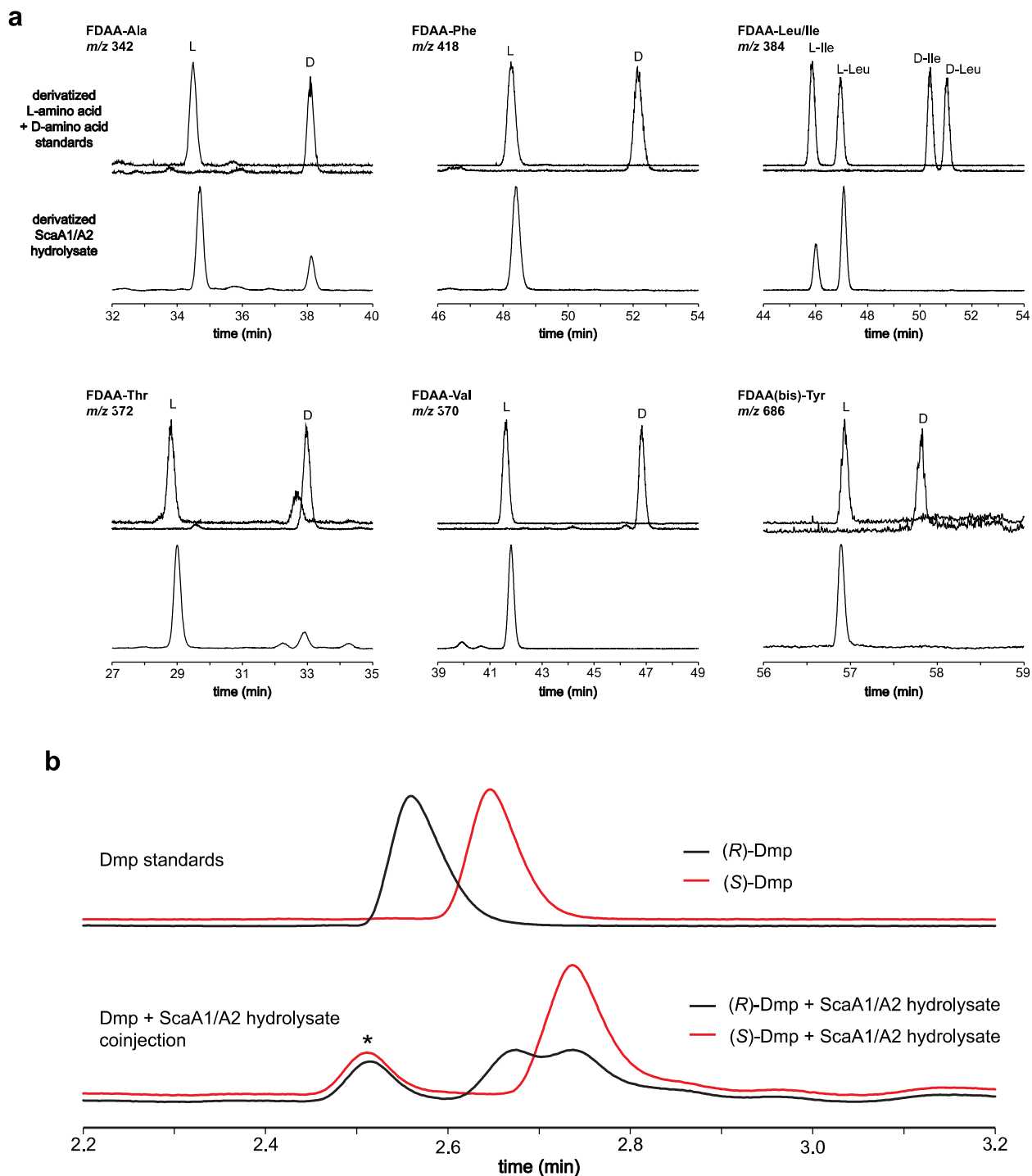


**Supplementary Figure 18: The *sca* BGC identified from *Streptomyces capuensis* NRRL B-3501.**

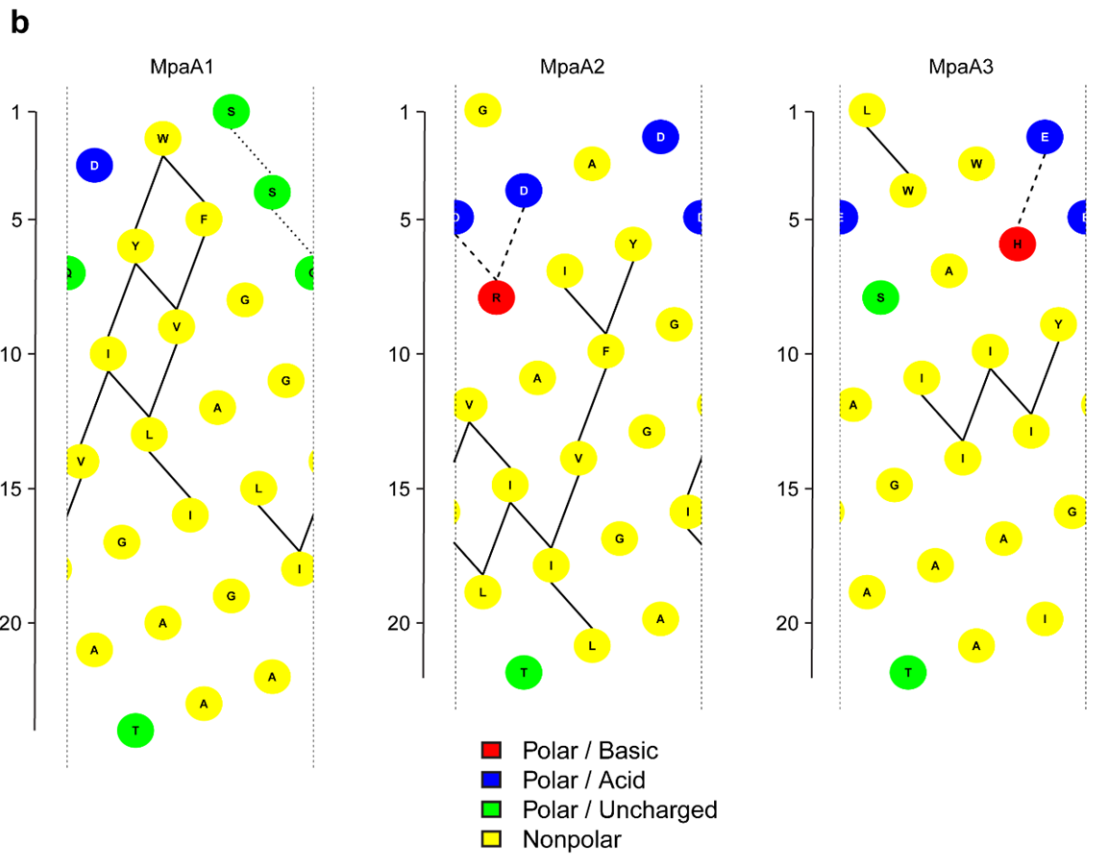
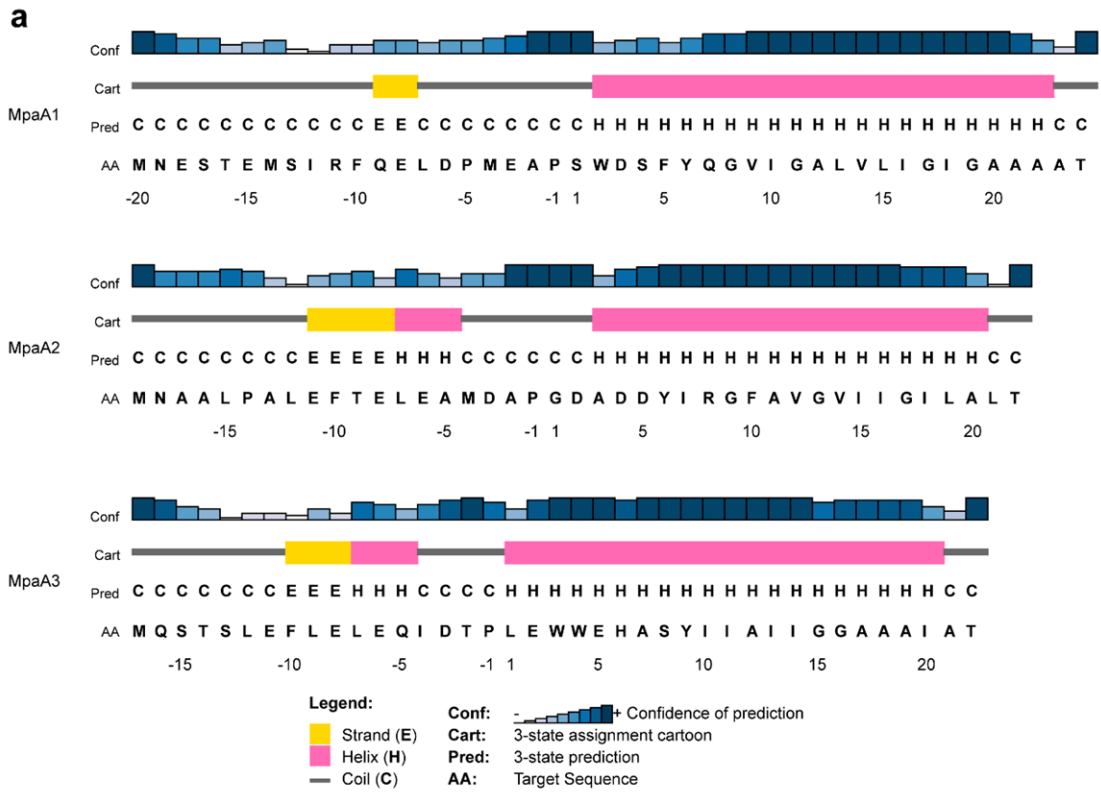
(a) Organization of the *sca* BGC. (b) Precursor peptide sequences. (c) Functional annotation and accession numbers of genes in the *sca* BGC

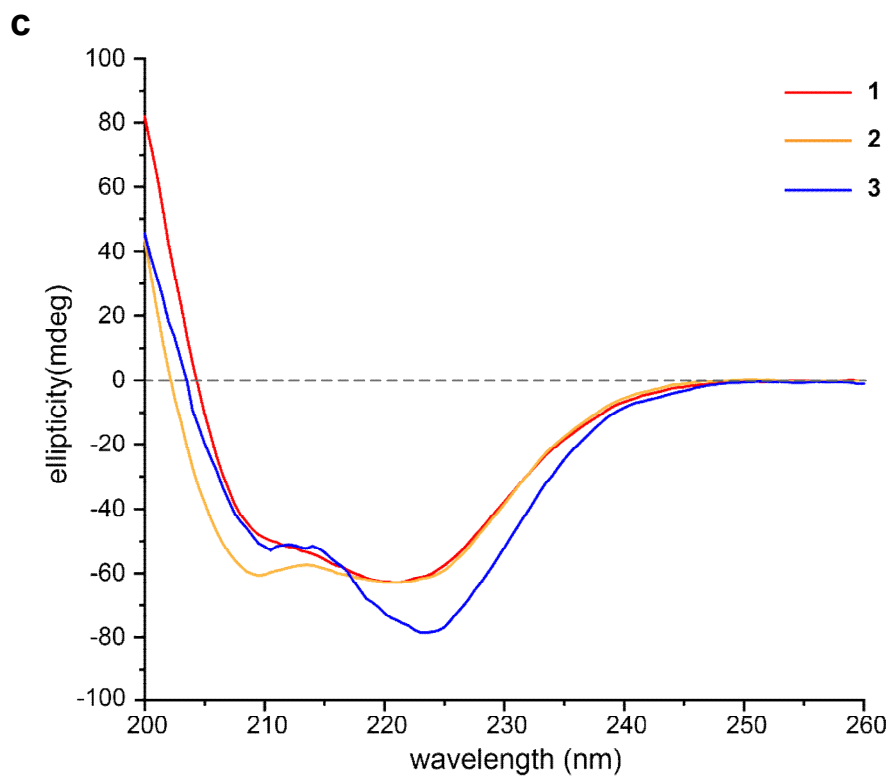


**Supplementary Figure 19: Heterologous expression and product characterization of *sca*.** (a) MALDI-TOF mass spectra of the methanol extracts of *S. albus* J1074 containing *sca* and the pBE45 empty vector. Sodium and potassium ions are denoted as '+Na' and '+K'. (b) MALDI LIFT-TOF/TOF mass spectrum of the modified ScaA2 core peptide acquired by the potassium adduct. Observed b- and y-ions are annotated. Ions are in the +1 charge state. Suspected sites of conversion to *D*-Ala are colored in red. Dmp: *N*<sub>2</sub>,*N*<sub>2</sub>-dimethyl-1,2-propanediamine. (c) MALDI LIFT-TOF/TOF mass spectrum of the modified ScaA2 core peptide acquired using the [M+H]<sup>+</sup> ion. Observed b- and y-ions are annotated. Ions are in the +1 charge state. Suspected sites of conversion to *D*-Ala are colored in red. Dmp: *N*<sub>2</sub>,*N*<sub>2</sub>-dimethyl-1,2-propanediamine.

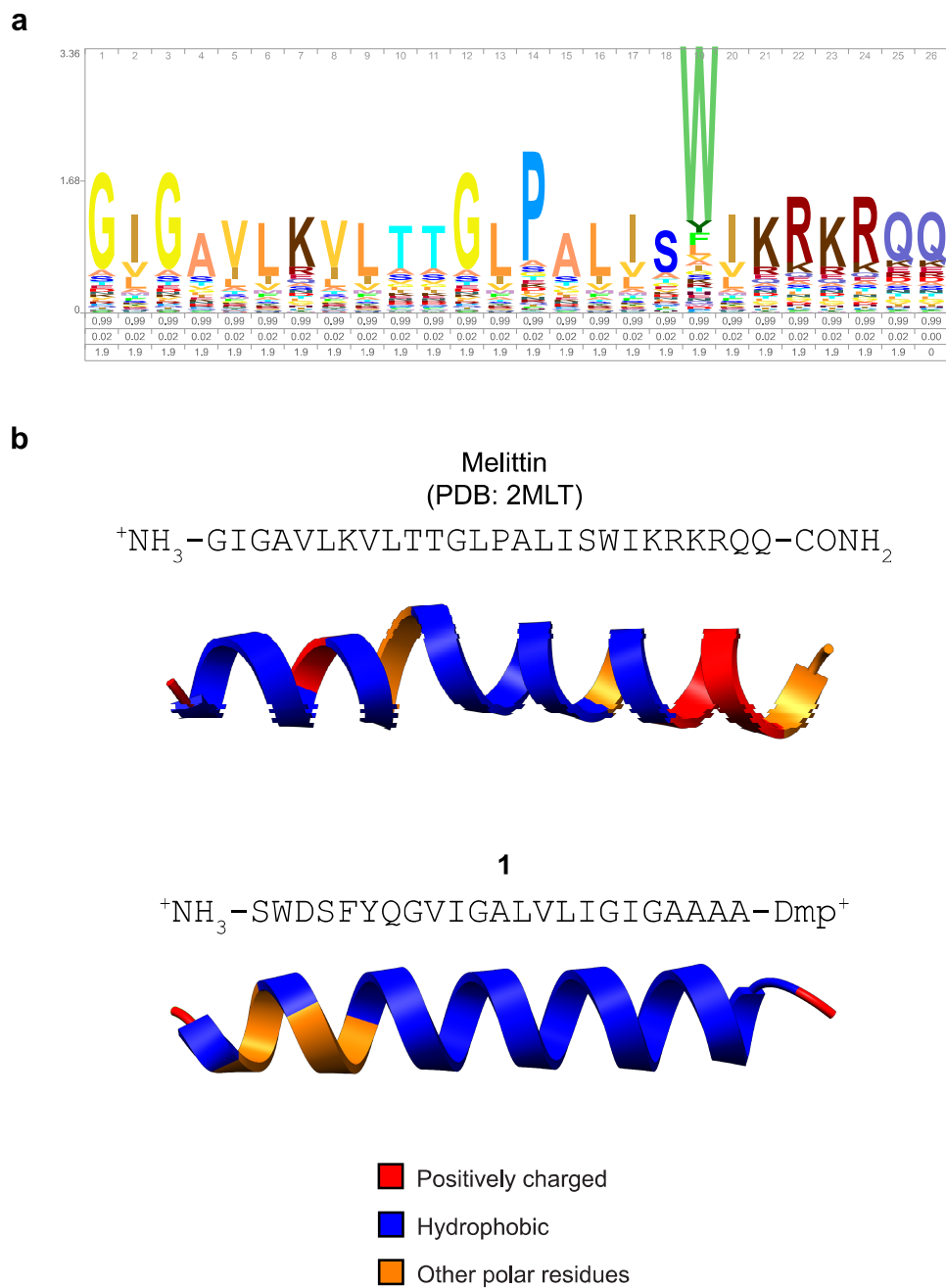


**Supplementary Figure 20: Determination of ScaA1/A2 residue stereochemistry.** (a) Ion count-normalized LC-MS chromatograms are shown for derivatized amino acid standards and for 1-fluoro-2-4-dinitrophenyl-5-alanine amide (FDAA)-derivatized hydrolysate of ScaA1/A2. L- and D-amino acid standards were run individually. FDAA-Trp adducts were not observed<sup>12</sup>. (b) Absorbance-normalized chromatograms are shown for single injections of FDAA-derivatized (*R*)-Dmp and (*S*)-Dmp, along with co-injections of derivatized hydrolysate of ScaA1/A2. Absorbance was monitored at 340 nm. Asterisk indicates possible FDAA adduct to unidentified hydrolysis product. Dmp: *N*<sub>2</sub>,*N*<sub>2</sub>-dimethyl-1,2-propanediamine.



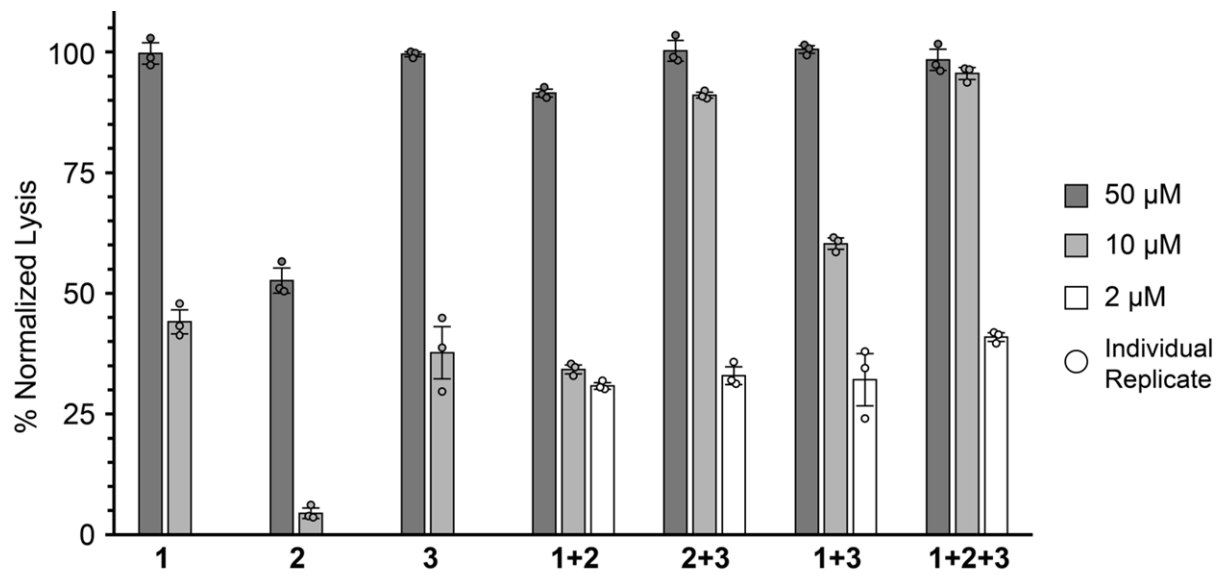


**Supplementary Figure 21: Secondary structure of daptides 1-3.** (a)  $\alpha$ -helices of MpaA1-3 predicted by PSI-PRED4.0<sup>13</sup> (<http://bioinf.cs.ucl.ac.uk/psipred/>). (b) Helical net diagrams showing predicted intra-helix interactions for MpaA1-3 core peptides. Diagrams were generated using NetWheels (<http://lbqp.unb.br/NetWheels/>). (c, following page) Circular dichroism spectra of **1-3**.

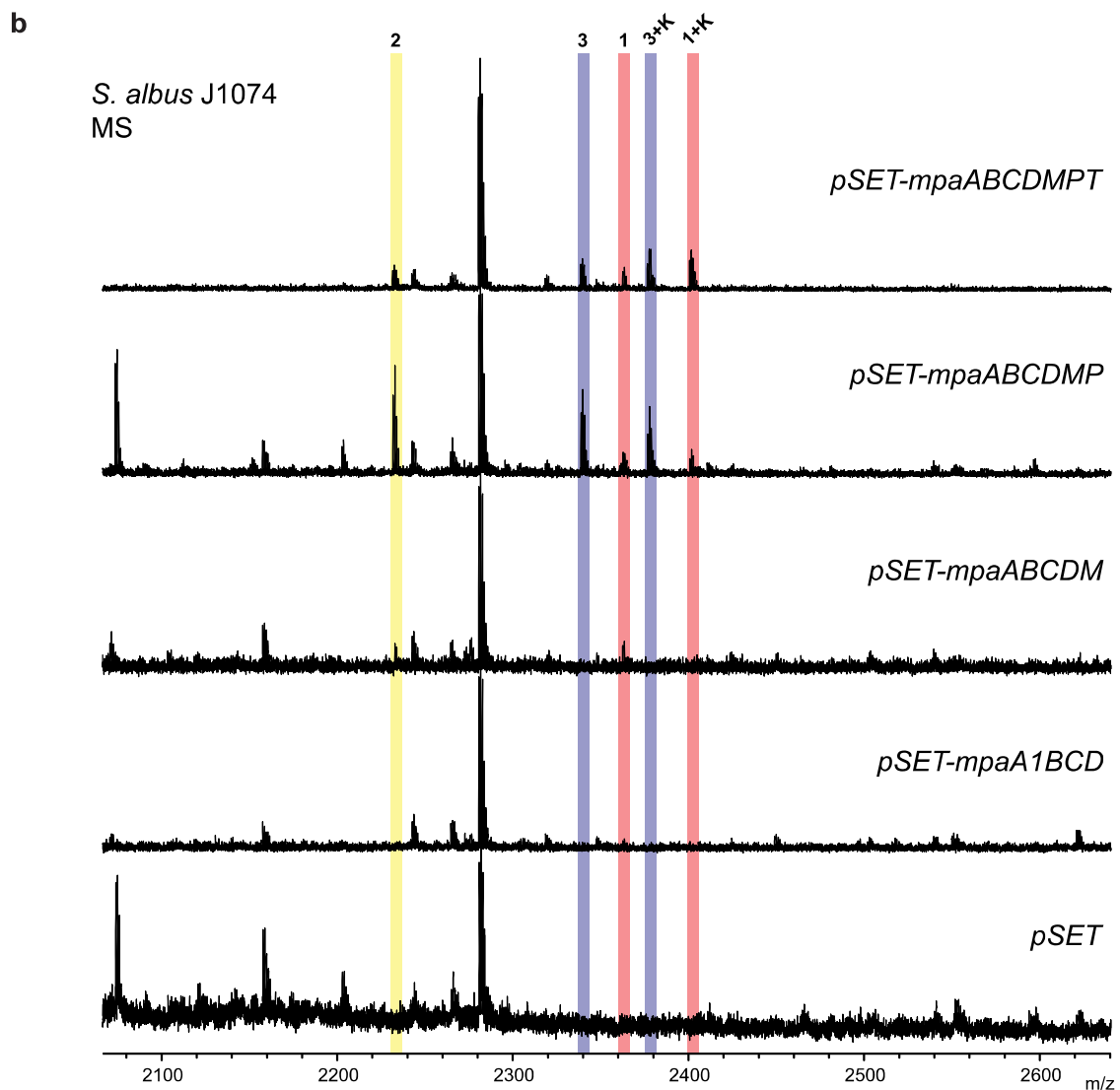
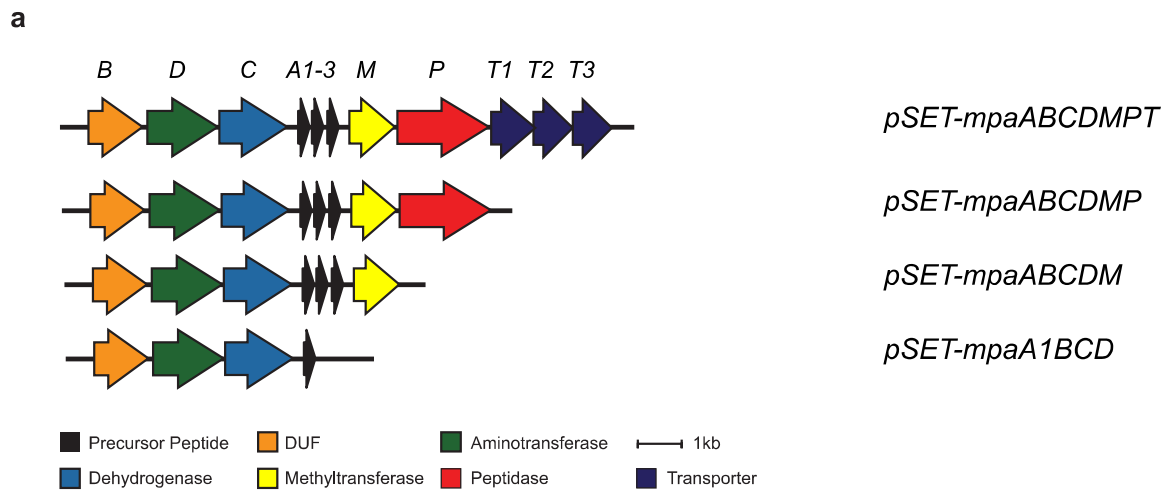


**Supplementary Figure 22: Comparison of melittin to daptide 1.** (a) Sequence logo for the melittin family is shown. The logo was generated using SkyLign<sup>9</sup> on the melittin pHMM (Pfam identifier: PF01372)<sup>5</sup>. (b) A crystal structure of melittin and predicted structure of **1** are shown. AlphaFold<sup>14</sup> was used to predict the MpaA1 complete sequence, and only the core region is shown. Melittin structure was re-created based on a review article<sup>15</sup>. Dmp: *N*<sub>2</sub>,*N*<sub>2</sub>-dimethyl-1,2-propanediamine.





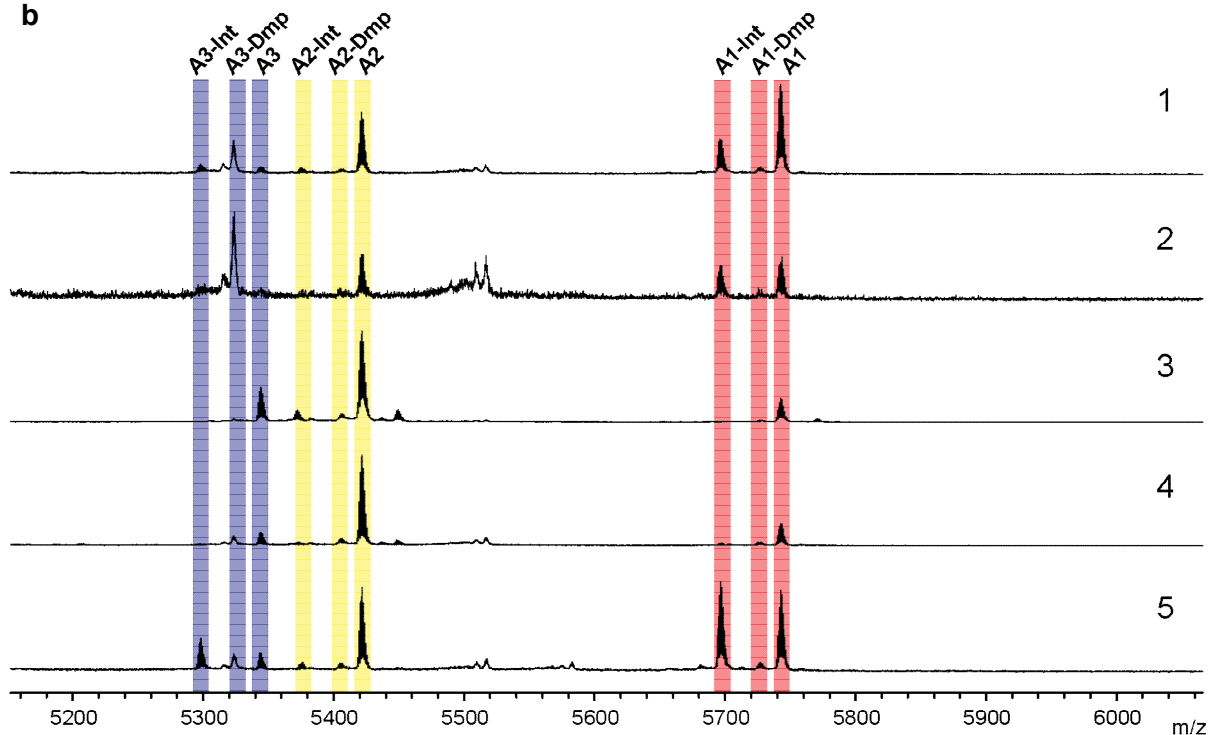
**Supplementary Figure 23: Hemolytic activity of daptides 1-3.** Hemolysis of bovine erythrocytes was normalized to the positive control [5% (v/v) Triton X-100]. All individual and combination daptide treatments were assessed. The percentage of hemolysis at total concentrations of 50  $\mu$ M and 10  $\mu$ M are shown as grey and white bars, respectively. In the combination treatments, the total daptide concentration is listed (i.e., each daptide contributes 1/2 or 1/3 of the total concentration). All data represent the mean of n = 3 biologically independent samples and error bars show standard deviation.



**Supplementary Figure 24: Heterologous expression and *mpa* gene omissions in *S. albus* J1074. (a)** Gene organization of the minimal *mpa* BGC (no flanking genes included) with examined gene omissions depicted. **(b)** MALDI-TOF mass spectra of the corresponding methanol extracts.

**a**

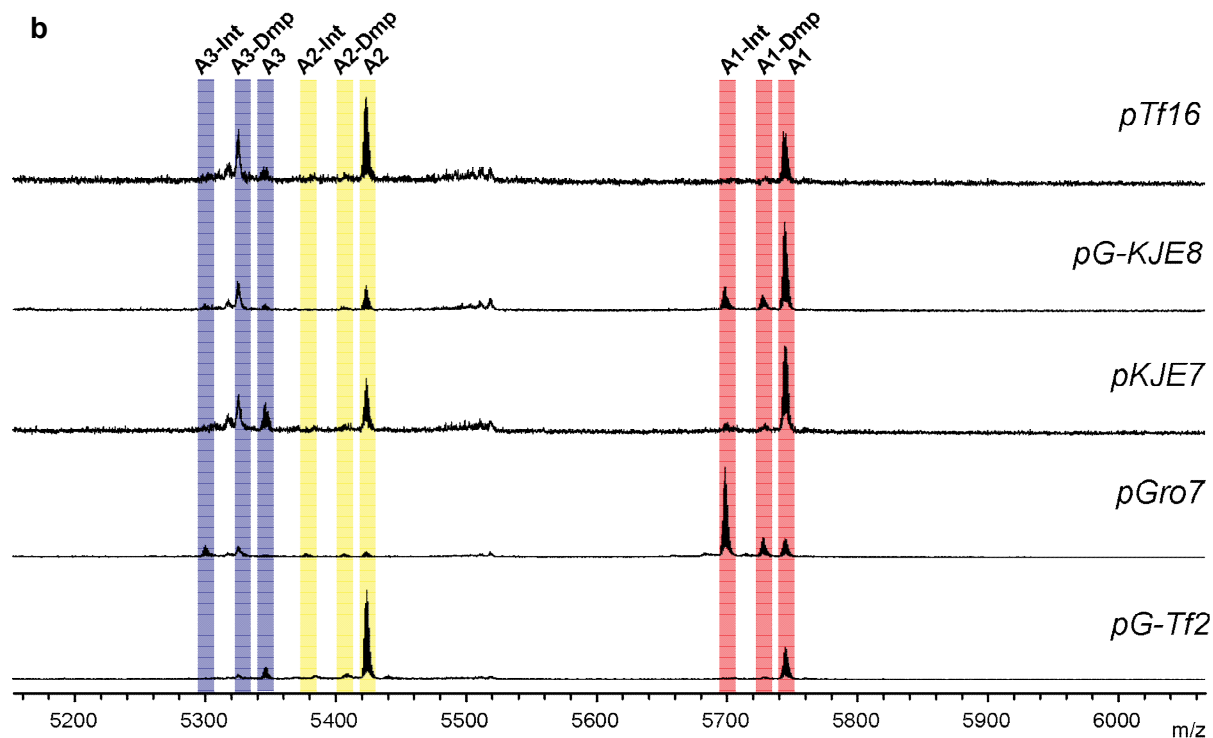
Condition	Medium	Induction Density OD <sub>600</sub>	Expression Time (h)	Expression Temperature (°C)
1	TB	1.0	20	18
2	TB	1.0	3	18
3	TB	1.5	3	37
4	LB	0.6	20	18
5	M9	0.7	36	18

**b**

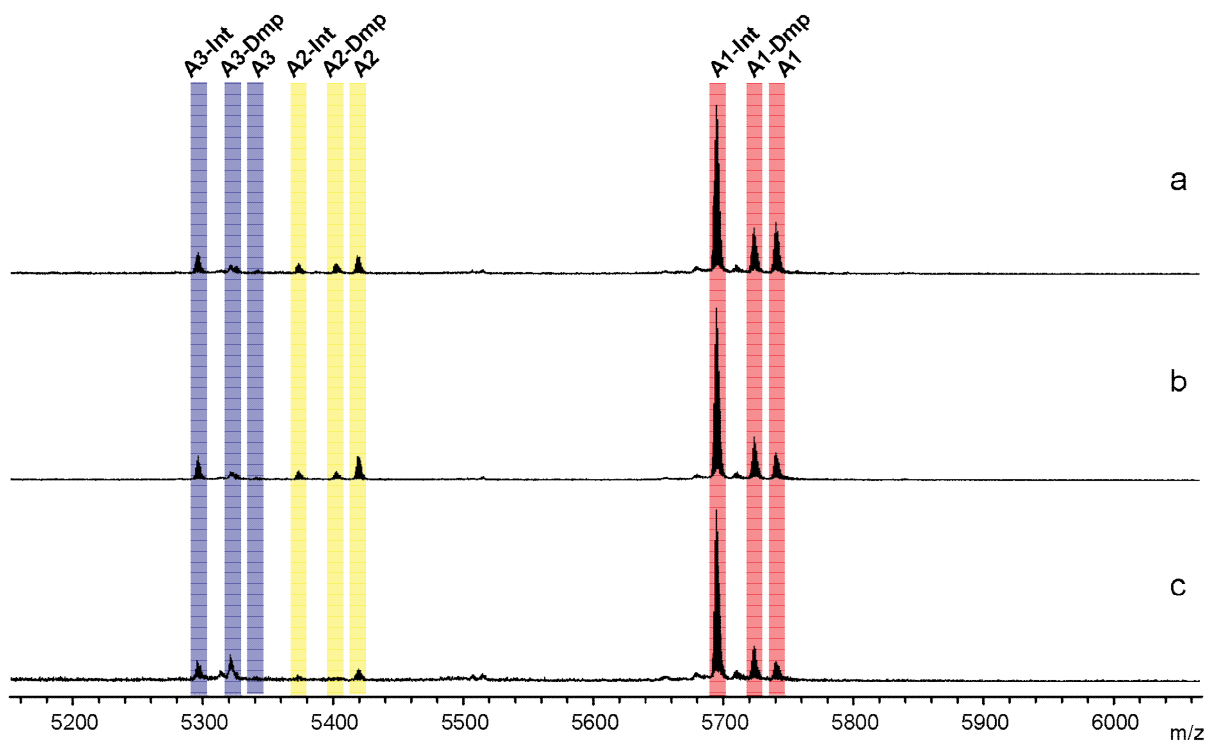
**Supplementary Figure 25: Expression of the refactored *mpaABCDE* under various cultivation conditions.** (a) List of variables for expression conditions 1-5, which used IPTG (0.5 mM final) for induction. (b) MALDI-TOF mass spectra of IMAC-purified products from expression conditions 1-5. The ketone/amine intermediates are denoted by “-Int” while the fully modified products are denoted by “-Dmp”. Dmp: *N*<sub>2</sub>,*N*<sub>2</sub>-dimethyl-1,2-propanediamine

a

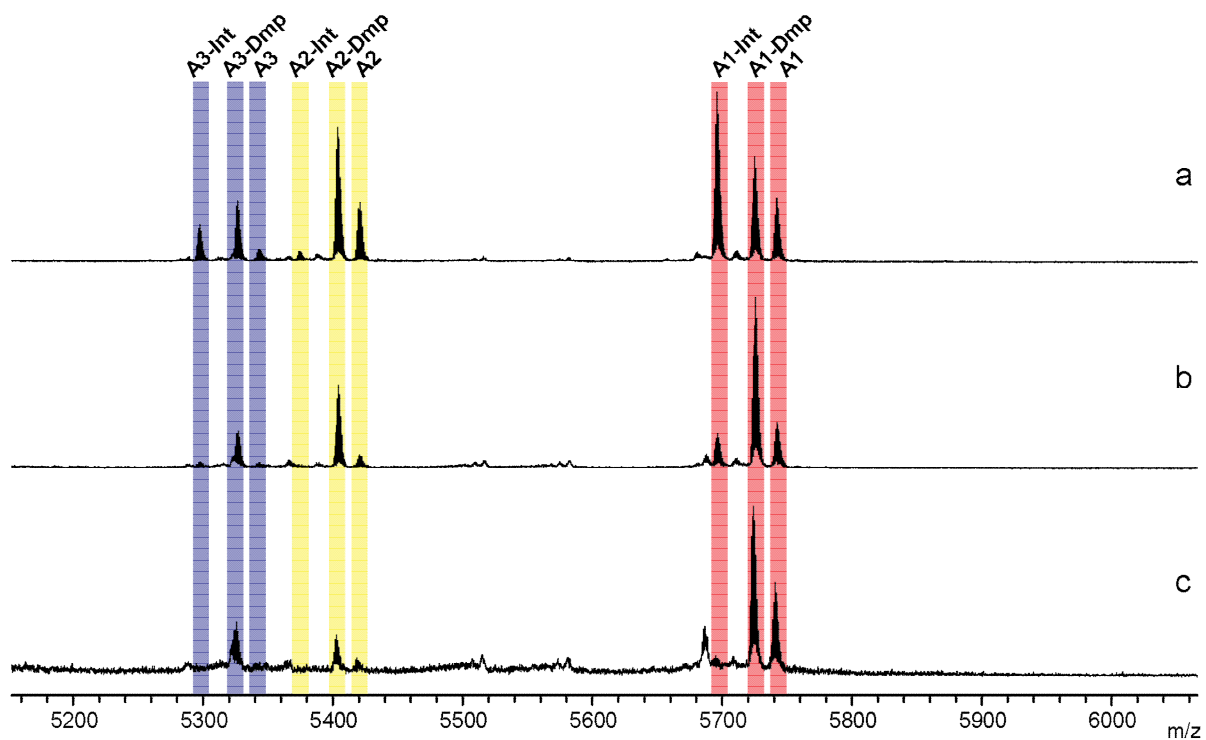
Plasmid	Chaperone Genes	Promoter	Inducer
pTf16	<i>tig</i>	<i>araB</i>	L-Arabinose: 0.5 mg/ml
pG-KJE8	<i>dnaK-dnaJ-grpE</i> <i>gro ES-groEL</i>	<i>araB</i> Pzt-1	L-Arabinose: 0.5 mg/ml Tetracycline: 1 ng/ml
pKJE7	<i>dnaK-dnaJ-grpE</i>	<i>araB</i>	L-Arabinose: 0.5 mg/ml
pGro7	<i>groES-groEL</i>	<i>araB</i>	L-Arabinose: 0.5 mg/ml
pG-Tf2	<i>groES-groEL-tig</i>	Pzt-1	Tetracycline: 1 ng/ml



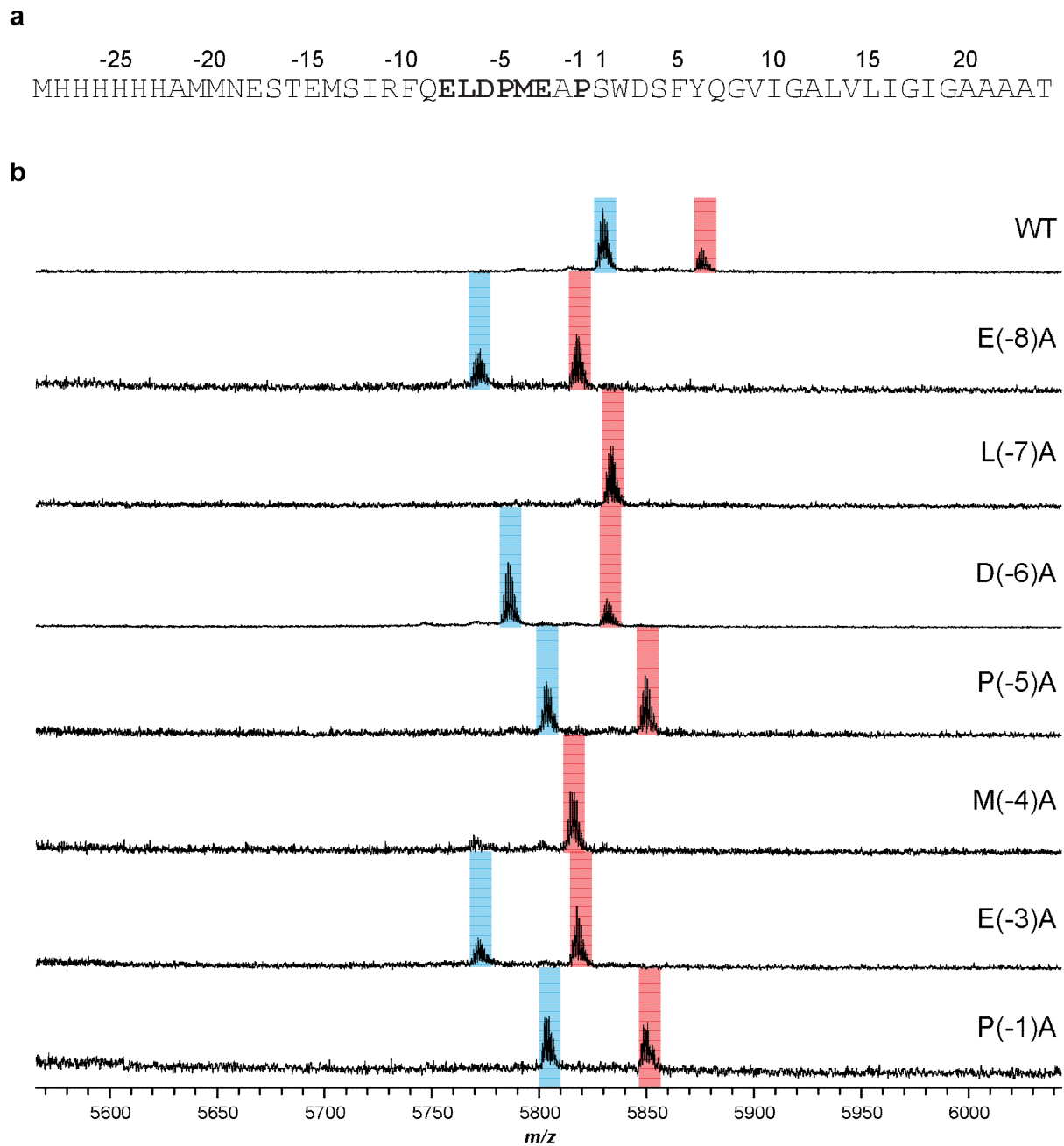
**Supplementary Figure 26: Expression of the refactored *mpaABCDE* with chaperone plasmids. (a)** Information for the genes involved in each plasmid. All chaperone plasmids were obtained from TaKaRa Bio Inc. Additional expression parameters were: medium, TB; induction OD<sub>600</sub>, 0.8; [IPTG] 0.1 mM; expression temperature, 18 °C; expression time, 18 h. **(b)** MALDI-TOF mass spectra of IMAC purified products. The ketone/amine intermediates are denoted by “-Int” while the fully modified products are denoted by “-Dmp”. Dmp: *N*<sub>2</sub>,*N*<sub>2</sub>-dimethyl-1,2-propanediamine.



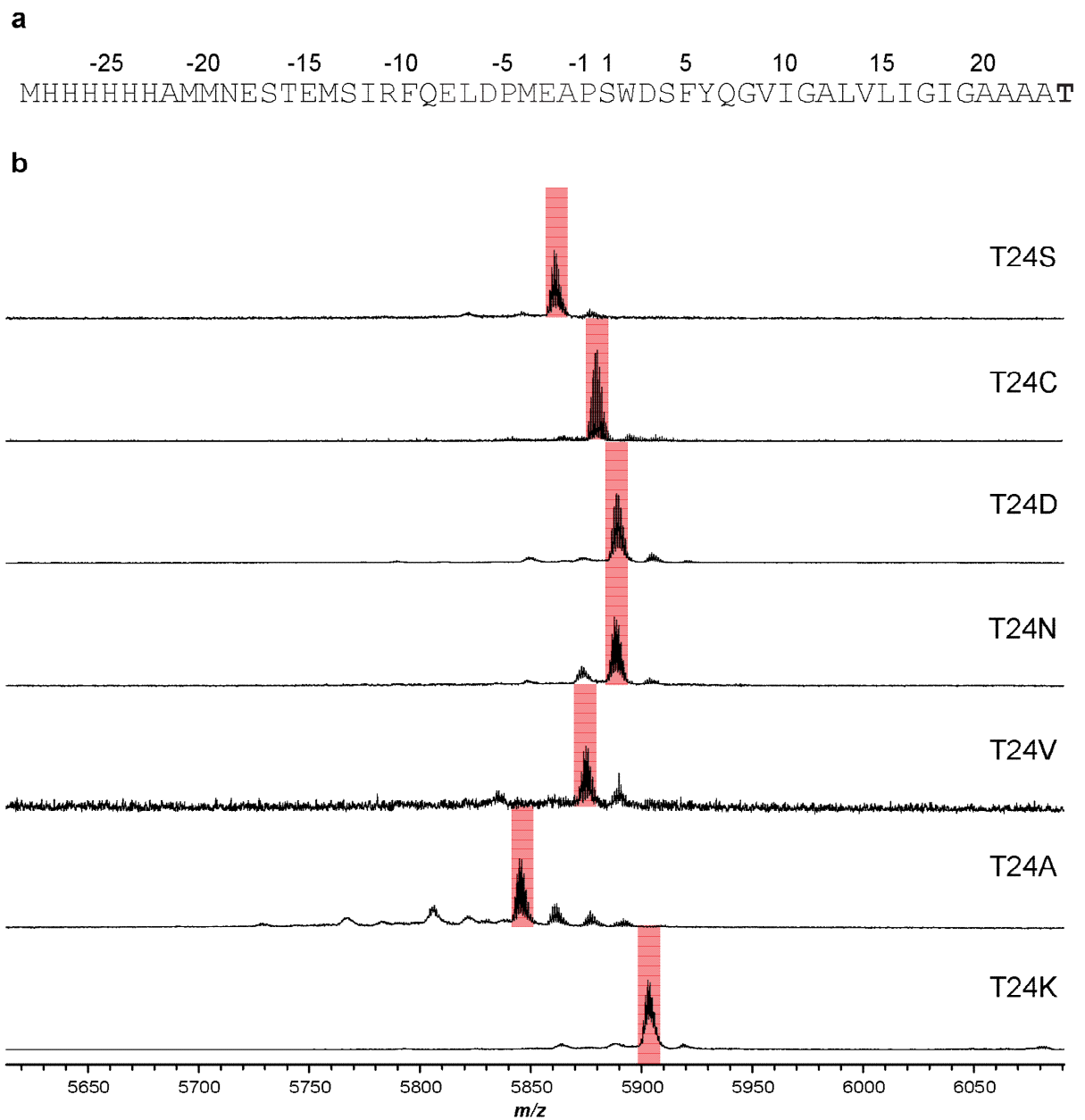
**Supplementary Figure 27: Expression of the refactored *mpaABCDE* with pGro7 chaperone plasmid under various arabinose concentrations** ( $a = 0.5$  mg/mL,  $b = 2.0$  mg/mL,  $c = 4.0$  mg/mL). Additional expression parameters were: medium, TB; induction  $OD_{600}$ , 0.8; [IPTG], 0.1 mM; expression temperature, 18 °C; expression time, 18 h. The ketone/amine intermediates are denoted by “-Int” while the fully modified products are denoted by “-Dmp”. Dmp:  $N_2,N_2$ -dimethyl-1,2-propanediamine.



**Supplementary Figure 28: Expression of the refactored *mpaABCDE* with pGro7 chaperone plasmid with extended expression time (a = 36 h; b = 72 h; c = 96 h). Additional expression parameters were: medium, M9; [arabinose], 0.5 mg/ml; induction OD<sub>600</sub>, 0.7; [IPTG], 0.5 mM; expression temperature, 18 °C. The ketone/amine intermediates are denoted by “-Int” while the fully modified products are denoted by “-Dmp”. Dmp: *N*<sub>2</sub>,*N*<sub>2</sub>-dimethyl-1,2-propanediamine.**

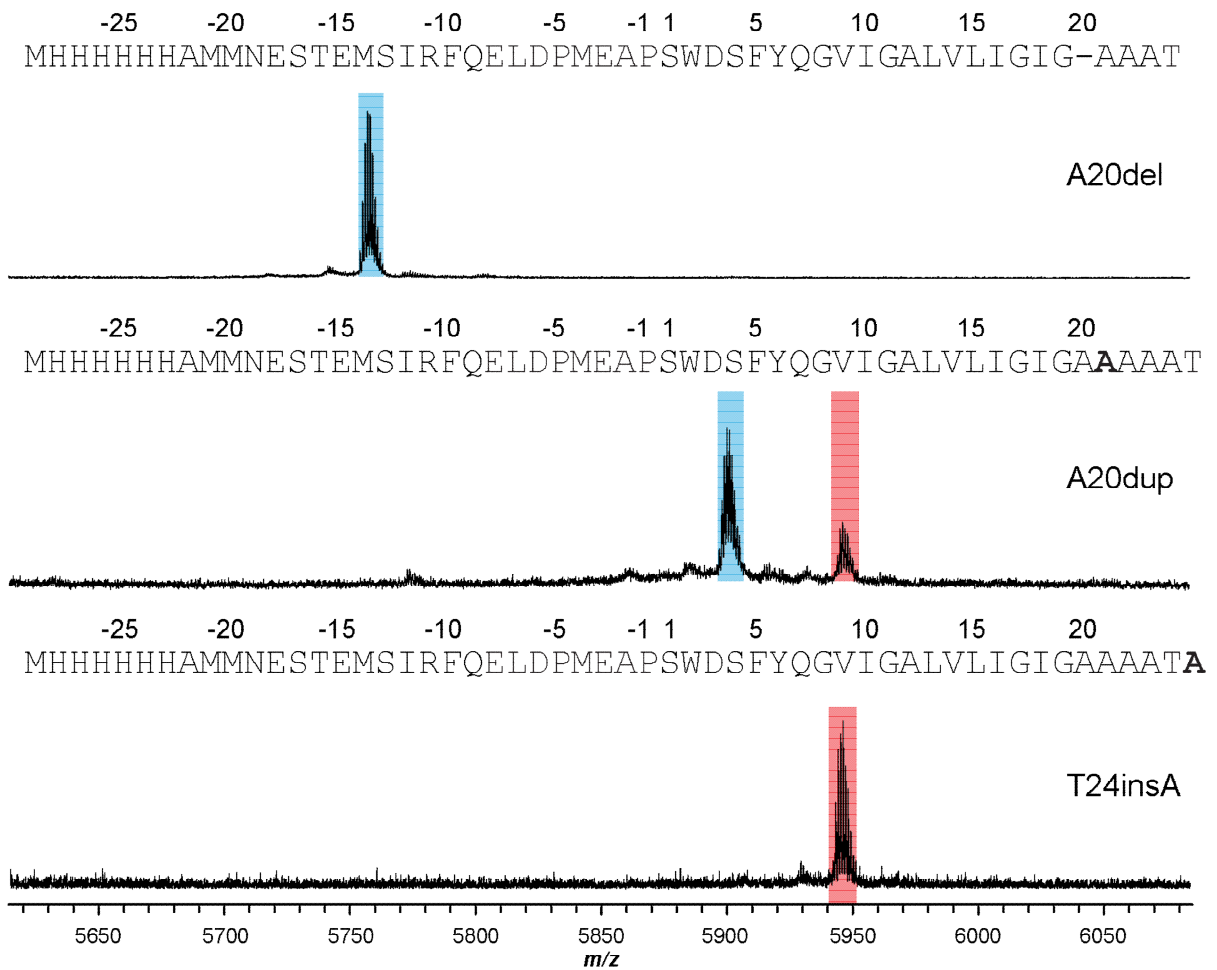


**Supplementary Figure 29: MALDI-TOF-MS analysis of MpaA1 leader region variants co-expressed with MpaB and MpaC.** (a) Sequence of MpaA1 with varied residues shown in bold. (b) MALDI-TOF mass spectra of IMAC-purified products after co-expression under the following condition: medium, TB; chaperone plasmid, pGro7; [arabinose], 0.5 mg/mL; induction OD<sub>600</sub>, 0.8; [IPTG], 0.1 mM; expression temperature, 18 °C; expression time, 18 h. Ions for unmodified and modified peptides are highlighted in red and blue, respectively.

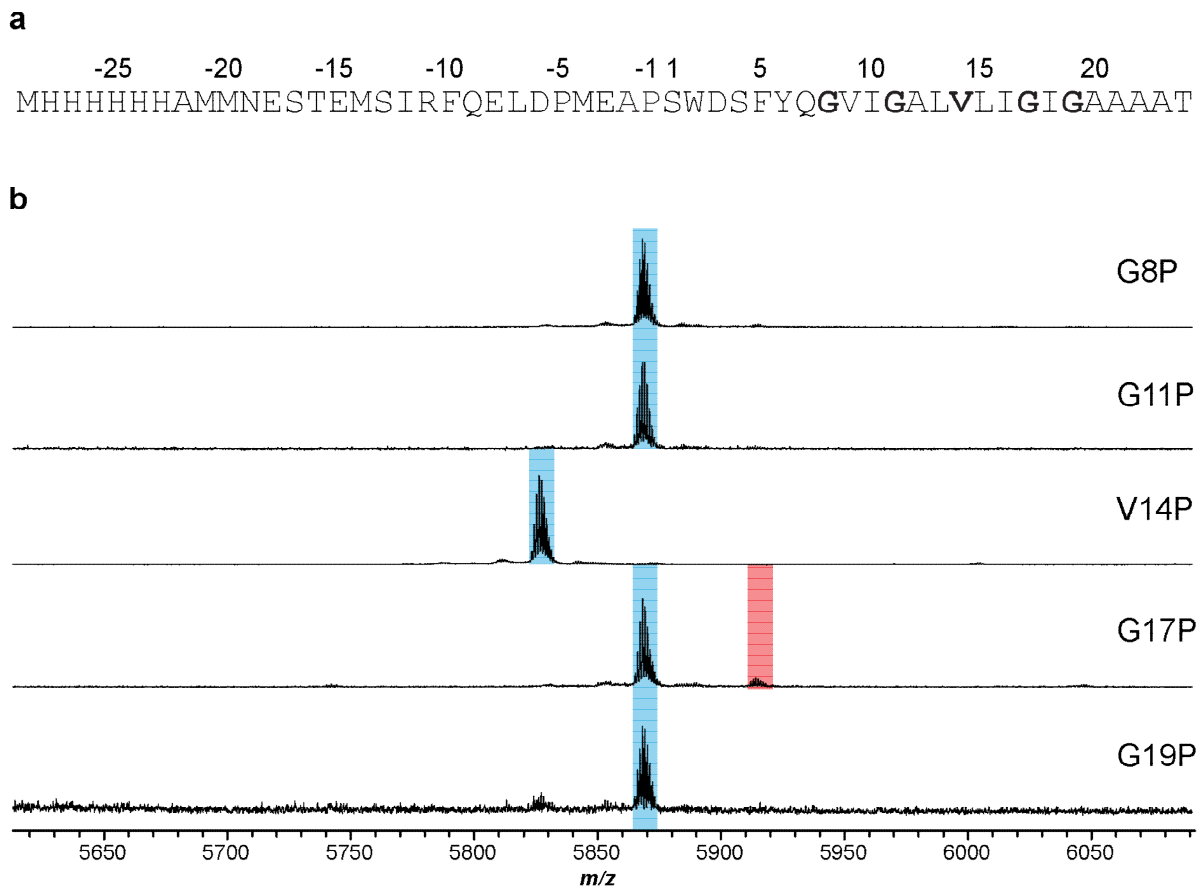


**Supplementary Figure 30: MALDI-TOF-MS analysis of MpaA1 C-terminal Thr variants that were co-expressed with MpaB and MpaC.** (a) Sequence of MpaA1 with the replaced C-terminal Thr shown in bold. (b) MALDI-TOF mass spectra of IMAC-purified products after co-expression under the following condition: medium, M9; chaperone plasmid, pGro7; [arabinose], 0.5 mg/mL; induction  $OD_{600}$ , 0.7; [IPTG], 0.5 mM; expression temperature, 18 °C; expression time, 72 h. Ions for unmodified peptides are highlighted in red. Minor peaks appearing at +16 are presumed to be from Met oxidation.

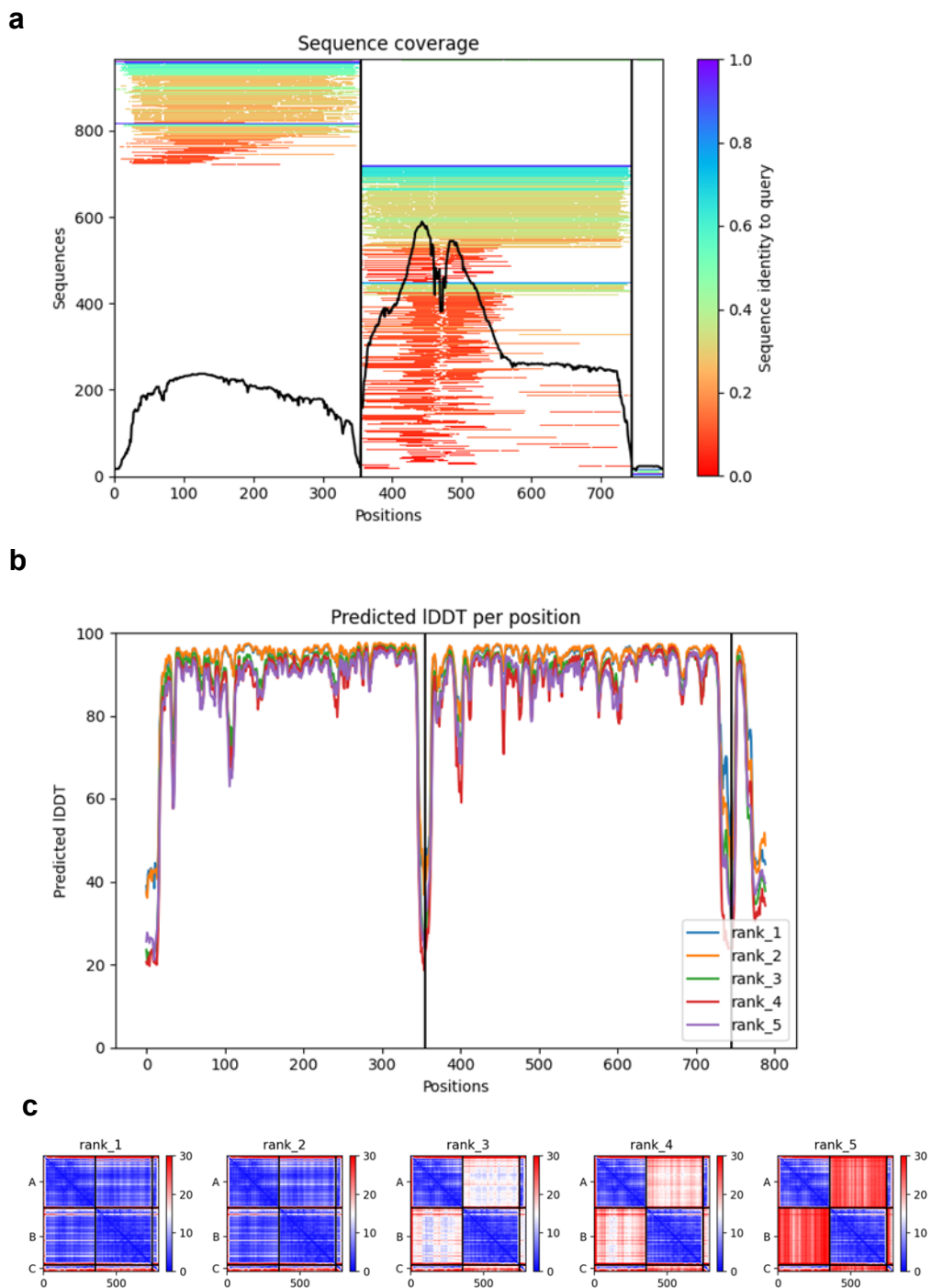




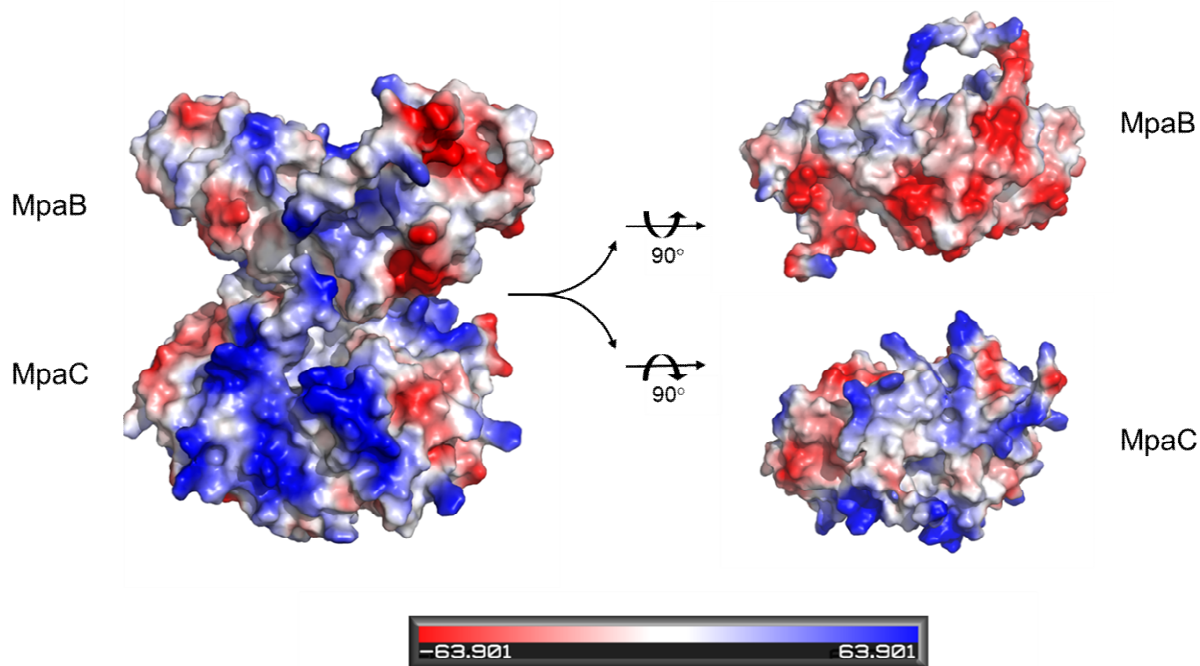
**Supplementary Figure 31: MALDI-TOF-MS analysis of MpaA1 insertion and deletion variants at the C-terminus that were co-expressed with MpaB and MpaC.** Products were purified by IMAC after co-expression under the following condition: medium, M9; chaperone plasmid, pGro7; [arabinose], 0.5 mg/mL; induction OD<sub>600</sub>, 0.7; [IPTG], 0.5 mM; expression temperature, 18 °C; expression time, 72 h. Sequences of the MpaA1 variants are shown above their corresponding mass spectra, with the inserted/deleted residues denoted in bold and dash respectively. Ions for unmodified and modified peptides are highlighted in red and blue, respectively.



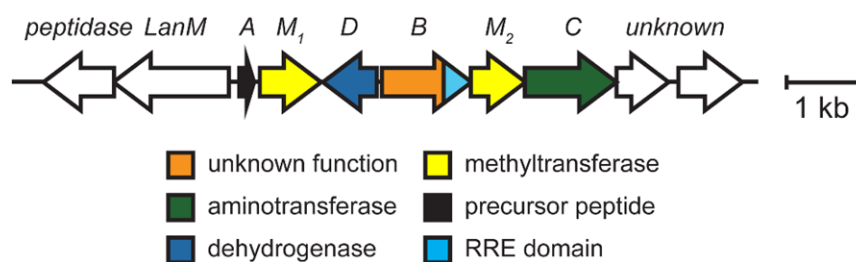
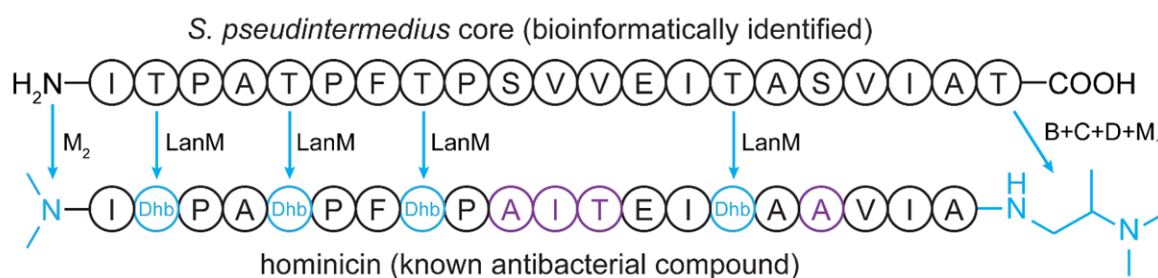
**Supplementary Figure 32: MALDI-TOF-MS analysis of MpaA1 variants in the core peptide region that were co-expressed with MpaB and MpaC.** (a) Sequence of MpaA1 with the mutated residues shown in bold. (b) MALDI-TOF mass spectra of IMAC-purified products after co-expression under the following condition: medium, M9; chaperone plasmid, pGro7; [arabinose], 0.5 mg/mL; induction  $OD_{600}$ , 0.7; [IPTG], 0.5 mM; expression temperature, 18 °C; expression time, 72 h. Ions for unmodified and modified peptides are highlighted in red and blue, respectively.



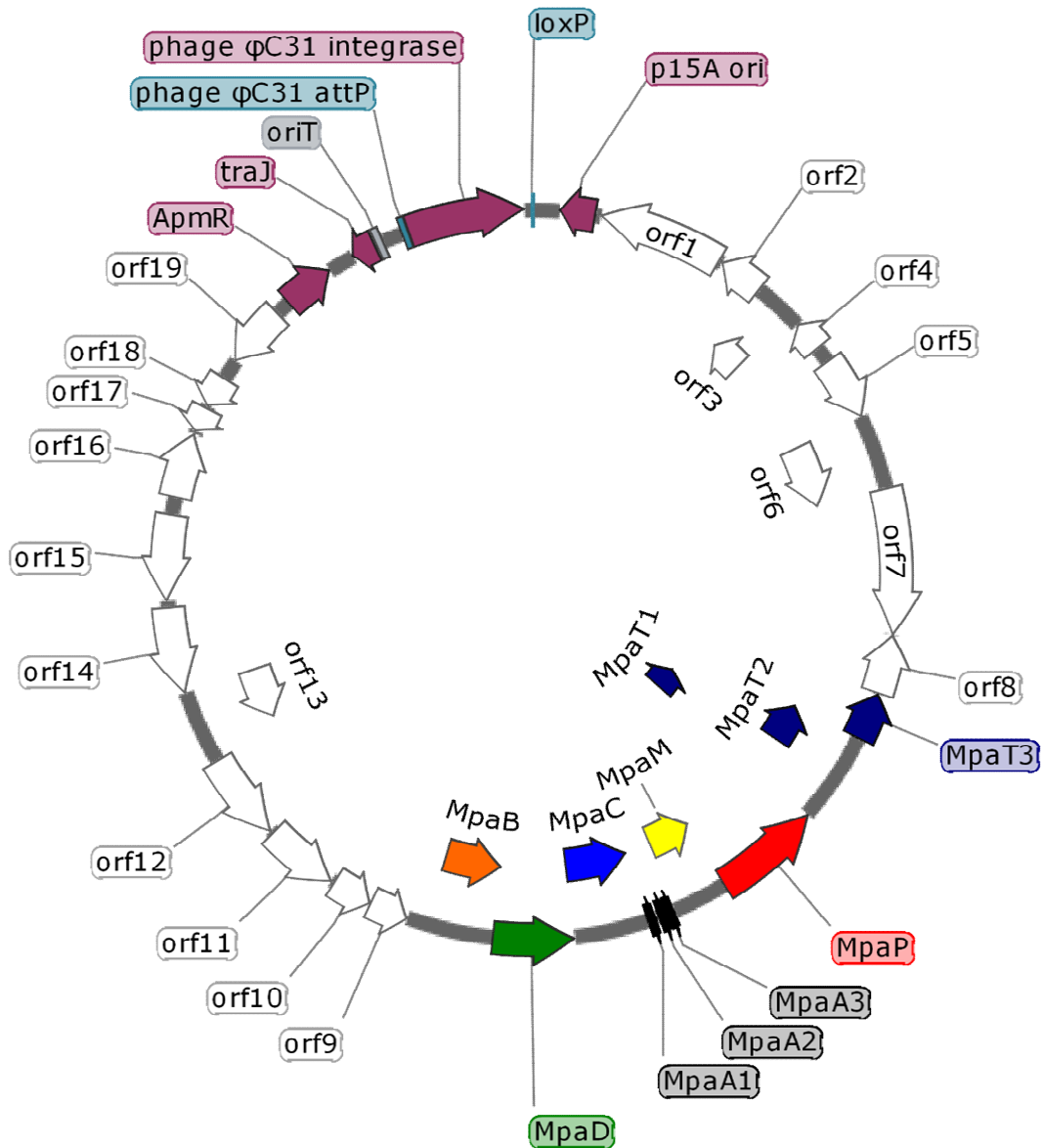
**Supplementary Figure 33: Assessment of the AlphaFold-Multimer prediction for the MpaB-MpaC-MpaA1 complex.** (a) The multiple sequence alignment (MSA) depth during MpaB-MpaC-MpaA1 complex prediction using AlphaFold- Multimer. (b) The predicted Local Distance Difference Test (pLDDT) for five predicted models. pLDDT is a per-residue measure of local confidence on a scale from 0-100. (c) Predicted Aligned Error (PAE) for five predicted models. The inter PAE between chains is low, indicating a confident prediction.



**Supplementary Figure 34: Electrostatic surface potential of MpaB and MpaC.** MpaB ( $pI = 4.8$ ) and MpaC ( $pI = 11.2$ ) are shown as a predicted protein complex on the left with positively and negatively charged surface shown in blue and red, respectively. Views of the interaction surfaces are shown on the right by a 90-degree rotation for each protein. The interaction surface is overall negatively charged for MpaB and positive for MpaC. The electrostatic surface potential is calculated by APBS in PyMOL<sup>16, 17</sup>.

**a***Staphylococcus pseudintermedius***b**

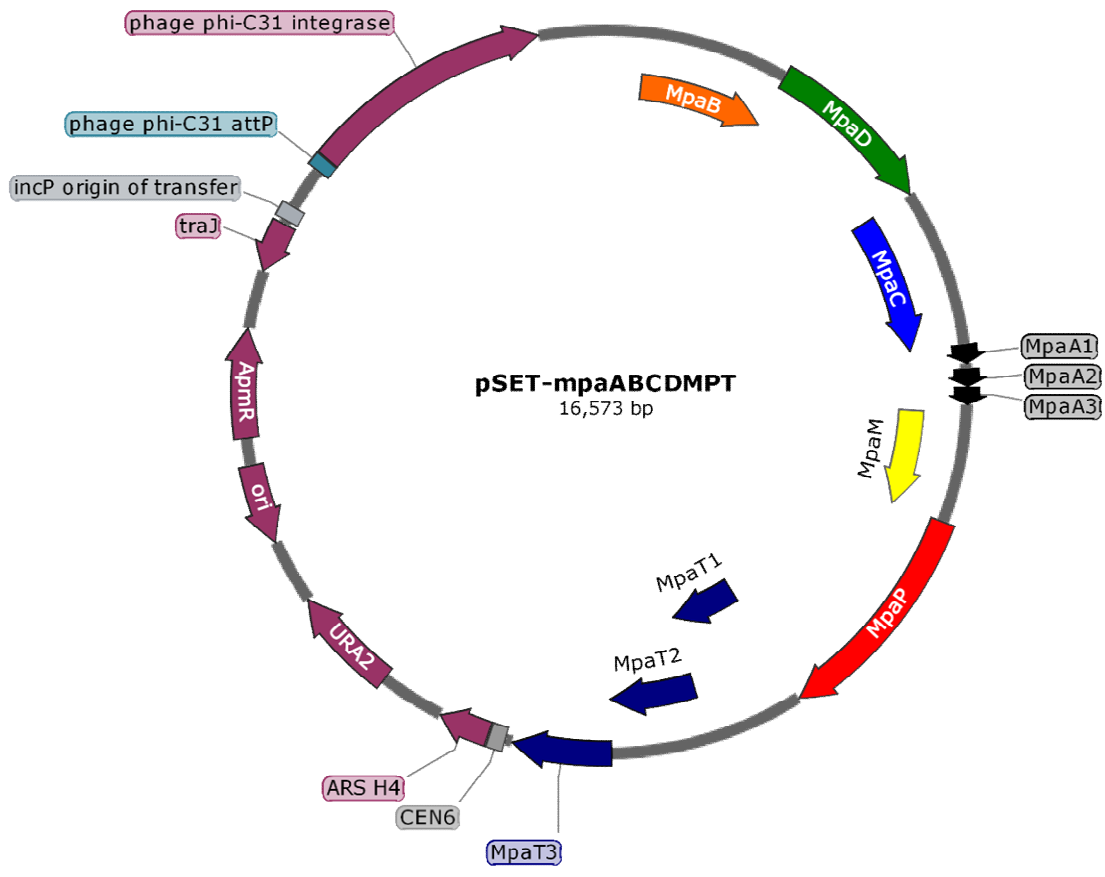
**Supplementary Figure 35: Identification of a hominicin-like BGC from *Staphylococcus pseudintermedius*.** (a) The BGC from *S. pseudintermedius* (DapC protein: WP\_214539449.1) is shown. Additionally encoded are a LanM which is proposed to convert the four internal Thr residues to dehydrobutyrine (Dhb), a second methyltransferase (putatively dimethylating the *N*-terminus), a peptidase, and two genes of unknown function. (b) Comparison of the core peptide region from the *S. pseudintermedius* BGC and the structure of hominicin<sup>8</sup>. Sites modified in hominicin are cyan and the predicted modifying enzymes are listed. Amino acid variations from the *S. pseudintermedius* core are purple.



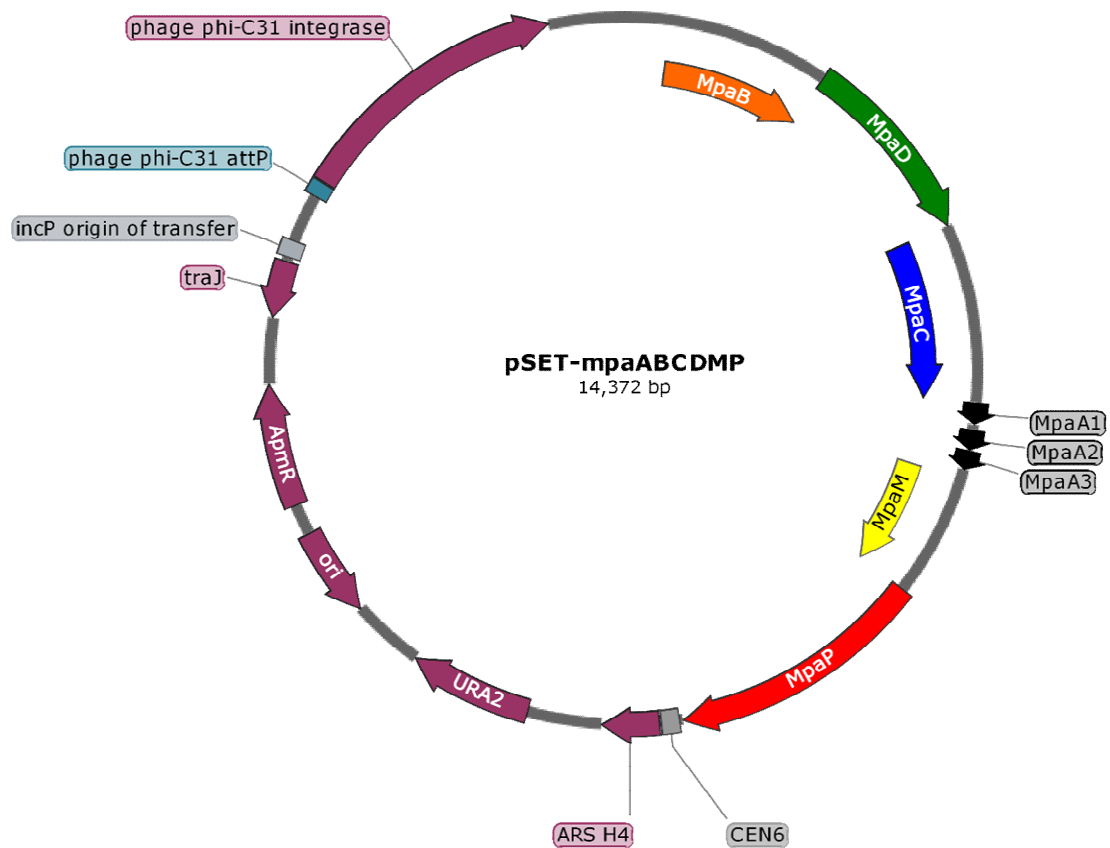
**Direct cloned mpa**

35,487 bp

**Supplementary Figure 36: The plasmid map of directly cloned *mpa* for heterologous expression in *S. albus* J1074.** ApmR: apramycin resistance marker; traJ: conjugal transfer transcriptional regulator traJ; oriT: origin of transfer; loxP: Cre-Lox recombination site; p15A ori: p15A plasmid origin of replication. The plasmid map was drawn with SnapGene (GSL Biotech LLC). The plasmid sequence is available in **Source Data**.

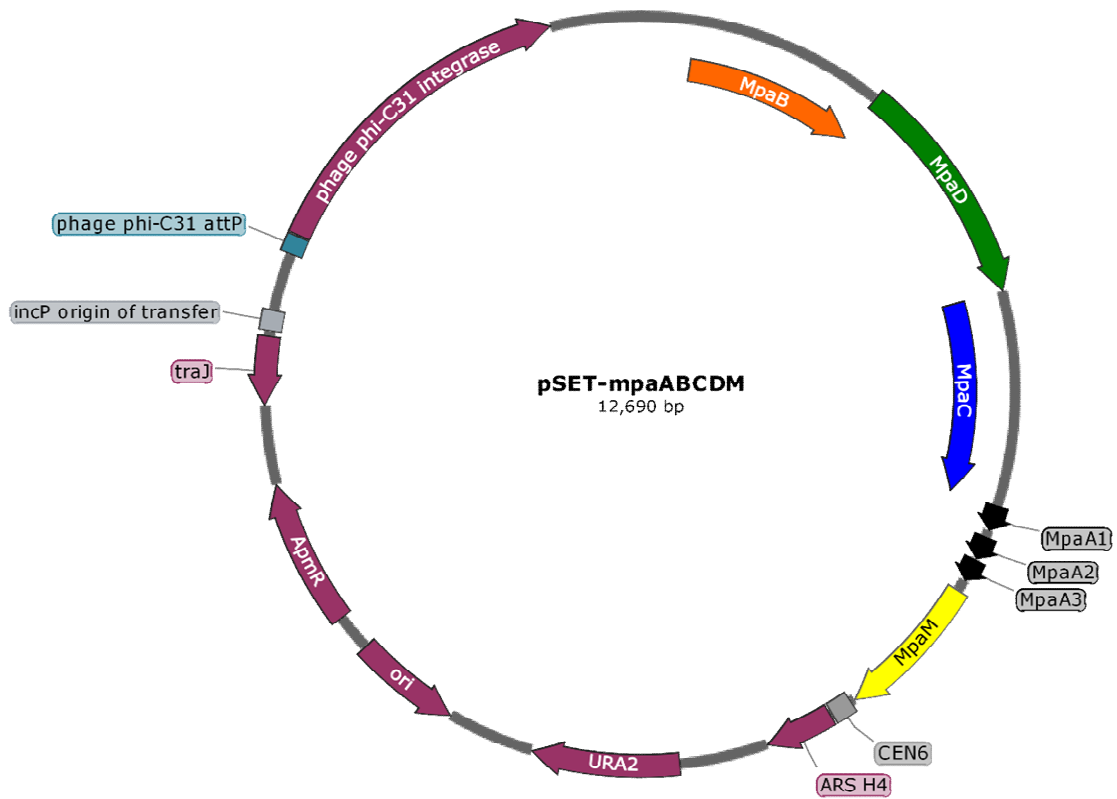


**Supplementary Figure 37: Plasmid maps of gene omission for heterologous expression in *S. albus* J1074: pSET-mpaABCDMPT.** ApmR: apramycin resistance marker; traJ: conjugal transfer transcriptional regulator traJ; oriT: origin of transfer; loxP: Cre-Lox recombination site; ori: p15A plasmid origin of replication; URA2: uracil auxotrophic marker; ARS H4: yeast artificial chromosome; CEN6: centromere in chromosome VI of *Saccharomyces cerevisiae*. The plasmid map was drawn with SnapGene (GSL Biotech LLC). The plasmid sequence is available in **Source Data**.

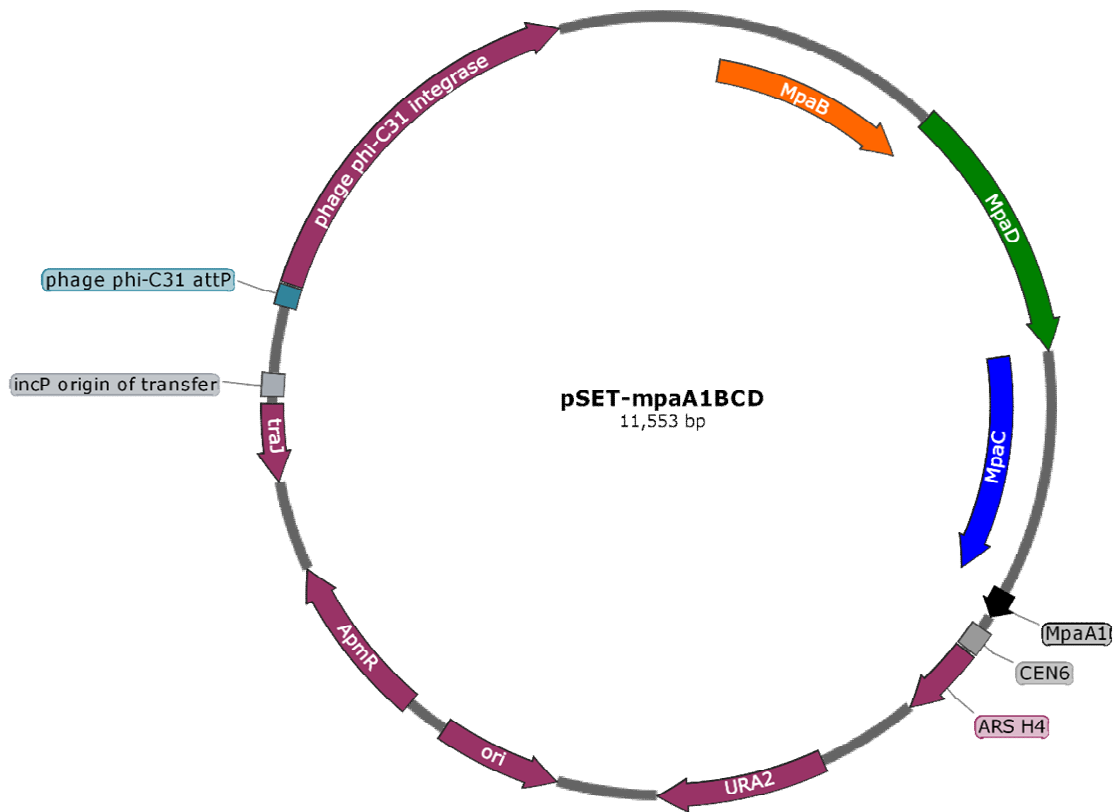


**Supplementary Figure 38: Plasmid maps of gene omission for heterologous expression in *S. albus* J1074: pSET-mpaABCDMP.** ApmR: apramycin resistance marker; traJ: conjugal transfer transcriptional regulator traJ; oriT: origin of transfer; loxP: Cre-Lox recombination site; ori: p15A plasmid origin of replication; URA2: uracil auxotrophic marker; ARS H4: yeast artificial chromosome; CEN6: centromere in chromosome VI of *Saccharomyces cerevisiae*. The plasmid map was drawn with SnapGene (GSL Biotech LLC). The plasmid sequence is available in **Source Data**.

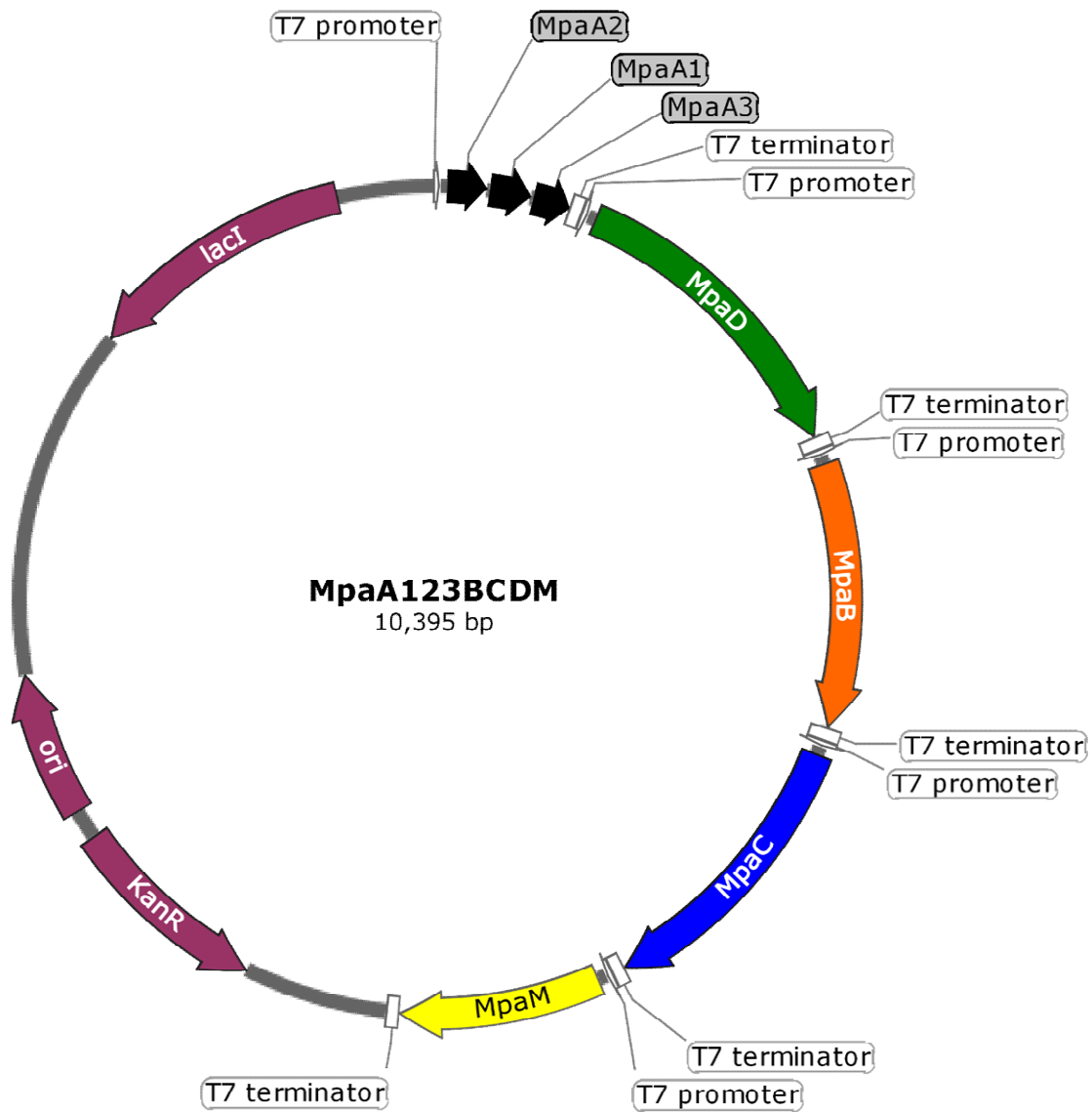




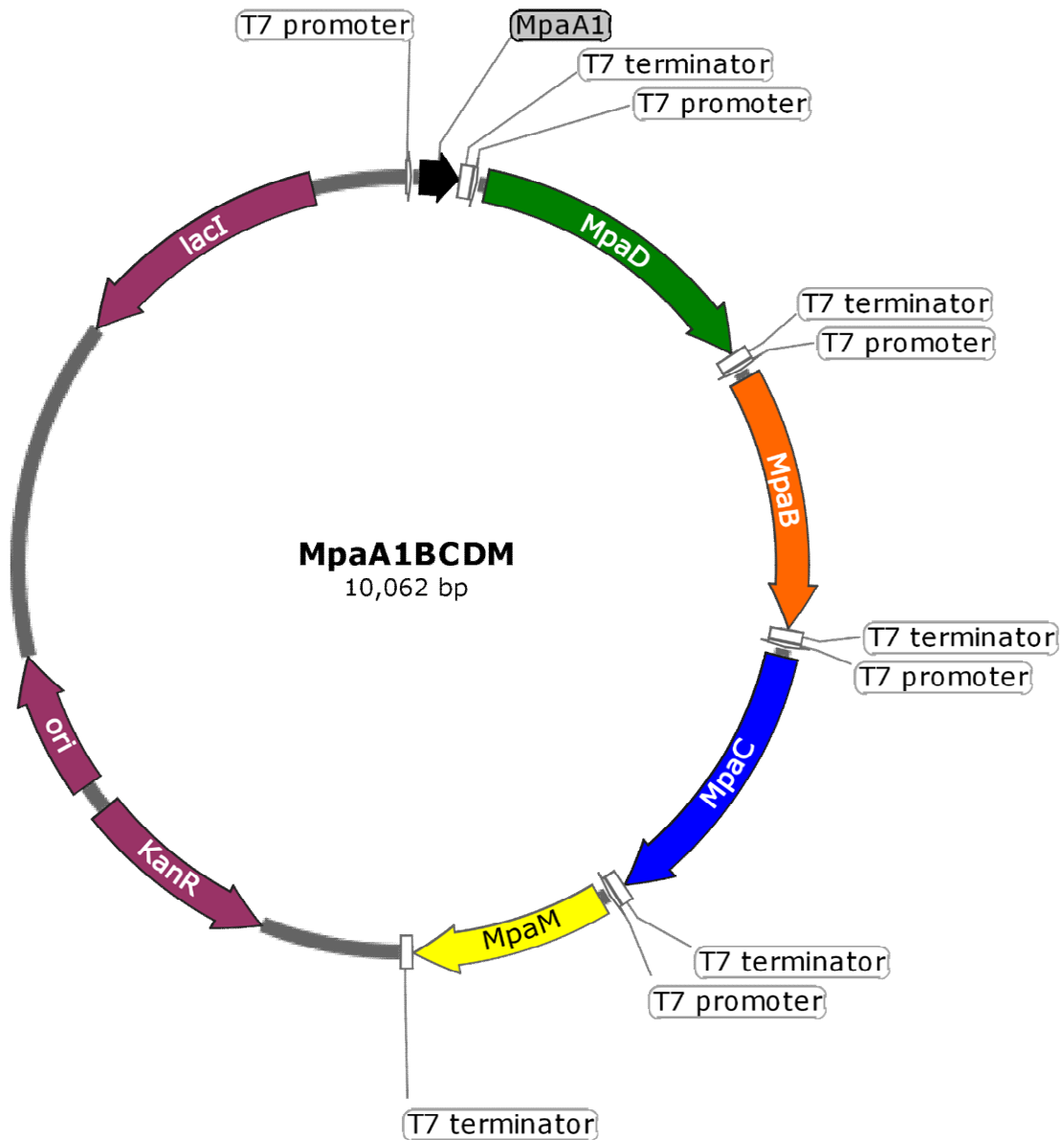
**Supplementary Figure 39: Plasmid maps of gene omission for heterologous expression in *S. albus* J1074: pSET-mpaABCDM.** ApmR: apramycin resistance marker; traJ: conjugal transfer transcriptional regulator traJ; oriT: origin of transfer; loxP: Cre-Lox recombination site; ori: p15A plasmid origin of replication; URA2: uracil auxotrophic marker; ARS H4: yeast artificial chromosome; CEN6: centromere in chromosome VI of *Saccharomyces cerevisiae*. The plasmid map was drawn with SnapGene (GSL Biotech LLC). The plasmid sequence is available in **Source Data**.



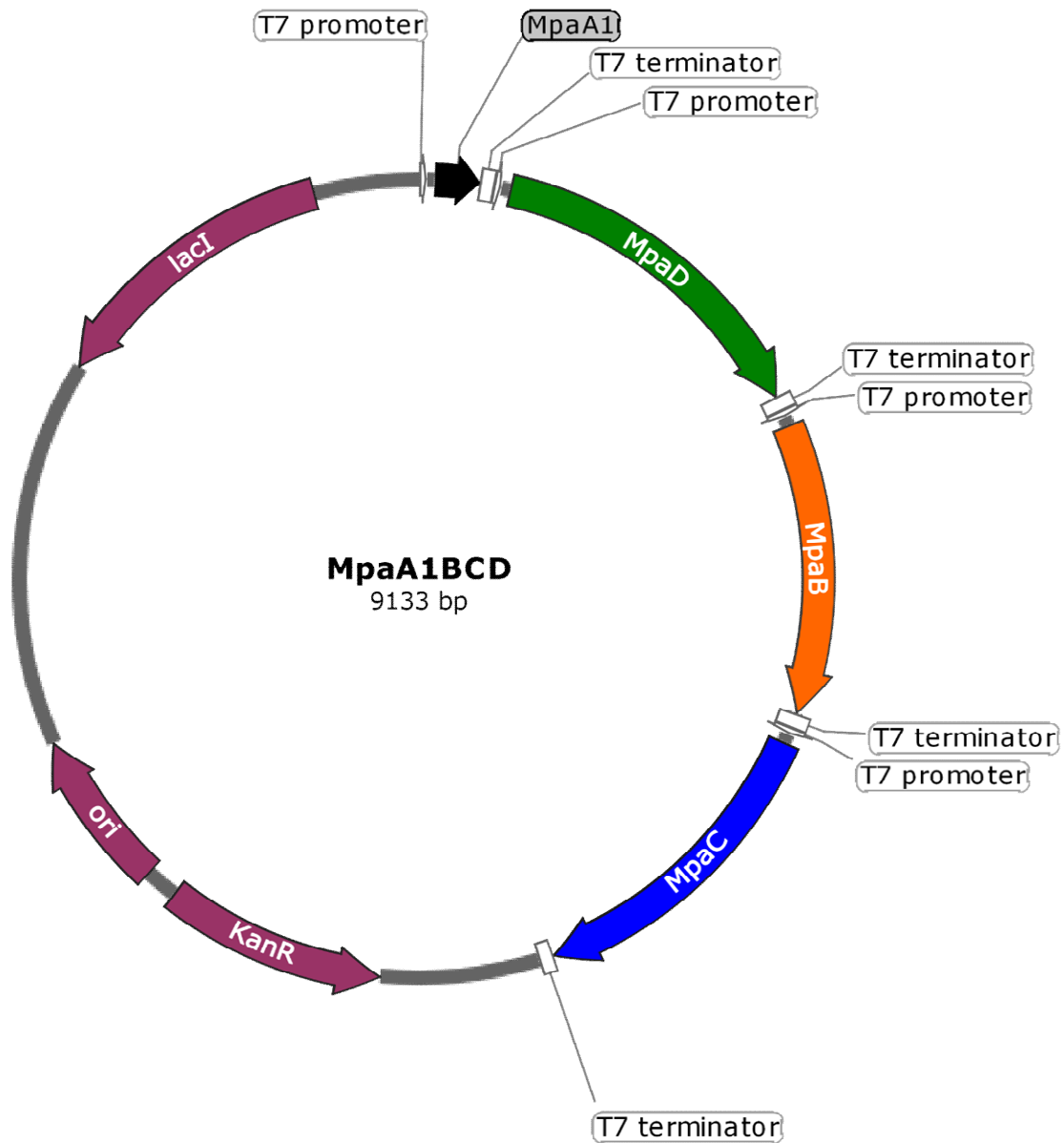
**Supplementary Figure 40: Plasmid maps of gene omission for heterologous expression in *S. albus* J1074; pSET-mpaA1BCD.** ApmR: apramycin resistance marker; traJ: conjugal transfer transcriptional regulator traJ; oriT: origin of transfer; loxP: Cre-Lox recombination site; ori: p15A plasmid origin of replication; URA2: uracil auxotrophic marker; ARS H4: yeast artificial chromosome; CEN6: centromere in chromosome VI of *Saccharomyces cerevisiae*. The plasmid map was drawn with SnapGene (GSL Biotech LLC). The plasmid sequence is available in **Source Data**.



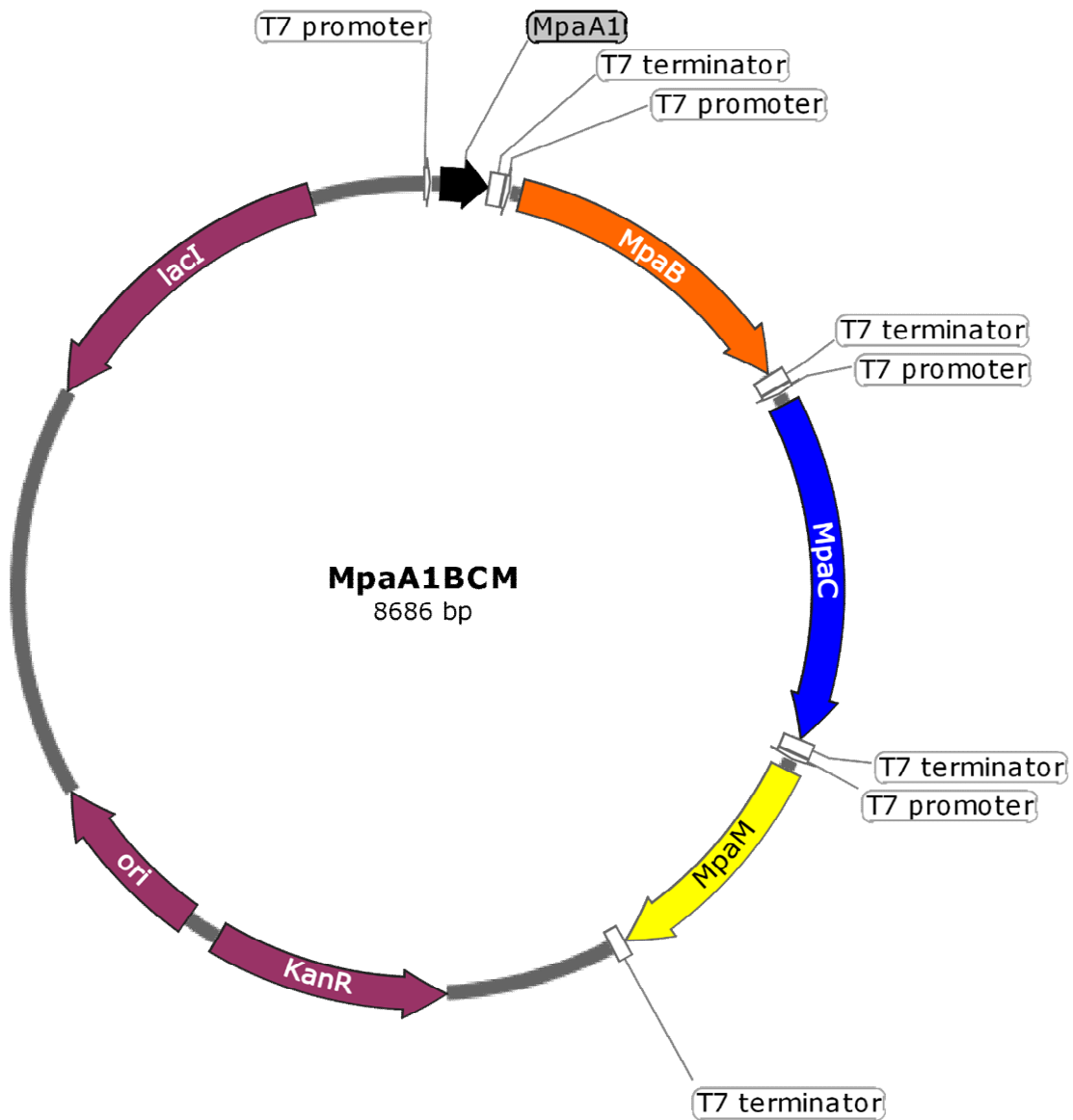
**Supplementary Figure 41: Plasmid maps of codon-optimized and refactored genes for heterologous expression in *E. coli*: MpaA1A2A3BCDM.** KanR: kanamycin resistance marker; ori: pBR322 plasmid origin of replication; lacI: lactose operon repressor lacI. The plasmid map was drawn with SnapGene (GSL Biotech LLC). The plasmid sequence is available in **Source Data**.



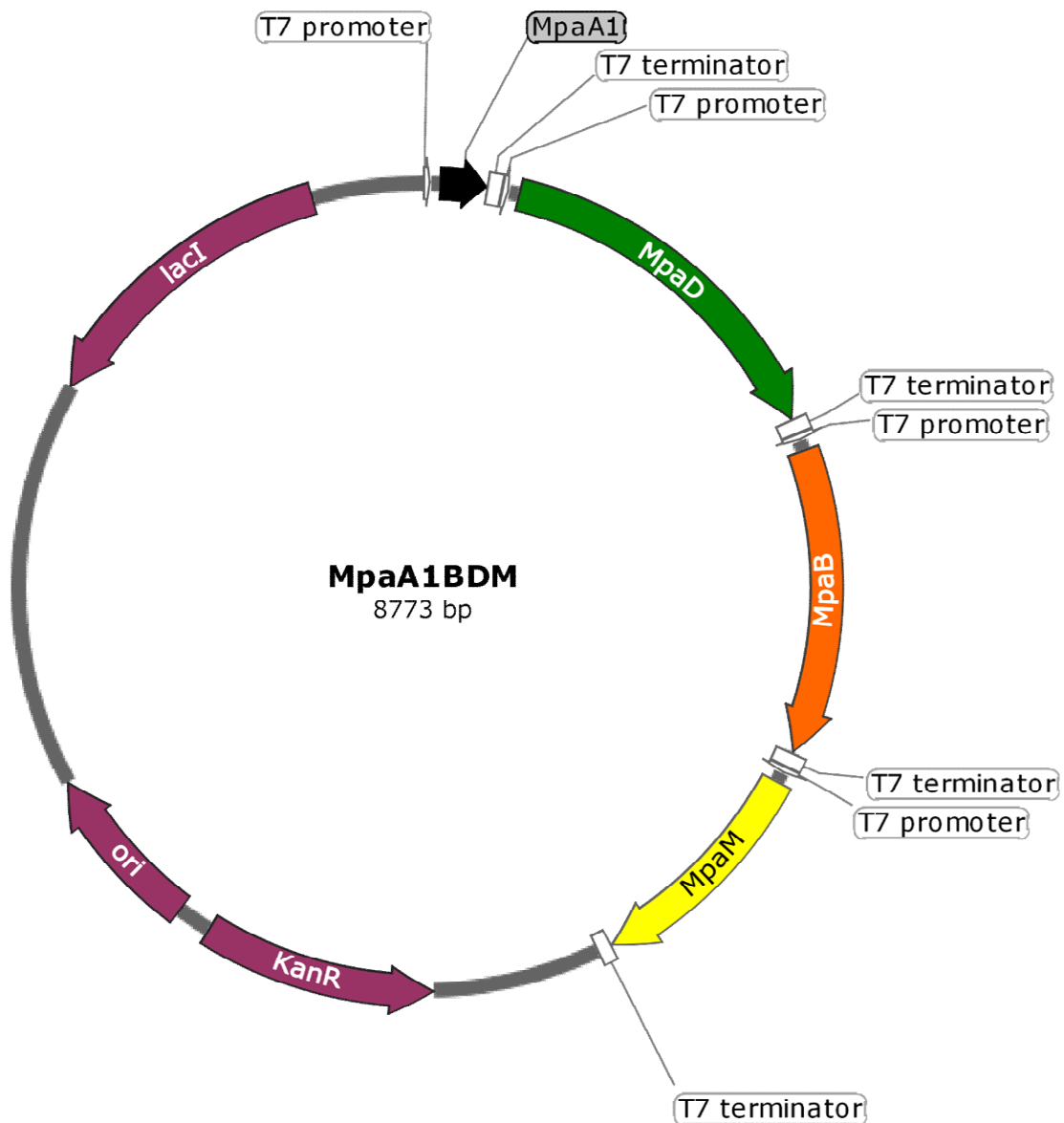
**Supplementary Figure 42: Plasmid maps of codon-optimized and refactored genes for heterologous expression in *E. coli*: MpaABCDM.** KanR: kanamycin resistance marker; ori: pBR322 plasmid origin of replication; lacI: lactose operon repressor lacI. The plasmid map was drawn with SnapGene (GSL Biotech LLC). The plasmid sequence is available in **Source Data**.



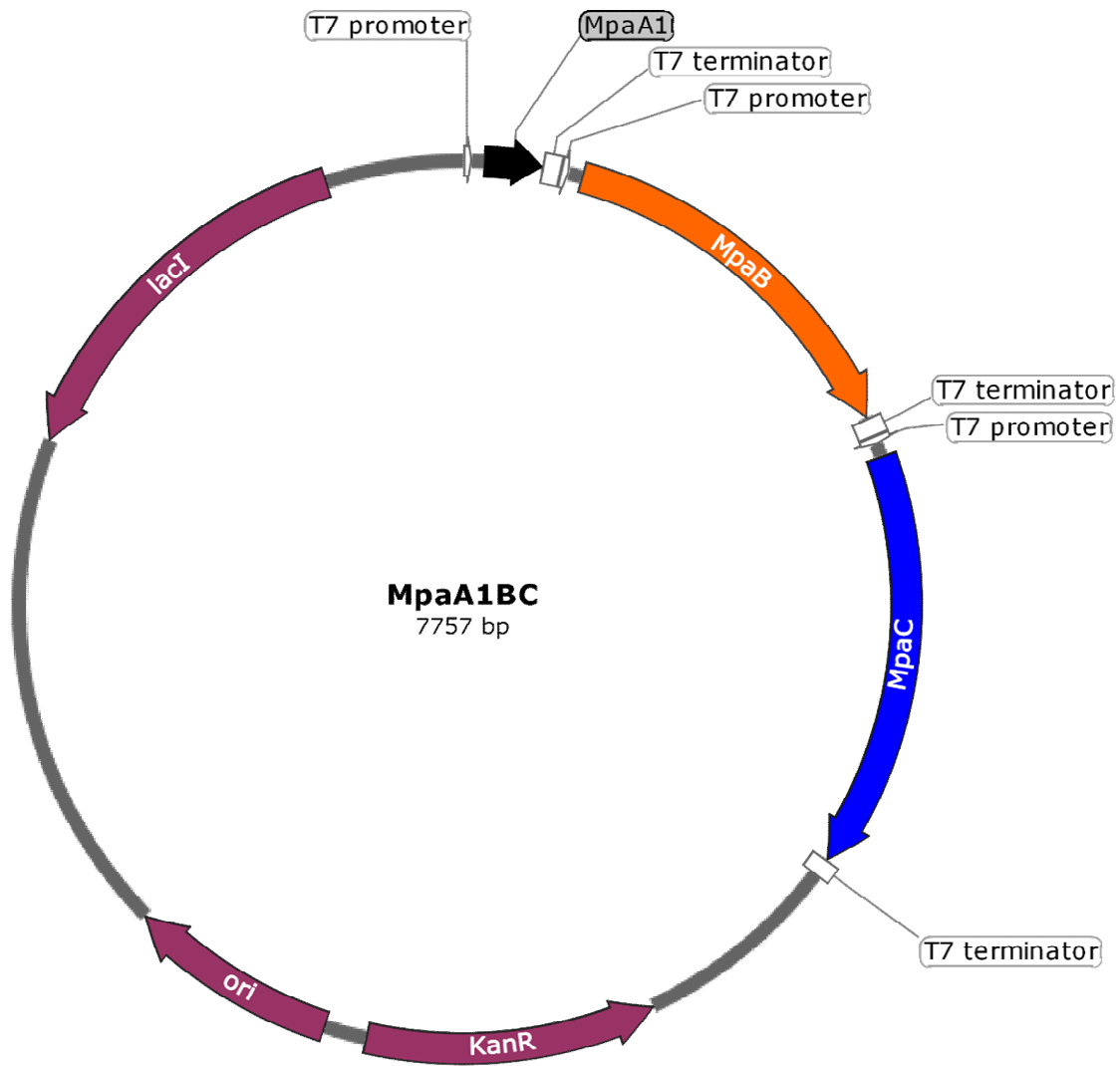
**Supplementary Figure 43: Plasmid maps of codon-optimized and refactored genes for heterologous expression in *E. coli*: MpaABCD.** KanR: kanamycin resistance marker; ori: pBR322 plasmid origin of replication; lacI: lactose operon repressor lacI. The plasmid map was drawn with SnapGene (GSL Biotech LLC). The plasmid sequence is available in **Source Data**.



**Supplementary Figure 44: Plasmid maps of codon-optimized and refactored genes for heterologous expression in *E. coli*: MpaABCM.** KanR: kanamycin resistance marker; ori: pBR322 plasmid origin of replication; lacI: lactose operon repressor lacI. The plasmid map was drawn with SnapGene (GSL Biotech LLC). The plasmid sequence is available in **Source Data**.

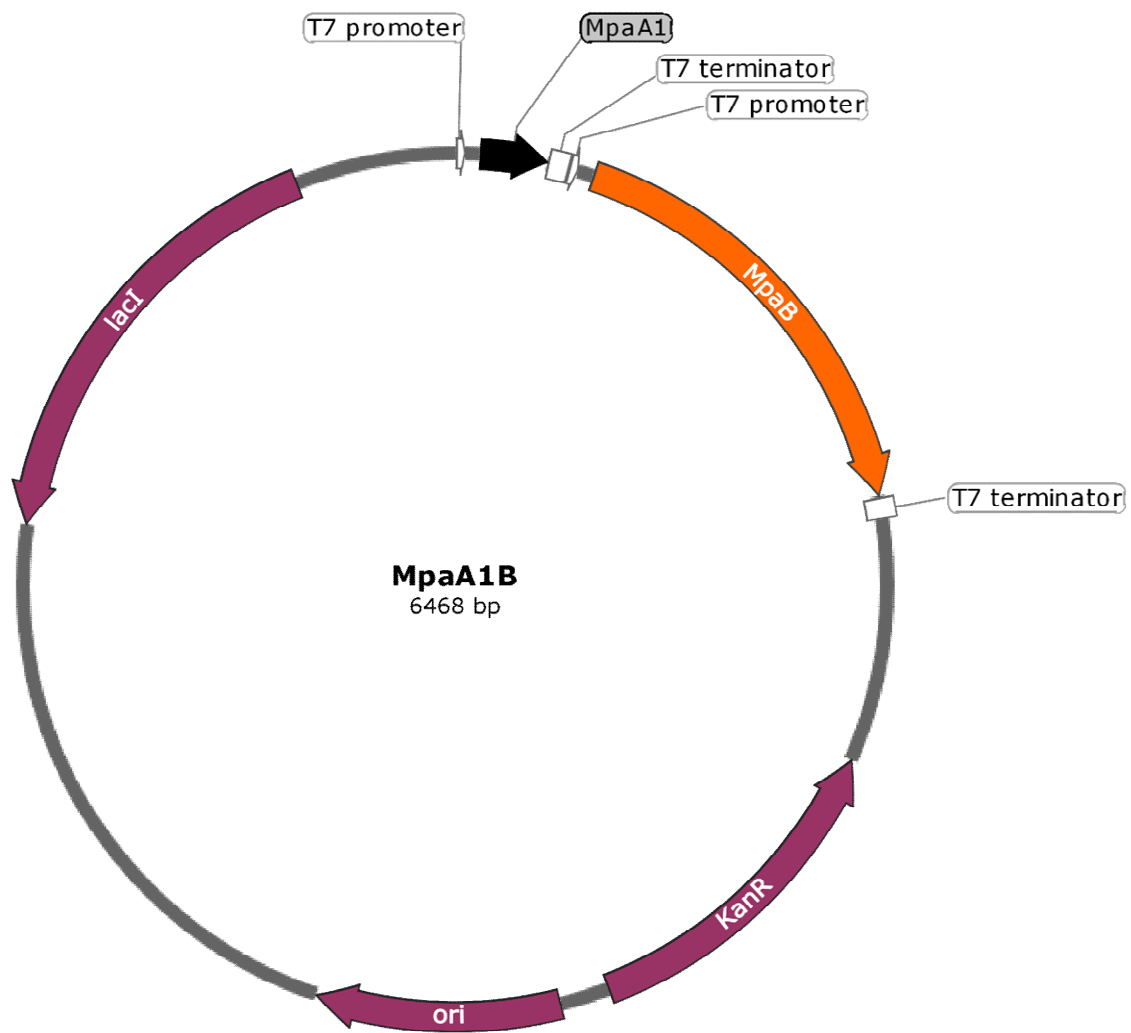


**Supplementary Figure 45: Plasmid maps of codon-optimized and refactored genes for heterologous expression in *E. coli*: MpaABDM.** KanR: kanamycin resistance marker; ori: pBR322 plasmid origin of replication; lacI: lactose operon repressor lacI. The plasmid map was drawn with SnapGene (GSL Biotech LLC). The plasmid sequence is available in **Source Data**.

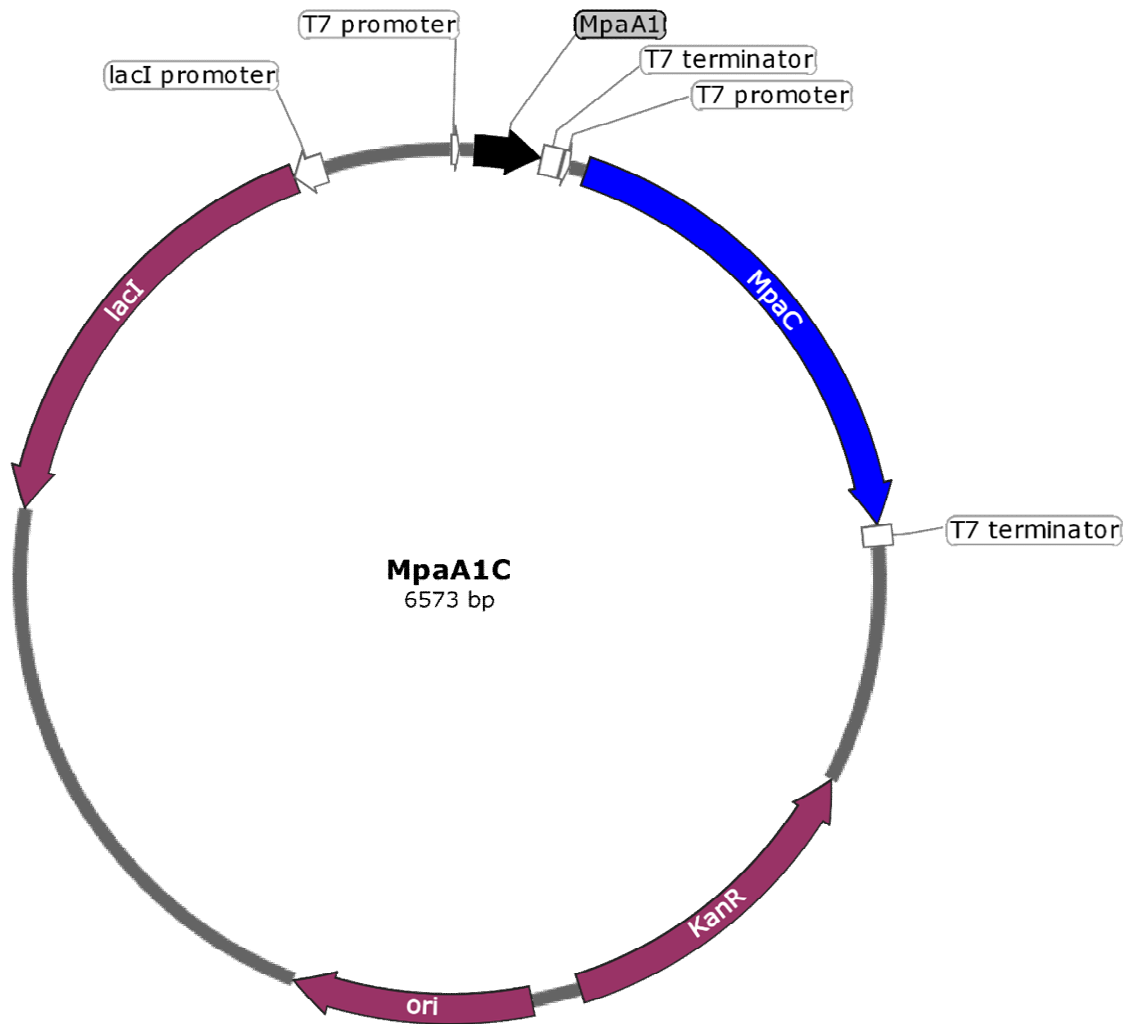


**Supplementary Figure 46: Plasmid maps of codon-optimized and refactored genes for heterologous expression in *E. coli*: MpaABC.** KanR: kanamycin resistance marker; ori: pBR322 plasmid origin of replication; lacI: lactose operon repressor lacI. The plasmid map was drawn with SnapGene (GSL Biotech LLC). The plasmid sequence is available in **Source Data**.





**Supplementary Figure 47: Plasmid maps of codon-optimized and refactored genes for heterologous expression in *E. coli*: MpaAB.** KanR: kanamycin resistance marker; ori: pBR322 plasmid origin of replication; lacI: lactose operon repressor lacI. The plasmid map was drawn with SnapGene (GSL Biotech LLC). The plasmid sequence is available in **Source Data**.



**Supplementary Figure 48: Plasmid maps of codon-optimized and refactored genes for heterologous expression in *E. coli*: MpaAC.** KanR: kanamycin resistance marker; ori: pBR322 plasmid origin of replication; *lacI*: lactose operon repressor *lacI*. The plasmid map was drawn with SnapGene (GSL Biotech LLC). The plasmid sequence is available in **Source Data**.

## References

1. Blodgett, J.A. et al. Unusual transformations in the biosynthesis of the antibiotic phosphinothricin tripeptide. *Nat Chem Biol* **3**, 480-485 (2007).
2. Gregor, V.E. Tricyclic compound derivatives useful in the treatment of neoplastic diseases, inflammatory disorders and immunomodulatory disorders. *US 2014/0228350 A1*, 314 (2014).
3. Andres, J.M., Manzano, R. & Pedrosa, R. Novel bifunctional chiral urea and thiourea derivatives as organocatalysts: enantioselective nitro-Michael reaction of malonates and diketones. *Chem-Eur J* **14**, 5116-5119 (2008).
4. Tietz, J.I. et al. A new genome-mining tool redefines the lasso peptide biosynthetic landscape. *Nat Chem Biol* **13**, 470-478 (2017).
5. Mistry, J. et al. Pfam: The protein families database in 2021. *Nucleic Acids Res* **49**, D412-D419 (2021).
6. Haft, D.H. et al. TIGRFAMs: a protein family resource for the functional identification of proteins. *Nucleic Acids Res* **29**, 41-43 (2001).
7. Kloosterman, A.M., Shelton, K.E., van Wezel, G.P., Medema, M.H. & Mitchell, D.A. RRE-Finder: a genome-mining tool for class-independent RiPP discovery. *Msystems* **5**, e00267 (2020).
8. Kim, P.I. et al. Characterization and structure identification of an antimicrobial peptide, hominicin, produced by *Staphylococcus hominis* MBBL 2-9. *Biochem Bioph Res Co* **399**, 133-138 (2010).
9. Wheeler, T.J., Clements, J. & Finn, R.D. Skylign: a tool for creating informative, interactive logos representing sequence alignments and profile hidden Markov models. *Bmc Bioinformatics* **15**, 7 (2014).
10. Zimmermann, L. et al. A completely reimplemented MPI bioinformatics toolkit with a new HHpred server at its core. *J Mol Biol* **430**, 2237-2243 (2018).
11. Price, M.N., Dehal, P.S. & Arkin, A.P. FastTree 2--approximately maximum-likelihood trees for large alignments. *PLoS One* **5**, e9490 (2010).
12. Fountoulakis, M. & Lahm, H.W. Hydrolysis and amino acid composition analysis of proteins. *J Chromatogr A* **826**, 109-134 (1998).
13. Buchan, D.W.A. & Jones, D.T. The PSIPRED protein analysis workbench: 20 years on. *Nucleic Acids Res* **47**, W402-W407 (2019).
14. Jumper, J. et al. Highly accurate protein structure prediction with AlphaFold. *Nature* **596**, 583-589 (2021).
15. Hong, J.J. et al. How melittin inserts into cell membrane: Conformational changes, inter-peptide cooperation, and disturbance on the membrane. *Molecules* **24**, 1775 (2019).
16. Jurrus, E. et al. Improvements to the APBS biomolecular solvation software suite. *Protein Sci* **27**, 112-128 (2018).
17. Pymol: the PyMOL molecular graphics system, version 1.2r3pre, Schrödinger, LLC.